Titre: Title:	Cellulose Nanofiber-Reinforced Polymer Biocomposites
Auteur: Author:	Fatemeh Safdari Shadlou
Date:	2017
Type:	Mémoire ou thèse / Dissertation or Thesis
Référence: Citation:	Safdari Shadlou, F. (2017). Cellulose Nanofiber-Reinforced Polymer Biocomposites [Thèse de doctorat, École Polytechnique de Montréal]. PolyPublie. https://publications.polymtl.ca/2505/

UNIVERSITÉ DE MONTRÉAL

CELLULOSE NANOFIBER-REINFORCED POLYMER BIOCOMPOSITES

FATEMEH SAFDARI SHADLOU

DÉPARTEMENT DE GÉNIE CHIMIQUE

ÉCOLE POLYTECHNIQUE DE MONTRÉAL

THÈSE PRÉSENTÉE EN VUE DE L'OBTENTION

DU DIPLÔME DE PHILOSOPHIAE DOCTOR

(GÉNIE CHIMIQUE)

AVRIL 2017

UNIVERSITÉ DE MONTRÉAL

ÉCOLE POLYTECHNIQUE DE MONTRÉAL

Cette thèse intitulée:

CELLULOSE NANOFIBER-REINFORCED POLYMER BIOCOMPOSITES

présentée par : SAFDARI SHADLOU Fatemeh

en vue de l'obtention du diplôme de : Philosophiae Doctor

a été dûment acceptée par le jury d'examen constitué de :

M. LAFLEUR Pierre, Ph. D., président

M. CARREAU Pierre, Ph. D., membre et directeur de recherche

Mme HEUZEY Marie-Claude, Ph. D., membre et codirectrice de recherche

M. KAMAL Musa, Ph. D., membre et codirecteur de recherche

M. AJJI Abdellah, Ph. D., membre

Mme KONTOPOULOU Marianna, Ph. D., membre

DEDICATION

To my dearly loved ones who make up my life!

ACKNOWLEDGMENTS

First of all, I wish to offer my heartfelt appreciation to my three supervisors, *Professor Pierre J. Carreau*, *Professor Marie-Claude Heuzey*, and *Professor Musa R. Kamal*. This thesis would not have been possible without their knowledge, patience, and, support. Their kind words always were indeed encouraging to advance more and more. The discussions I have had with them on scientific matters (and the matters beyond science) and the experiences I have gained, these are invaluable and not easily achievable, and so, it is my great honor to be a member of their research group.

I also acknowledge *Professor Mohini M. Sain* from University of Toronto who kindly provided the cellulose nanofibers to perform this dissertation.

Besides, I would like to thank the thesis committee, *Professor Pierre G. Lafleur*, *Professor Abdellah Ajji*, and *Professor Marianna Kontopoulou* for accepting to evaluate this dissertation.

My especial thanks are dedicated to *Professor Hossein Nazockdast*, my supervisor in Amirkabir University of Technology, who taught me great scientific and life lessons, and also, *Professor Hormoz Eslami*, who motivated me to continue my studies.

I am also grateful to technical and administrative staffs of Chemical Engineering Department, *Evelyne Rousseau*, *Valerie Beaudart*, *Martine Lamarche*, and especially, *Melina Hamdine*, our ex-research associate, for her kind cooperation and encouragement during my first year of Ph.D.

Many thanks to all the present (and the past) *members of the Rheology Group* who are truly kind and have generously shared their knowledge and experiences during the years of my Ph.D.

I also would like to convey my sincere appreciation to all *my friends*, in Iran and Canada, who have always supported and helped me in research, and more important, in life.

I owe gratitude to *Teodora Gancheva* for kindly translating the abstract of this thesis to French.

Definitely, my accomplishments throughout my life would not have been achievable without unconditional love and support of *my beloved parents and two sisters*. I am also so proud to be the aunt of *my lovely niece and nephew*, who could make me smile even in the hardest time I have had during the years being far from. I apologize that I could not be there for you in important moments of your life. Know that I love you all so much; my life has been short in you, no matter where I am.

Finally, my deepest gratitude goes to my spouse, *Davood*, for overwhelming help, support, and forgiveness he provided so far; someone who has never left my side. I am just lucky to have a caring friend as you in my life. Thanks!

RÉSUMÉ

L'intérêt d'incorporer des nanofibres de cellulose (CNFs) comme agents de renforcement pour améliorer les propriétés des matrices polymères a considérablement augmenté dernièrement, compte tenu de l'origine biologique de ces nanoparticules ainsi que leurs bonnes propriétés physiques et mécaniques, comparées aux renforts inorganiques. Cependant, il existe des défis importants liés à leur grand facteur de forme, nature fibrillaire, flexibilité élevée et hydrophilicité qui rendent les CNFs fortement enchevêtrées, et qui compliquent leur dispersion/distribution dans les polymères, en particulier dans les matrices hydrophobes.

Cette thèse vise à développer des biocomposites polymères/CNF avec une microstructure bien dispersée et des propriétés améliorées. Nous avons choisi deux polymères qui nécessitent des améliorations au niveau de leurs propriétés thermomécaniques: le polylactide (PLA), qui est un polymère hydrophobe et d'origine biologique, et le poly(oxyde d'éthylène) (PEO), qui est un polymère hydrophile, biocompatible et biodégradable. Les biocomposites ont été préparés par des méthodes de mélange simple, soit en utilisant du N,N-diméthylformamide (DMF), soit en utilisant de l'eau comme solvant. À titre de comparaison, certains composites ont aussi été préparés à l'état fondu.

Des composites à haute performance comprenant du PLA et des CNFs (0,25–5% massique) ont été d'abord préparés par coulée de solvant sans aucune comptabilisation. La viscosité complexe et le module élastique des biocomposites PLA/CNF ont été augmentés jusqu'à deux et cinq ordres de grandeur, respectivement, à basses fréquences comparativement au PLA. Une amélioration jusqu'à 50% pour le module d'Young du PLA a été obtenue par incorporation des CNFs. De même, la résistance à la traction a été augmentée de 31%. Le module élastique en flexion dans l'analyse thermique mécanique dynamique (DMTA) a été augmenté jusqu'à 51 et 264% à température ambiante et 70 °C, respectivement. Une bonne transparence a été retenue pour les films biocomposites dans la plage de lumière visible, comparativement à celle du PLA.

La seconde partie de ce projet était liée à la préparation de biocomposites de PEO/CNF renforcés avec différents chargements de nanofibres, c'est-à-dire de 1 à 3% massique, par mélange en solution aqueuse. À basses fréquences, pour les biocomposites PEO/CNF, on a obtenu des augmentations allant jusqu'à deux et trois ordres de grandeur pour la viscosité complexe et le module élastique, respectivement, comparé au PEO seul. Le module d'Young et le module élastique en DMTA à

température ambiante ont été améliorés par environ 48% en ajoutant 3% massique de CNFs au PEO; la résistance à la traction a également augmenté de 35%. De plus, la transparence des films composites dans la plage de lumière visible était similaire à celle du film de PEO non chargé. Pour les biocomposites préparés à l'état fondu, les CNFs étaient mal dispersés et, par conséquence, aucune amélioration des propriétés n'a été observée.

Dans la dernière partie, un polyéthylène glycol (PEG) a été utilisé comme agent comptabilisant pour le système PLA/CNF. Initialement, un « masterbatch » CNF/PEG (rapport 1:2) a été préparé en solution aqueuse. Ensuite, les biocomposites ont été élaborés par la méthode de coulée de solvant. Différentes techniques microscopiques ont montré que les CNFs étaient mieux dispersées/distribuées dans le PLA lorsque l'agent comptabilisant était présent. La viscosité complexe et le module élastique de composites comptabilisés ont été augmentés d'un ordre de grandeur par rapport aux composites non compatibilisés. En utilisant un agent comptabilisant, les modules élastiques en DMTA du PLA contenant 2% massique de nanofibres, à température ambiante et à 80 °C, ont été augmentés jusqu'à 42 et 553%, respectivement, par rapport au PLA. L'effet de nucléation des CNFs sur la cristallisation du PLA était plus prononcé par rapport aux échantillons non compatibilisés. Aussi, une meilleure transmission de la lumière a été mesurée pour les films composites PLA/CNF/PEG par rapport aux films PLA/CNF. D'autre part, aucune amélioration des propriétés, par rapport à la matrice, n'a été observée pour les biocomposites préparés à l'état fondu.

En conclusion, la morphologie, la rhéologie, les propriétés mécaniques et les résultats de transmission de la lumière ont confirmé qu'en utilisant des méthodes de préparation en solution simples, une bonne dispersion et distribution des CNFs dans les matrices polymères PLA, PEO et PLA/PEG a été obtenue. Des améliorations substantielles des propriétés thermomécaniques des composites ont été constatées à faibles teneurs en nanofibres.

ABSTRACT

The interest to incorporate cellulose nanofibers (CNFs) as reinforcing agents to enhance the properties of polymer matrices has recently grown considerably, as these nanoparticles are bio-based and have good physical and mechanical properties, comparable to those of inorganic fillers. However, one faces important challenges associated with their large aspect ratio, fibrillated nature, high flexibility and hydrophilicity that make CNFs highly entangled, which render their dispersion/distribution in polymers quite difficult, especially in hydrophobic matrices.

This thesis aims at developing polymer/CNF biocomposites with well-dispersed microstructure and enhanced properties. We chose two polymers that need improvements in thermomechanical properties: polylactide (PLA), which is a commonly used bio-based hydrophobic polymer, and poly(ethylene oxide) (PEO), which is a biocompatible/biodegradable hydrophilic polymer. The biocomposites were prepared via simple mixing methods, either using N,N-dimethylformamide (DMF) or water as solvents. For comparison, some composites were prepared in the molten state.

High-performance composites comprising PLA and CNFs (0.25–5 wt%) were first prepared via solvent casting without any compatibilization. The complex viscosity and storage modulus of the PLA/CNF biocomposites were increased by up to two and five orders of magnitude, respectively, at low frequencies compared to the neat PLA. An improvement of up to 50% for the Young modulus of PLA was achieved by incorporating CNFs. Similarly, the tensile strength was raised by 31%. The flexural storage modulus in dynamic mechanical thermal analysis (DMTA) was increased by up to 51 and 264% at room temperature and 70 °C, respectively. Good transparency was retained for the biocomposite films in the visible light range comparable to that of neat PLA.

The second part of this project was related to the preparation of enhanced PEO/CNF biocomposites with different nanofiber loadings, i.e., 1–3 wt%, via aqueous solution mixing. At low frequencies, increases of up to two and three orders of magnitude were obtained for the complex viscosity and storage modulus, respectively, of PEO/CNF biocomposites relative to the neat PEO. The Young modulus and the room temperature DMTA storage modulus were improved by ca. 48% by adding 3 wt% CNFs to PEO; the tensile strength also increased by 35%. Moreover, the transparency of the composite films in the visible range was similar to that of the neat PEO film. For the melt-prepared biocomposites, however, the CNFs were poorly dispersed and consequently no property enhancement was observed.

In the last part, poly(ethylene glycol) (PEG) was used as a compatibilizer for the PLA/CNF system. Initially, a CNF/PEG masterbatch (ratio of 1/2) was prepared in an aqueous solution. Then, the biocomposites were prepared using a solvent-casting method. Different microscopic techniques showed that CNFs were better dispersed/distributed within PLA when the compatibilizer was employed. The complex viscosity and storage modulus were increased by one order of magnitude for the compatibilized composites compared to those of the uncompatibilized composites. With compatibilization, the DMTA storage moduli of the PLA containing 2 wt% nanofibers at room temperature and 80 °C were enhanced by up to 42 and 553%, respectively, compared to the neat PLA. The nucleation effect of the CNFs on PLA crystallization was more pronounced relative to the uncompatibilized samples. Also, better light transmittance was measured for the PLA/CNF/PEG composite films relative to the PLA/CNF composite films. On the other hand, no property enhancement, compared to the matrix, was observed for the biocomposites prepared in the melt.

In conclusion, the morphology, rheology, mechanical properties and light transmittance results confirmed that, using simple solution methods, good dispersion and distribution of CNFs within the host polymer matrices, PLA, PEO and PLA/PEG, was achieved. Substantial enhancements in the thermomechanical properties of the composites were obtained at low nanofiber contents.

TABLE OF CONTENTS

LIST OF TABLES

LIST OF FIGURES

CHAPTER 1 INTRODUCTION

The overdependence on petroleum-based products (synthetic polymers, resins, etc.) in the past half-century has increased consistently. This has encouraged researchers to consider green materials, especially those based on cellulose, as possible alternatives. Cellulose fibers at the micro and nano scales are attractive as promising candidates for replacing non-biodegradable fillers in the production of environmentally friendly green products, such as biocomposites [1]. Cellulose nanofibers (CNFs) can be extracted from various sources by mechanical separation of fibers into smaller elementary constituents, which typically requires high energy input. However, chemical and/or enzymatic fiber pretreatments have been developed to overcome this problem [2-4]. Such new materials that are the subject of continuing research are commercially interesting due to the abundance of the sources in nature, high strength and stiffness, large aspect ratio and surface area, low density, biocompatibility and biodegradability [5-16].

CNFs offer a series of advantages compared to glass fibers that is the most common reinforcement, such as lower density, flexibility during processing, less abrasive machine wear, and also minimal health hazards [17]. Their use as reinforcing agents in thermoplastics, especially bio-derived polymers, has attracted great interest. Polylactide (PLA) is the frontrunner among different biopolymers [5] and has numerous applications, e.g. in the medical, packaging and automotive fields [8-10, 13, 18, 19]. On the other hand, poly(ethylene oxide) (PEO) is a biocompatible and biodegradable polymer [20] that has already found applications in the biomedical and electrochemical fields, and is used as hydrogel, flocculating agent, and rheology modifier [2, 20, 21]. However, both PLA and PEO suffer from deficiencies in mechanical and thermal properties. The incorporation of CNFs can improve the thermomechanical properties of PLA and PEO while maintaining their unique properties such as biocompatibility, biodegradability and film transparency [2, 7, 22, 23]. This would result in biodegradable and biocompatible products comprising components from renewable sources, all or in parts that open various application prospects.

Nanofibers with high aspect ratios and flexibility such as CNFs, have strong tendency to entangle and form agglomerates with a non-uniform state of dispersion in a polymer matrix. This is the result of strong hydrogen bond attraction between the fibers [8-11, 13, 14, 16, 19]. Besides, the insufficient adhesion between hydrophilic CNFs and hydrophobic polymer matrices, such as PLA

[24], may hamper the use of CNFs as reinforcement in such matrices. Therefore, to improve the compatibility between CNFs and non-polar polymers, either surface modification or the use of a compatibilizer may have to be proposed.

This thesis focuses on developing biocomposites based on both hydrophilic and hydrophobic matrices, e.g. PEO and PLA, reinforced with CNFs through efficient preparation methods that lead to enhanced properties. It also presents a promising approach to increase the compatibility between CNFs and PLA, as one of the most commonly used bioplastics [5], which results in further improving the mechanical and thermal properties of PLA/CNF composites. This route includes the use of a miscible compatibilizer with PLA, i.e., poly(ethylene glycol) (PEG) [25-28], which has a better affinity with CNFs compared to PLA.

The main contributions of the current project are found in three papers; the first and second have been published in the journals of *Polymer Composites* and *Cellulose*, respectively, and the third one has been accepted in *Cellulose*.

In this thesis, the following chapters are presented:

- Chapter 1: Introduction
- Chapter 2: Literature review
- Chapter 3: Objectives
- Chapter 4: Organization of the articles
- Chapters 5 to 7: The three papers reporting the main results of this project
- Chapter 8: General discussion
- Chapter 9: Conclusions and recommendations

CHAPTER 2 LITERATURE REVIEW

2.1 Overview

Composite preparation is one of the methods to produce materials with new and/or enhanced properties compared to neat matrices. In recent years, polymers derived from renewable resources have been considered as promising alternatives to petroleum-based polymers thanks to their biodegradability. They reduce environmental concerns about greenhouse gas emissions and pollution and our reliance on fossil resources that currently have raised challenges [5]. Therefore, the preparation of composites from fully bio-based components is more desirable over traditional composites to minimize environmental impacts. The term "biocomposites" refers to composite materials made of bio-based components, all or in parts. All three biocomposites prepared in this project comprise matrices such as bio-based, biodegradable, and biocompatible polylactide (PLA), and biodegradable and biocompatible poly(ethylene oxide) (PEO) in the presence of a bio-based reinforcement, i.e., cellulose nanofibers (CNFs). Also, poly(ethylene glycol) (PEG) is used as a compatibilizer for the PLA/CNF system.

CNFs have interesting mechanical and physical properties that make them a good alternative to mineral reinforcements. Therefore, in this research dissertation, we investigate the use of CNFs to improve the properties of two biodegradable and biocompatible polymers, namely PLA and PEO.

2.2 Cellulose nanofibers (CNFs)

Cellulose is a long linear chain carbohydrate polymer with a large number of hydroxyl groups, three per anhydroglucose (AGU), the repeating unit of the molecular structure of cellulose. The chemical structure of cellulose is presented in Figure 2.1.

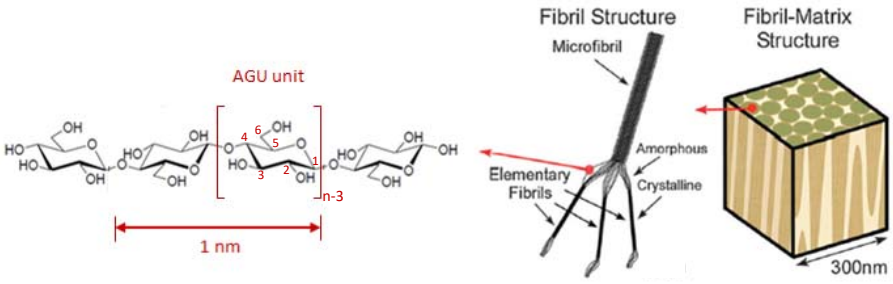

Figure 2.1: Chemical structure of cellulose molecule showing the AGU repeating unit [29, 30].

Cellulose is a molecule that is flexible [31] and the presence of the hydroxyl groups forms intra- and inter-molecular hydrogen bonds, which allow the creation of a 3D structure [1]. It is considered as the most common organic polymer and is an almost endless raw material for the increasing demand for environmentally friendly and biocompatible products [31]. The most important source for cellulose is wood pulp (soft and hard). Cellulosic fibers have high tensile strength, as a result of their fibrillar structure and the large amounts of hydrogen bonds. Therefore, the structural element of a plant that bears the load in tensile mode is cellulose. Also, it can be isolated from other sources including cotton, algae, tunicates and even bacteria in which the main role of cellulose is to act as the reinforcement material [1]. Several processes such as mechanical and chemical pulping, homogenization, acid hydrolysis, steam explosion, and high-intensity ultrasonication have been used to extract highly purified nanofibers from cellulosic materials [1, 2]. Depending on what source cellulose is extracted from and the extraction method, cellulosic particles vary in characteristic size, aspect ratio, morphology, crystallinity, and crystal structure [1, 30].

The first successful isolation of cellulosic microfibrils/microfibers (CMFs) was reported in 1983 via a Gaulin laboratory homogenizer. Dilute slurries of cut cellulose fibers from softwood pulp were subjected to high shear forces to yield individualized CMFs. The resulting gels showed a significant increase in viscosity after several passes through the homogenizer. It should be mentioned that a completely homogeneous sample of single CMFs cannot be achieved and mechanical disintegration of pulps usually results in cellulose fibril bundles having diameters below 100 nm, which are called cellulose nanofibrils/nanofibers (CNFs) [1]. However, considering their characteristic size, CNFs may be sometimes found under other nomenclatures in the literature, e.g. CMFs and micro-fibrillated cellulose (MFC).

CNFs, with diameter in the nanometer scale, provide a high surface area that can result in a strong interaction between the fibrils and surrounding species, such as organic and polymeric compounds, and living cells [32]. Compared to some inorganic fillers, the main advantages of CNFs that make them an interesting choice to replace inorganic fillers are: renewable nature, non-food agricultural based economy, low energy consumption in their production, low density, high specific strength and modulus, relatively reactive surface, which can be used for grafting specific groups, high sound attenuation of resultant composites, comparatively easy processability due to their nonabrasive nature, which allows high filling levels, resulting in significant cost savings. Moreover, disposal issues are easier to resolve by the combustion of cellulosic particle-filled composites in comparison

with inorganic fillers systems. Therefore, the possibility of using CNFs in the plastics industry has received considerable interest, particularly for the fabrication of automotive parts [33, 34]. Other potential applications could be in aircraft, railways, irrigation systems, furniture industries, sports and leisure items [34, 35]. Some new applications for cellulosic particles are based on their biocompatibility and chirality that can be utilized for the immobilization of proteins, heparin and antibodies [32].

2.3 Polylactide (PLA)

Polylactide (PLA) is a bio-derived, semi-crystalline, thermoplastic polyester [36-39] that is nowadays commercially used in a number of industrial sectors. PLA is the product of the ring opening polymerization of lactide monomer. Figure 2.2 presents the chemical structures of lactide and PLA. Although, PLA has oxygen single and double bounds in its chemical structure, it is classified as a hydrophobic polymer [24], rarely as a partially-hydrophilic one.

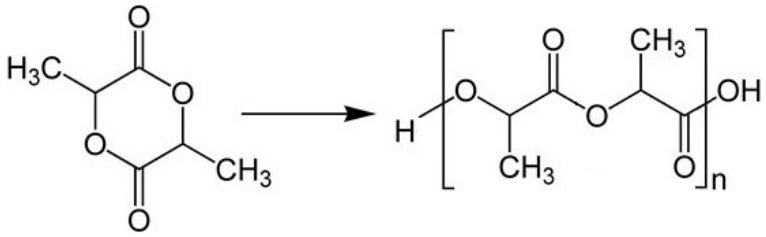

Figure 2.2: Chemical structure of lactide (left), and PLA (right) [40].

PLA has glass transition and melting temperatures of 55–60 °C and 155–170 °C, respectively. It has interesting mechanical properties, such as high modulus and tensile strength at room temperature, UV stability, gloss, low toxicity, and is of moderate cost [2, 5, 7, 13, 37-39, 41-45]. In addition, its other unique properties such as biocompatibility and biodegradability make it the frontrunner among many other polymers. Biomedical, automotive and textile applications, in addition to electronics and packaging industries, as disposable bottles/bags, food containers and plastic utensils, are examples of different sectors for which PLA has already found considerable applications [8-10, 13, 18, 19, 38, 39, 46-49]. Moreover, it has relatively good processability in conventional industrial processing techniques used for polyolefins (i.e., extrusion, injection molding, film blowing and blow molding) [8-10, 18, 19, 46, 47]. However, major drawbacks limit its applications: slow crystallization [47] and low heat resistance (low stiffness at elevated temperatures) [2, 7, 36, 42, 44, 47]. To overcome these deficiencies, the use of reinforcements is a

possible route [2, 36]. However, appropriate reinforcements should be chosen to maintain PLA biocompatibility, biodegradability and film transparency. In this regard, some common nanofillers (e.g. carbon nanotubes) may not be appropriate due to the lack of biocompatibility, biodegradability, and gloss of the final composites.

2.4 Poly(ethylene oxide) (PEO)

Poly(ethylene oxide) (PEO) is another nontoxic, semi-crystalline, thermoplastic polymer that is highly hydrophilic [20, 21, 50]. Figure 2.3 presents the chemical structure of PEO that is the product of the ring opening polymerization of ethylene oxide monomer.

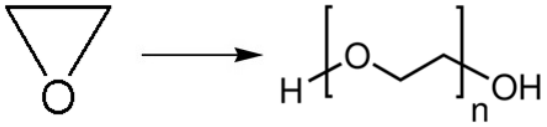

Figure 2.3: Chemical structure of ethylene oxide (left), and PEO (right) [51].

PEO has glass transition and melting temperatures of ca. -40 °C and 63–66 °C, respectively. It is worth mentioning that for molecular weights of 20,000 g/mol and lower the polymer with a similar chemical structure to PEO is referred as poly(ethylene glycol) (PEG) [52], which is the result of polycondensation of ethylene glycol molecules. PEO has found applications in biomedical, energy storage [20, 21, 53-55], and the electrochemical field as electrolyte in lithium polymer cells [21, 56-58]. Other uses are hydrogel, dispersant, surfactant, flocculating agent and rheology modifier [2, 21]. However, its deficient mechanical and thermal properties and high crystallinity are drawbacks for many applications. Thermomechanical properties of PEO can also be improved by incorporating reinforcements. It is important to preserve its advantageous properties, such as high biocompatibility, biodegradability [2, 21, 54] and film transparency [22, 23].

2.5 PLA/cellulose biocomposites

Mathew et al. [59] investigated the effect of 5 wt% cellulose microfibers (CMFs), diameters up to 1 μm, on mechanical properties of PLA. The CMF aqueous suspension was pumped into the PLA melt stream during extrusion. Table 2.1 presents the results of a mechanical test for PLA and PLA/5CMF samples. The Young modulus of PLA increased by 30% for the composite; however, the tensile strength remained unchanged and the elongation at break decreased.

Table 2.1: Tensile properties of PLA and PLA/5CMF [59].

Sample	Young's modulus (GPa)	Tensile strength (MPa)	Elongation at break (%)
PLA	2.0 ± 0.2	58 ± 6	4.2 ± 0.6
PLA/5CMF	2.6 ± 0.1	58 ± 5	2.8 ± 0.5

They also prepared PLA composite containing 5 wt% cellulose nanocrystals (CNCs) of diameter of 10–15 nm and average aspect ratio of 40, with a similar preparation method to that of PLA/CMF composites [59], to compare the effect of the two cellulosic reinforcements on mechanical properties. The Young modulus of PLA increased by 20% in the presence of 5 wt% CNCs; however, the improvement was lower compared to the composite with the same content of CMFs (see Table 2.1). Moreover, the tensile strength of PLA slightly decreased by incorporating CNCs.

Wang and Sain [14] freeze-dried hemp nanofibers (HPNs) and prepared a PLA composite containing 5 wt% fibers using an internal mixer in the molten state. In that study, the nanofibers had diameters between 50 and 100 nm and lengths in the micrometer scale. Figure 2.4 presents a scanning electron microscopy (SEM) micrograph of the freeze-dried HPNs.

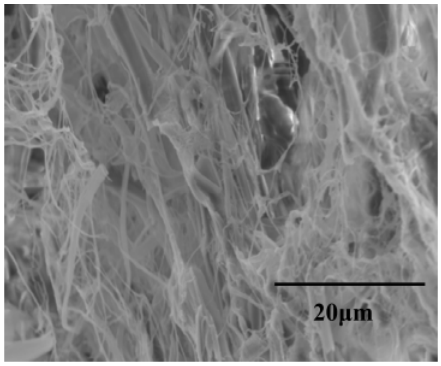

Figure 2.4: SEM micrograph of the freeze-dried HPNs [14].

Table 2.2 reports the results of the tensile test for the neat PLA and PLA/5HPN. The Young modulus and tensile strength were negligibly increased for PLA containing 5 wt% HPNs, 3 and 5%, respectively, compared to those of the neat PLA.

Table 2.2: The Young modulus and tensile strength for PLA and PLA/5HPN [14].

Sample	Young's modulus (GPa)	Tensile strength (MPa)
PLA	2.72 ± 0.09	65.49 ± 0.21
PLA/5HPN	2.80 ± 0.06	68.97 ± 0.40

Iwatake et al. [11] prepared PLA reinforced with 3–20 wt% micro-fibrillated cellulose (MFC) via a solution preparation method using acetone. The suspensions were dried and finally the samples were kneaded by a twin rotary roller mixer in the molten state. For the sake of comparison one sample was prepared by direct mixing of MFC aqueous suspension, containing 10 wt% solids, into molten PLA using the same mixer. Figure 2.5 shows the SEM micrograph of MFC consisting of fibers with diameters of nanometer to submicron forming a web-like network.

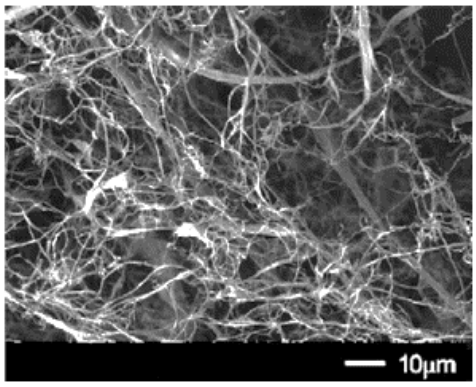

Figure 2.5: SEM micrograph of MFC [11].

The micrographs of composites containing 5 wt% MFC prepared via solution and melt mixing are presented in Figure 2.6. A uniform dispersion was observed for the solution-based composite (Figure 2.6 left), while agglomerates remained in the composite prepared via melt mixing (Figure 2.6 right).

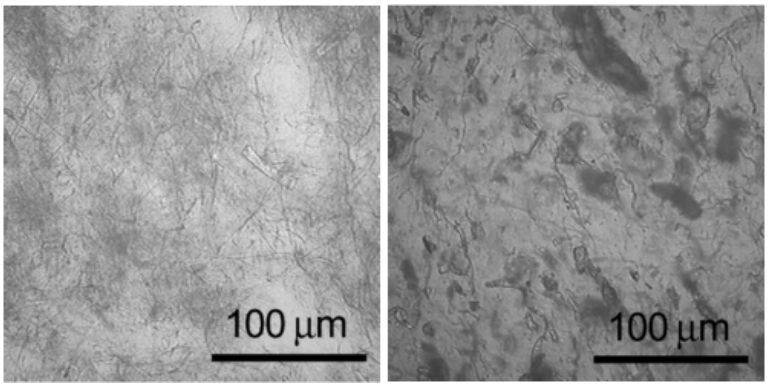

Figure 2.6: SEM micrographs of the samples prepared in solution (left), and melt (right) with MFC concentration of 5 wt% [11].

Figure 2.7 depicts tensile stress-strain curves for the neat PLA and samples containing 5 wt% MFC prepared using both preparation methods and solution-prepared composites with 3–20 wt% fibers.

The mechanical properties of PLA were improved for the solution-based sample over the melt-prepared sample with the same content of fibers, i.e., 5 wt% (Figure 2.7 left). The Young modulus and tensile strength were improved by 38 and 33%, respectively, for solution-based samples with the addition of MFC up to 10 wt%, and for larger concentrations they decreased (Figure 2.7 right).

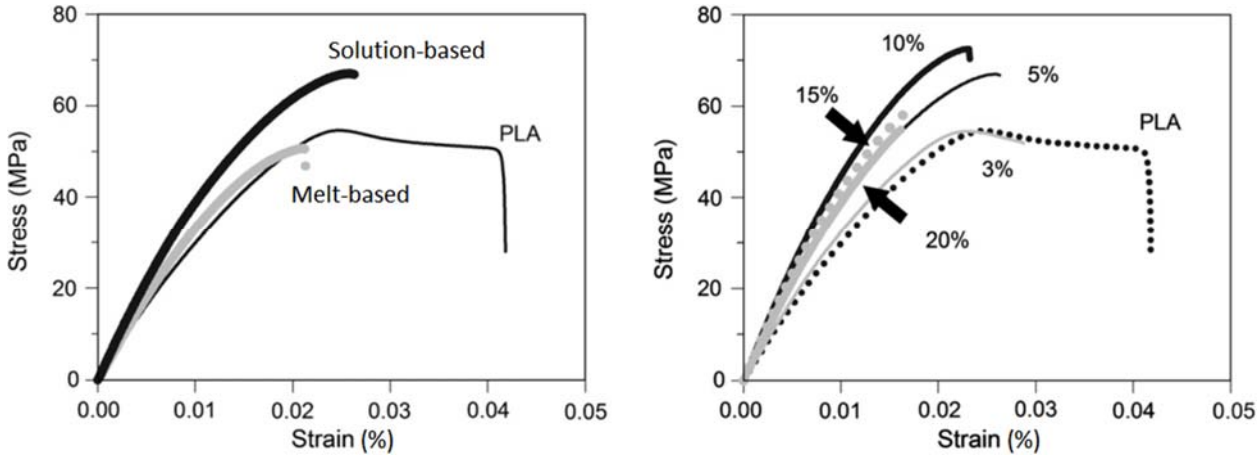

Figure 2.7: Stress-strain curves for the samples containing 5 wt% MFC prepared by solution and melt mixing methods (left), and solution-prepared samples containing different fiber contents (right) [11].

Iwatake et al. [11] also prepared a sample containing 5 wt% bleached Kraft pulp of smooth surface with 30–50 μm in diameter, via the same preparation method described for solution-based PLA/MFC composites, to study the effect of fiber morphology. The Young modulus increased negligibly and the yield strain and the tensile strength were reduced by 30 and 15%, respectively, at a fiber content of 5 wt% compared to those of the neat PLA. However, these properties were improved in the presence of the same content of MFC (see Figure 2.7).

Suryanegara et al. [47] incorporated up to 20 wt% of MFC reinforcement into PLA using a solution method with dichloromethane, followed by drying and kneading using a twin rotary roller mixer in the molten state. Thereafter, they annealed the samples to prepare highly-crystalized composites. Table 2.3 presents the data of the tensile tests and Figure 2.8 reports the results of the storage modulus in dynamic mechanical thermal analysis (DMTA). The maximum enhancements were obtained at the highest MFC concentration, i.e., 20 wt%. The Young modulus and tensile strength of PLA increased by ca. 42 and 14%, respectively, while the elongation at break decreased (Table 2.3); the storage modulus at 20 and 80 °C improved by 37 and 220%, respectively, relative to the

PLA (Figure 2.8). However, more enhancements in tensile and DMTA properties of PLA were achieved when the samples were quenched in liquid nitrogen (amorphous state).

Table 2.3: Tensile properties of the PLA/MFC composites [47].

Sample	Young's modulus (GPa)	Tensile strength (MPa)	Elongation at break (%)
PLA	4.0 ± 0.1	60.9 ± 1.6	3.1 ± 0.4
PLA/3MFC	4.4 ± 0.1	63.6 ± 0.7	2.0 ± 0.1
PLA/5MFC	4.6 ± 0.1	64.4 ± 0.8	2.0 ± 0.1
PLA/10MFC	4.7 ± 0.1	66.2 ± 3.5	2.0 ± 0.2
PLA/20MFC	5.7 ± 0.1	69.4 ± 1.4	1.7 ± 0.1

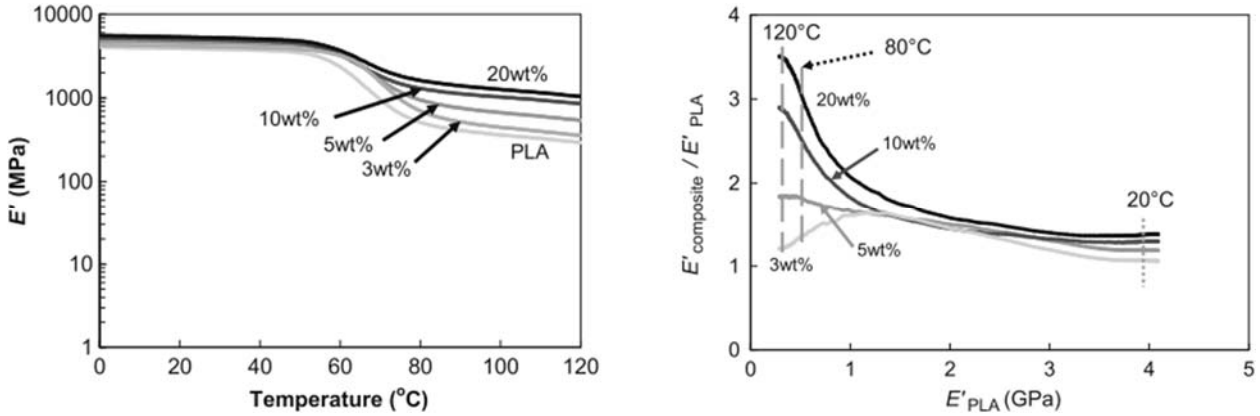

Figure 2.8: Storage modulus vs temperature (left), and normalized storage modulus (right) for various PLA/MFC composites [47].

Jonoobi et al. [10] developed PLA/CNF composites via masterbatch preparation in a mixture of acetone and chloroform. The resulting masterbatch, after drying, was diluted with PLA using a twin-screw extruder to produce composites of 1–5 wt% CNFs. Figure 2.9 shows the atomic force microscopy (AFM) image of CNFs and the SEM micrograph of the fractured surface for the PLA/5CNF composite. The CNFs used in that study had diameters in the range from 40 to 70 nm (Figure 2.9 left), and the estimated length of several micrometers. However, agglomerates of ca. 10 µm size are evident in Figure 2.9 (right).

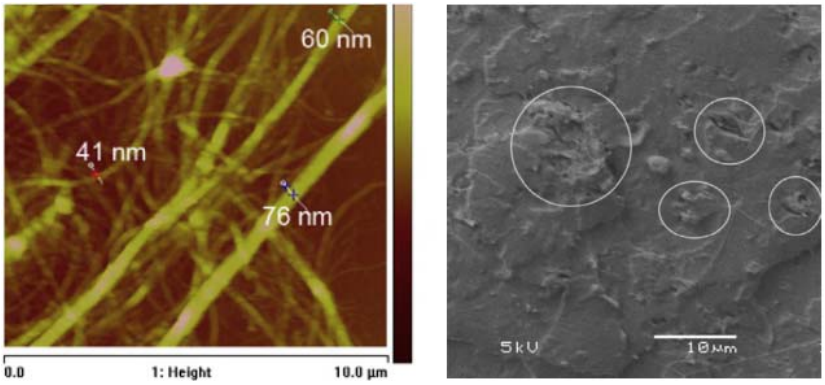

Figure 2.9: AFM image of CNFs (left), and SEM micrograph of the fractured surface of PLA/5CNF composite (right) [10].

A visual comparison of PLA/CNF composite films with different CNF contents is also presented in Figure 2.10. Large agglomerates (white spots) are observed in thin films, especially, as the CNF concentration increases.

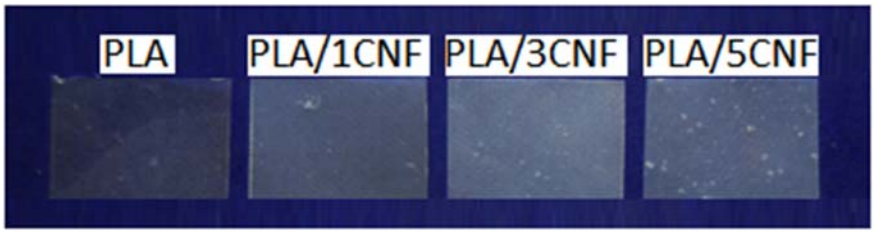

Figure 2.10: Visual comparison of PLA/CNF composite films with different CNF contents [10].

The mechanical properties of the samples are reported in Table 2.4. The Young modulus and tensile strength of PLA increased by 24 and 21%, respectively, by incorporating 5 wt% CNFs; as expected, the elongation at break decreased.

Table 2.4: Tensile properties of the PLA/CNF composites [10].

Sample	Young's modulus (GPa)	Tensile strength (MPa)	Elongation at break (%)
PLA	2.9 ± 0.6	58.9 ± 0.5	3.4 ± 0.4
PLA/1CNF	3.3 ± 0.4	63.1 ± 0.9	2.8 ± 0.3
PLA/3CNF	3.4 ± 0.1	65.1 ± 0.6	2.7 ± 0.2
PLA/5CNF	3.6 ± 0.7	71.2 ± 0.6	2.7 ± 0.1

Qu et al. [44] also prepared a PLA/1CNF composite via a solvent-casting method using N,N-dimethylacetamide (DMAc) as the solvent. The CNFs were 50 nm wide and several micrometers long. Figure 2.11 presents the results of a tensile test. The tensile strength decreased from ca. 40 MPa for PLA to ca. 30 MPa for the PLA/1CNF.

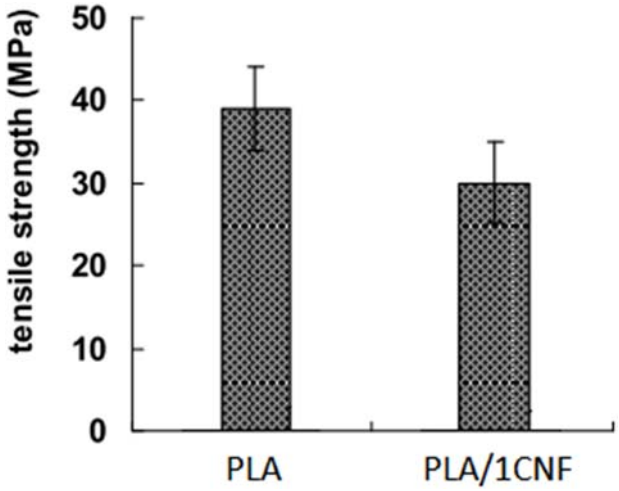

Figure 2.11: Tensile strength of PLA and PLA/1CNF composite [44].

Kowalczyk et al. [60] employed a solution-based method in dichloromethane followed by drying and then melt mixing to prepare a PLA/CNF composite containing 2 wt% nanofibers. The CNFs employed in that investigation had the diameter and length of 200–300 nm and less than 300 µm, respectively. Figure 2.12 shows a SEM micrograph of the nanofibers and a micrograph of the cryo-fractured surface of PLA/2CNF. A good distribution of the CNFs within the PLA matrix was obtained (Figure 2.12 right).

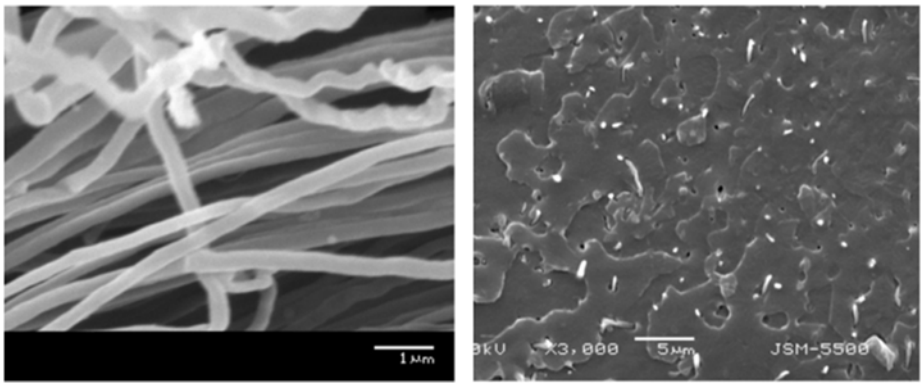

Figure 2.12: SEM micrograph of CNFs (left), and cryo-fractured surface of the composite containing 2 wt% CNFs (right) [60].

Table 2.5 reports tensile properties at 25 °C. A decrease in the elongation at break and slight increases in the yield stress (5%) and the tensile strength (3%) were observed for PLA/2CNF compared to those of the neat PLA. However, the enhancement of the yield stress was more evident when the tensile test was performed at 55 °C.

Table 2.5: Tensile properties of the neat PLA and PLA/2CNF at 25 °C [60].

Sample	Yield stress (MPa)	Tensile strength (MPa)	Elongation at break (%)
PLA	48.2 ± 1.1	46.9 ± 1.1	21 ± 6
PLA/2CNF	50.7 ± 1.5	48.2 ± 1.2	12 ± 3

Figure 2.13 presents the results of the DMTA test. The storage modulus of PLA at 20 °C increased by only 14% for PLA/2CNF. Moreover, the CNFs did not promote nucleation.

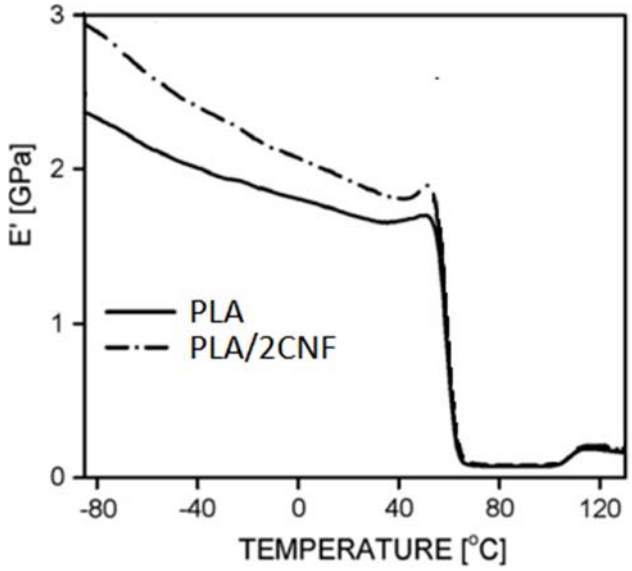

Figure 2.13: DMTA properties of PLA and PLA/2CNF samples [60].

Kowalczyk et al. [60] also prepared a sample containing 2 wt% cellulose fibers, with diameter in the range of 10–17 μm and length of less than 300 μm, to evaluate the effect of a significant increase of the size of cellulose fibers on the composite tensile properties at 25 °C. Reductions in both the yield stress and tensile strength of PLA in the presence of 2 wt% cellulose fibers were reported. However, these properties were increased in the presence of CNFs with a similar content (see Table 2.5).

Lee et al. [49] incorporated 5 wt% bacterial cellulose nanofibers (BCNFs) into PLA using 1,4-dioxane as the media for composite preparation. The suspension was then immersed in liquid nitrogen and subsequently dried via freeze-drying prior to injection molding. Table 2.6 reports the differential scanning calorimetry (DSC) data for the samples. The glass transition, T_g, melting, T_m, and crystallization, T_c, temperatures of the matrix were reduced for the PLA/5BCNF, while the crystalline content, X_c, of PLA increased.

Table 2.6: Results of DSC tests for PLA and PLA/5BCNF [49].

Sample	T_g (°C)	T_m (°C)	T_c (°C)	$X_c^{heating}$ (%)
PLA	63 ± 3	171 ± 2	113 ± 2	18 ± 2
PLA/5BCNF	58 ± 5	167 ± 2	89 ± 4	25 ± 5

Table 2.7 presents the results of mechanical tests for PLA and the PLA/5BCNF composite. The Young modulus of the composite was improved by 11%; however, its tensile strength decreased and the elongation at break remained unchanged compared to neat PLA.

Table 2.7: Tensile properties of PLA and its composite containing 5 wt% BCNFs [49].

Sample	Young's modulus (GPa)	Tensile strength (MPa)	Elongation at break (%)
PLA	4.08 ± 0.07	63.1 ± 2.0	1.7 ± 0.1
PLA/5BCNF	4.55 ± 0.03	57.8 ± 5.9	1.7 ± 0.2

Frone et al. [8] investigated the influence of CNFs, with diameters ranging from 11 to 44 nm, on the properties of PLA. To that end, a composite was produced via melt mixing of 2.5 wt% dried CNFs with PLA in an internal mixer. AFM images of PLA and PLA/2.5CNF are presented in Figure 2.14. The agglomerates (white-colored) are heterogeneously distributed in the composite sample (Figure 2.14 right).

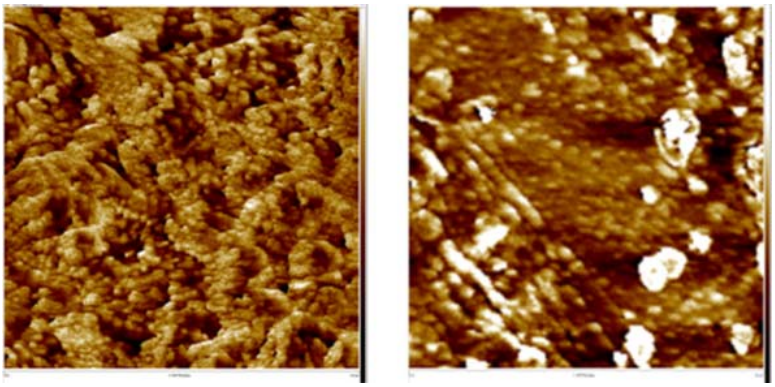

Figure 2.14: AFM modulus images of PLA (left), and PLA/2.5CNF composite (right) at a scan size of 3 μm × 3 μm [8].

DSC results for the first heating and cooling scans are presented in Table 2.8. The CNFs were reported to act as nucleating agents as the cold-crystallization temperature, T_{cc}, decreased; however, the crystallization temperature decreased too. Also, a higher degree of crystallinity was achieved for the composite sample, whereas the glass transition and melting temperatures were not affected by the presence of the CNFs.

Table 2.8: DSC results of the first heating and cooling scans [8].

Sample	T_g (°C)	T_{cc} (°C)	T_m (°C)	T_c (°C)	$X_c^{cooling}$ (%)
PLA	56.9	87.3	168.1	104.3	38.9
PLA/2.5CNF	56.3	85.2	168.0	102.9	47.1

Frone et al. [19] also investigated the effect of adding cellulose microfibrils (CMFs), diameters ranging from 5 to 15 μm and aspect ratios from 8 to 14 [19], to PLA with the same fiber loading, i.e., 2.5 wt%, following the same processing procedure described in [8]. Table 2.9 presents the results of the storage modulus recorded from a DMTA test. The storage modulus at 25 °C increased by 18% for composite containing 2.5 wt% CMFs compared to that of PLA; however, the storage modulus at 80 °C decreased for that composite.

Table 2.9: DMTA properties of the neat PLA and its composite with 2.5 wt% CMFs [19].

Sample	Storage modulus at 25 °C (GPa)	Storage modulus at 80 °C (MPa)
PLA	3.4 ± 0.1	260 ± 10
PLA/2.5CMF	4.0 ± 0.1	130 ± 10

Kiziltas et al. [61] reinforced PLA with 10 wt% CNFs using an internal batch mixer. The nanofibers had diameter and length of 10–500 nm and 1–10 µm, respectively. Figure 2.15 shows the SEM micrograph of the CNFs used in that investigation. The melt flow index (MFI) results are presented in Figure 2.16. The PLA/10CNF composite had a 65% lower MFI than that of PLA at temperature of the test.

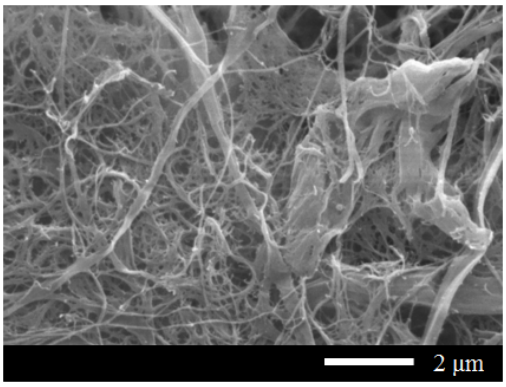

Figure 2.15: SEM micrograph of CNFs [61].

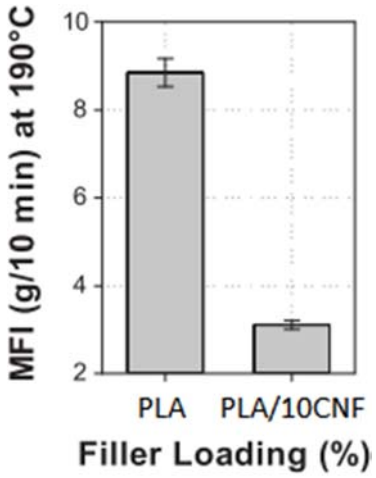

Figure 2.16: MFI results regarding the effect of 10 wt% CNFs on the flowability of PLA [61].

The results of a tensile test are reported in Table 2.10. The Young modulus of PLA increased by 21% in the presence of 10 wt% CNFs; however, the tensile strength and elongation at break decreased.

Table 2.10: Tensile properties of neat PLA and PLA/10CNF samples [61].

Sample	Young's modulus (GPa)	Tensile strength (MPa)	Elongation at break (%)
PLA	2.98 ± 0.07	59.9 ± 1.3	2.40 ± 0.09
PLA/10CNF	3.60 ± 0.08	56.6 ± 0.9	1.78 ± 0.07

2.6 Compatibilized PLA/cellulose biocomposites

Mathew et al. [59] also developed CMF-reinforced PLA by adding PEG as a processing aid. A CMF/PEG aqueous suspension was pumped into PLA melt stream during extrusion, as described earlier. Table 2.11 reports the tensile properties of the samples. The tensile strength negligibly increased and the Young modulus increased by only 15% for the PLA/CMF/PEG composite containing 5 wt% fibers and 5 wt% PEG compared to the values of the neat PLA. Moreover, both properties were lower than for the uncompatibilized case (see Table 2.1). The elongation at break of PLA decreased for PLA/5CMF/5PEG composite (Table 2.11).

Table 2.11: Tensile properties of different samples [59].

Sample	Young's modulus (GPa)	Tensile strength (MPa)	Elongation at break (%)
PLA	2.0 ± 0.2	58 ± 6	4.2 ± 0.6
PLA/5CMF/5PEG	2.3 ± 0.1	59 ± 2	3.3 ± 0.2

Mathew et al. [59] produced a compatibilized PLA/5CNC composite, i.e., PLA/5CNC/5PEG, too. The Young modulus increased by only 5% compared to the PLA and the enhancement was lower compared to the PLA/5CMF/5PEG composite (see Table 2.11) and the PLA/5CNC composite; the tensile strength decreased by 19% compared to that of PLA.

Wang and Sain [14] modified HPNs using a styrene maleic anhydride copolymer (SMA) in aqueous suspension. The freeze-dried modified nanofibers were then used to produce a PLA composite with 5 wt% nanofibers via an internal batch mixer. SEM micrograph of the freeze-dried SMA-modified HPNs (SMA-HPNs) is presented in Figure 2.17 and the SEM micrograph of HPNs was presented earlier in Figure 2.4. They claimed that SMA could reduce the entanglements of the nanofibers. However, the dispersion of the modified nanofibers in PLA was not uniform and agglomerates were still evident.

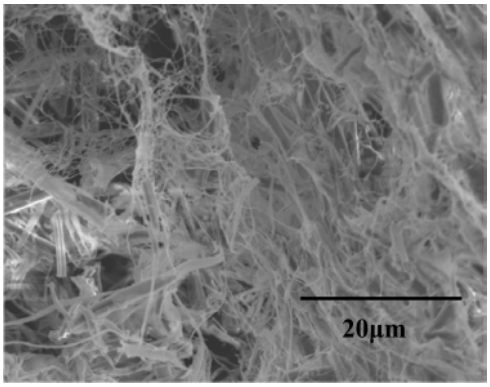

Figure 2.17: SEM micrograph of the freeze-dried SMA-HPNs [14].

Table 2.12 reports the results of tensile tests for the neat PLA and modified composite. The Young modulus and tensile strength increased slightly by 10 and 9%, respectively, for the composite containing 5 wt% SMA-HPNs. Moreover, the enhancements were less in the case of unmodified composite (see Table 2.2).

Table 2.12: Young's modulus and tensile strength of PLA and its modified composite [14].

Sample	Young's modulus (GPa)	Tensile strength (MPa)
PLA	2.72 ± 0.09	65.49 ± 0.21
PLA/5SMA-HPN	2.99 ± 0.01	71.14 ± 0.64

Qu et al. [44] also prepared PLA/CNF composites containing 1 wt% nanofibers using DMAc as a solvent and PEG as a compatibilizer in a solvent-casting method. All the components were added into DMAc with CNF/PEG at a ratio of 3/2. Figure 2.18 depicts the results of the tensile strength for the samples. The tensile strength slightly increased from ca. 40 MPa for PLA to ca. 45 MPa for the PLA/CNF/PEG sample containing 1 wt% fibers.

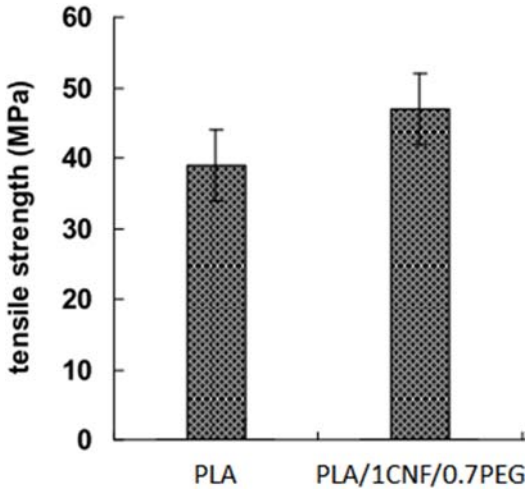

Figure 2.18: The results of tensile strength for various samples [44].

Lee et al. [49] incorporated a bio-derived polylactide carbohydrate copolymer (Co) to compatibilize PLA/BCNFs containing 5 wt% nanofibers. They added PLA, freeze-dried CNFs and the copolymer into 1,4-dioxane. The suspension was then immersed in liquid nitrogen and subsequently dried via freeze-drying prior to injection molding. Table 2.13 presents the results of DSC tests performed for different samples. The glass transition, melting, and crystallization temperatures of the matrix were reduced for the composite containing 5 wt% BCNFs with 4.75 wt% Co, while the crystalline content of PLA increased in that sample.

Table 2.13: DSC results of various samples [49].

Sample	T_g (°C)	T_m (°C)	T_c (°C)	$X_c^{heating}$ (%)
PLA	63 ± 3	171 ± 2	113 ± 2	18 ± 2
PLA/5BCNF/4.75Co	57 ± 2	166 ± 6	87 ± 3	28 ± 2

Table 2.14 reports the results of the Young modulus and tensile strength of the PLA/5BCNF/4.75Co composite, which are shown to be improved by 15 and 7%, respectively, compared to PLA. The elongation at break of PLA also slightly increased by incorporating 5 wt% BCNFs with 4.75 wt% Co (Table 2.14).

Table 2.14: Tensile properties of different samples [49].

Sample	Young's modulus (GPa)	Tensile strength (MPa)	Elongation at break (%)
PLA	4.08 ± 0.07	63.1 ± 2.0	1.7 ± 0.1
PLA/5BCNF/4.75Co	4.71 ± 0.13	67.4 ± 1.1	1.9 ± 0.1

Kiziltas et al. [61] incorporated polyhydroxybutyrate (PHB) in order to compatibilize PLA/CNF composites containing 1.25–5 wt% nanofibers. A masterbatch of CNF aqueous suspension and PHB was prepared in an internal batch mixer; however, the ratio of CNFs to PHB was not kept constant that makes the results inconclusive. Thereafter, PLA/CNF/PHB composites were prepared by melt mixing of PLA and the dried masterbatch. Figure 2.19 presents the results of rheology measurements for the samples. Even the composite containing the largest CNF content, i.e., 5 wt%, showed similar complex viscosity as the neat PLA, probably due to the lack of a CNF network and possible matrix degradation.

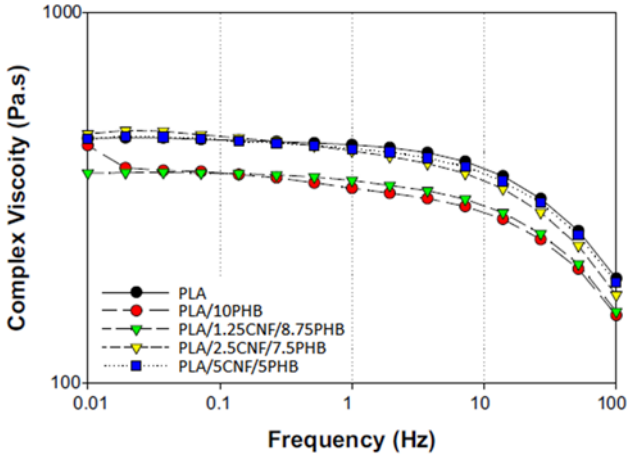

Figure 2.19: Complex viscosity vs frequency at 180 °C for different samples [61].

Table 2.15 reports the results of the Young modulus, tensile strength and elongation at break for various samples. The Young modulus remained unchanged for the compatibilized composite with 5 wt% CNFs and decreased for lower concentrations relative to that of the neat PLA; the tensile strength and elongation at break of PLA decreased by incorporating CNFs and PHB.

Table 2.15: The results of tensile tests for various samples [61].

Sample	Young's modulus (GPa)	Tensile strength (MPa)	Elongation at break (%)
PLA	2.98 ± 0.07	59.9 ± 1.3	2.40 ± 0.09
PLA/1.25CNF/8.75PHB	2.70 ± 0.01	44.8 ± 1.0	2.16 ± 0.02
PLA/2.5CNF/7.5PHB	2.79 ± 0.01	44.9 ± 1.3	2.52 ± 0.09
PLA/5CNF/5PHB	2.99 ± 0.05	43.2 ± 1.7	1.92 ± 0.03

Jonoobi et al. [62] prepared acetylated CNFs (A-CNFs) to improve the properties of PLA. The nanofibers were acetylated in acetic anhydride and 5 wt% pyridine as catalyst. Thereafter, a

masterbatch of PLA/A-CNF was prepared in a mixture of acetone and chloroform and, after drying, it was diluted with PLA by extrusion (as described earlier in [10]). Figure 2.20 presents the SEM micrographs of PLA and PLA/5A-CNF composites. They reported that the dispersion/distribution of modified nanofibers in the matrix (Figure 2.20 right) was similar to that of the unmodified composite (see Figure 2.9 right).

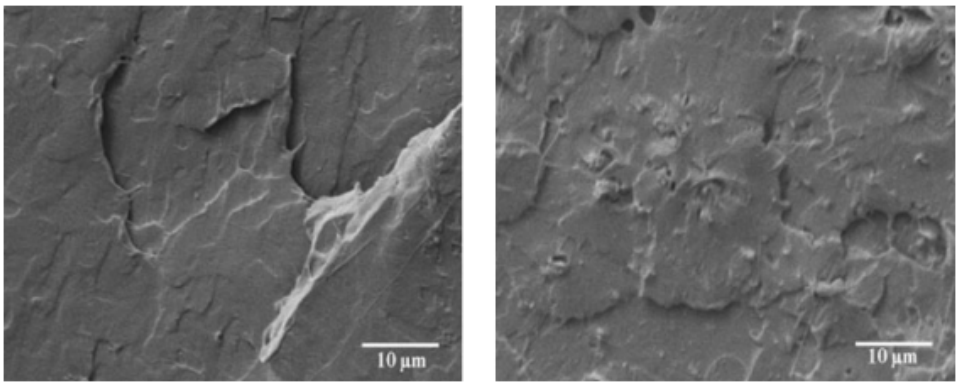

Figure 2.20: SEM micrographs of the fractured surface of PLA (left), and PLA/5A-CNF composite (right) [62].

Table 2.16 reports the Young modulus, tensile strength, and elongation at break for the neat PLA and its modified composite containing 5 wt% A-CNFs. The Young modulus and tensile strength were increased compared to the neat PLA; however, the enhancements were lower in comparison with the unmodified composite at similar content of CNFs, i.e., PLA/5CNF (see Table 2.4). As expected, the elongation at break of PLA decreased for the PLA/5A-CNF composite (Table 2.16).

Table 2.16: Tensile properties of PLA and PLA/5A-CNF [62].

Sample	Young's modulus (GPa)	Tensile strength (MPa)	Elongation at break (%)
PLA	2.9 ± 1.0	58 ± 0.5	3.4 ± 0.4
PLA/5A-CNF	3.5 ± 0.3	69 ± 0.6	2.9 ± 0.1

Frone et al. [8] investigated the influence of silane-modified CNFs on properties of PLA. To that end, a mixture of ethanol/water containing 3-aminopropyltriethoxysilane (APS) was added to a CNF aqueous suspension. Then, composites were prepared via melt mixing of dried modified CNFs with PLA using an internal mixer. Figure 2.21 shows AFM images of PLA and its compatibilized composite containing 2.5 wt% APS-modified CNFs (APS-CNFs). Better

dispersion/distribution of the APS-CNFs was observed in the matrix, as compared to the unmodified CNFs (see Figure 2.14).

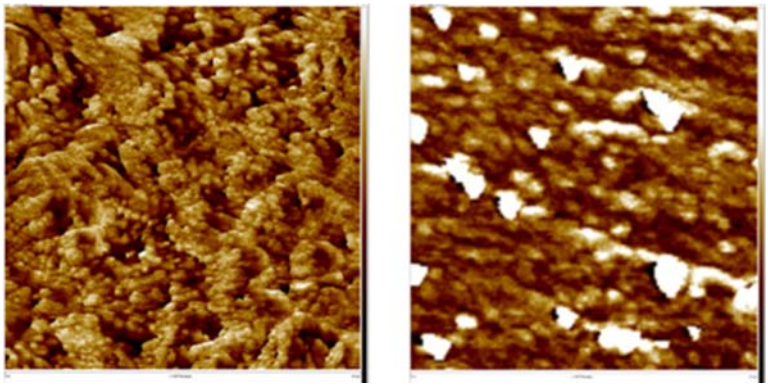

Figure 2.21: AFM modulus images of PLA (left), and PLA/2.5APS-CNF composite (right) at a scan size of 3 μm × 3 μm [8].

Table 2.17 reports the results of DSC test for PLA and PLA/2.5APS-CNF samples. The CNFs were reported to slightly increase the degree of crystallinity of PLA. However, that increase was more evident for the composite containing unmodified CNFs (see Table 2.8) compared to the composites with APS-CNFs. Moreover, for compatibilized composite, the CNFs did not act as nucleating agent; the crystallization temperature decreased and the cold-crystallization temperature increased. The glass transition and melting temperatures of PLA remained unchanged.

Table 2.17: DSC values for PLA and PLA/2.5APS-CNF samples [8].

Sample	T_g (°C)	T_{cc} (°C)	T_m (°C)	T_c (°C)	$X_c^{cooling}$ (%)
PLA	56.9	87.3	168.1	104.3	38.9
PLA/2.5APS-CNF	57.2	89.8	167.9	101.1	41.1

Frone et al. [19] also investigated the effect of 2.5 wt% silane-modified CMFs on PLA properties with the same processing procedure described in [8]. Table 2.18 reports the results of the storage modulus from DMTA measurements. The storage modulus at 25 °C increased by 18% for the composites containing 2.5 wt% APS-CMFs compared to that of PLA; however, the storage modulus of that composite at 80 °C decreased. Similar changes to those of the compatibilized composite were observed for the uncompatibilized composite, i.e., PLA/2CMF, relative to those of the neat PLA (see Table 2.9).

Table 2.18: Values of storage modulus at 25 and 80 °C extracted from DMTA [19].

Sample	Storage modulus at 25 °C (GPa)	Storage modulus at 80 °C (MPa)
PLA	3.4 ± 0.1	260 ± 10
PLA/2.5APS-CMF	4.0 ± 0.1	240 ± 10

2.7 PEO/cellulose biocomposites

To prepare PEO/BCNF composites, Brown and Laborie [54] incorporated PEO in a culture medium of *acetobacter xylinum* (used for BCNF culture) to achieve finely dispersed nanofibers in PEO. Table 2.19 reports the data regarding DSC tests. No change in the melting temperature of PEO and a decrease in the crystalline content (from 67% for PEO to 49% for the PEO/15BCNF composite) are observed.

Table 2.19: Melting temperature and crystalline content of PEO and PEO/15CNF [54].

Sample	T_m (°C)	$X_c^{heating}$ (%)
PEO	68 ± 1	67 ± 1
PEO/15CNF	68 ± 3	49 ± 6

Xu et al. [55] prepared PEO/CNF composite films by solution casting. A CNF hydrogel was mixed with a PEO solution, allowing PEO molecules to penetrate in the CNF network. The nanofibers used in that investigation had an average width of 20 ± 14 nm and length of 1030 ± 334 nm (aspect ratio greater than 52). Figure 2.22 presents a transmission electron microscopy (TEM) image of the CNFs.

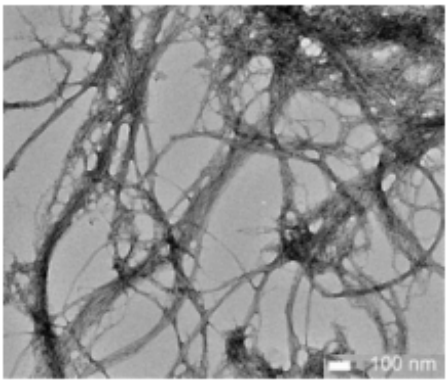

Figure 2.22: TEM image of CNFs [55].

Table 2.20 reports the melting temperature and crystalline content of PEO and PEO/CNF composites. A 4 °C decrease in the melting temperature and a small decrease in the crystalline content of PEO (from 82 to 79%) by adding 4 wt% CNFs are observed.

Table 2.20: DSC results of the neat PEO and PEO/CNF composites [55].

Sample	T_m (°C)	$X_c^{heating}$ (%)
PEO	71.2	82
PEO/1CNF	70.7	74
PEO/4CNF	66.8	79

The results of tensile tests, Young's modulus and yield strength, are reported in Table 2.21. A 31% enhancement in the Young modulus and a 46% improvement in the yield strength of PEO were reported in the presence of 4 wt% CNFs.

Table 2.21: The results of tensile tests for different PEO/CNF samples [55].

Sample	Young's modulus (MPa)	Yield strength (MPa)
PEO	760 ± 109	14.2 ± 0.9
PEO/1CNF	896 ± 99	17.7 ± 0.9
PEO/4CNF	994 ± 222	20.8 ± 0.7

Xu et al. [55] also prepared composites of PEO and CNCs of diameter of 19 ± 5 nm and 151 ± 39 nm in length (aspect ratio of 8), with the same nanoparticle loadings to investigate the effect of fiber size. Table 2.22 reports the results of DSC measurements for composites based on PEO and CNCs. Both melting temperature and crystalline content are lower for the composites, regardless of CNC content, compared to those of the PEO (see Table 2.20).

Table 2.22: DSC properties of PEO/CNC composites [55].

Sample	T_m (°C)	$X_c^{heating}$ (%)
PEO/1CNC	66.9	77
PEO/4CNC	66.8	78

Tensile tests were also performed for PEO/CNC composites and the data are reported in Table 2.23. The Young modulus and yield strength of PEO increase with the CNC content; however,

PEO/4CNC exhibits a similar Young's modulus as PEO/1CNF (see Table 2.21). This emphasizes the higher capacity of large-aspect ratio reinforcements, e.g. CNFs relative to CNCs, to improve the properties of polymer matrices.

Table 2.23: Results of tensile tests for different PEO/CNC samples [55].

Sample	Young's modulus (MPa)	Yield strength (MPa)
PEO/1CNC	820 ± 195	15.9 ± 0.1
PEO/4CNC	895 ± 141	16.0 ± 0.8

2.8 Summary

Various approaches to try to disperse/distribute cellulosic reinforcements within the hydrophobic and hydrophilic matrices of PLA and PEO, respectively, and improve their thermomechanical properties have been reported. Also, compatibilization for the case of PLA/cellulose composites has been discussed. Not all the investigations were successful in preparing high-performance composites with low cellulose loadings, i.e., 1–5 wt%. Moreover, modification/compatibilization efforts to improve the properties of PLA/CNF composites were not completely successful. On the other hand, the effects of CNFs and their network structure on the rheological, thermomechanical, and optical properties of PLA/CNF and PEO/CNF systems have not been thoroughly investigated. Hence, the focus of this investigation is to explore the potential use of CNFs to enhance the properties of the two thermoplastics, i.e., PLA and PEO; it also attempts to employ rheology to investigate the effect of CNFs on the behavior of PLA and PEO in the molten state. CNFs are chosen in view of their superior characteristics, e.g. large aspect ratio and surface area, which may lead to higher property enhancement, if dispersed/distributed well in the host polymer matrices, compared to other types of cellulosic reinforcements from nanometer to micron size such as CNCs, CMFs, MFC, flax fibers, etc. On the other hand, the preparation of CNFs is much easier and safer and, definitely, more cost effective compared to CNCs, as it does not include an acid hydrolysis step. Moreover, in this dissertation the use of a compatibilizer, i.e., PEG, with the aim of preparing PLA/CNF composites with improved dispersion/distribution and properties is investigated. The next chapter is dedicated to the statement of the main and specific objectives of this work.

CHAPTER 3 OBJECTIVES

Taking into account the importance of the use of renewable and bio-based alternatives to petroleum-based components in order to reduce dependency on fossil fuels and decrease ecological footprints, the main objective of this thesis is **to develop high-performance polymer biocomposites reinforced with cellulose nanofibers (CNFs)**.

To achieve the main objective, two thermoplastic polymer matrices are used: polylactide (PLA) and poly(ethylene oxide) (PEO), and the specific objectives are defined as:

1. To enhance the thermomechanical properties, e.g. heat resistance and crystallinity, of PLA by incorporating CNFs without using a compatibilizer.
2. To improve the thermomechanical properties, e.g. modulus and strength, of PEO by the addition of CNFs, comparing solution and melt preparation methods.
3. To further enhance the dispersion/distribution of nanofibers in PLA/CNF composites in the presence of a miscible compatibilizer, i.e., poly(ethylene glycol) (PEG). Two different preparation methods, solution and melt, to develop PLA/CNF/PEG biocomposites with improved thermal and mechanical properties are studied.

CHAPTER 4 ORGANIZATION OF THE ARTICLES

The main results from this research project are presented in the form of three scientific papers in the following chapters, 5, 6 and 7:

Chapter 5 presents the paper "*Rheological, mechanical, and thermal properties of polylactide/cellulose nanofiber biocomposites*" that has been published in *Polymer Composites*, 2015 impact factor: 2.0 (DOI 10.1002/pc.24127).

This chapter reports the development of polylactide (PLA)/cellulose nanofiber (CNF) biocomposites via a solution technique that results in well dispersed/distributed CNFs without the use of a compatibilizer. The biocomposites are characterized in terms of morphology and rheological, mechanical, thermal, and optical properties to investigate the effects of the CNFs on different properties of PLA.

Chapter 6 reports the paper "*Enhanced properties of poly(ethylene oxide)/cellulose nanofiber biocomposites*" that has been published in *Cellulose*, 2015 impact factor: 3.2 (DOI 10.1007/s10570-016-1137-1).

The preparation of poly(ethylene oxide) (PEO)/CNF biocomposites using a simple aqueous solution method is investigated to disperse/distribute nanofibers in PEO. This chapter also compares the efficiency of two different preparation methods, i.e., solution and melt, on PEO/CNF composite properties. The effects of the CNFs on rheological, mechanical, thermal, and optical properties of PEO are studied, as well.

The better dispersion of CNFs in PEO (Chapter 6) compared to PLA (Chapter 5) inspired us to study the use of poly(ethylene glycol) (PEG), a low molecular weight PEO, as a miscible compatibilizer in PLA/CNF system. Hence, Chapter 7 presents the paper entitled "*Effects of poly(ethylene glycol) on the morphology and properties of biocomposites based on polylactide and cellulose nanofibers*" that has been accepted in *Cellulose*.

This chapter aims at further dispersing/distributing the nanofibers in the PLA/CNF composites from Chapter 5 using PEG in order to promote the thermomechanical properties of PLA. A masterbatch of PEG and CNFs is prepared via a simple aqueous solution technique, and, two different preparation methods, i.e., solution and melt, are employed to prepare the biocomposites.

Then, the effects of PEG-compatibilized CNFs on the morphological, rheological, thermal, mechanical, and optical properties of PLA/CNF composites are studied.

CHAPTER 5 ARTICLE 1 : RHEOLOGICAL, MECHANICAL, AND THERMAL PROPERTIES OF POLYLACTIDE/CELLULOSE NANOFIBER BIOCOMPOSITES[1]

Fatemeh Safdari[a], Davood Bagheriasl[a], Pierre J. Carreau[a*], Marie C. Heuzey[a], Musa R. Kamal[b]

[a] *Research Center for High Performance Polymer and Composite Systems (CREPEC), Chemical Engineering Department, Polytechnique Montreal, Montreal, Quebec H3C 3A7, Canada*

[b] *CREPEC, Chemical Engineering Department, McGill University, Montreal, Quebec H3A 0C5, Canada*

Parts of this chapter have been published in:

- *SPE Plastics Research Online*; DOI 10.2417/spepro.006650

and presented at the:

- *NIPMMP Annual Conference*, Montreal, Canada (May 2015), winner of the "*First Prize Award*" in poster competition
- *CREPEC Student Conference*, Montreal, Canada (June 2015)

[1] Published in *Polymer Composites*; DOI 10.1002/pc.24127.

5.1 Abstract

Biocomposites based on polylactide (PLA) and cellulose nanofibers (CNFs) were prepared via a solution method. The effects of CNFs on rheological, mechanical, thermal, and optical properties of PLA were investigated. Scanning electron microscopy showed that the CNFs were fairly dispersed/distributed in the PLA. Significant increases in the rheological properties of PLA/CNF composites and a remarkable shear-thinning behavior were observed. Also, apparent yield stress and a transition from liquid- to solid-like behavior indicated a strong 3D network of CNFs. At room temperature, the storage and Young's moduli were increased by 50% for the composite containing 5 wt% CNFs as compared to the neat PLA, whereas the tensile strength was increased up to 31%. The Krenchel model was shown to predict well the Young modulus for lower concentrations of CNFs. Moreover, relative to the neat PLA the storage modulus in flexion at 70 °C increased by 264% for PLA containing 5 wt% CNFs. Increased crystalline content and a positive shift of the crystallization temperature by incorporating the CNFs in PLA were observed. Also, good light transparency was retained for these PLA/CNF biocomposites. These results show that the preparation method employed in this work leads to PLA/CNF composites with considerably enhanced properties.

5.2 Introduction

The use of bio-based materials has been the focus of many studies as a result of their biodegradability and renewability of their sources, which cause less harmful environmental impacts. Among different biopolymers, polylactide (PLA) has already found applications in tissue engineering, medical, textile, automotive and packaging industries, for example as water/milk bottles and degradable plastic bags, by employing various industrial processing techniques similar to those used for polyolefins (i.e., extrusion, injection molding, film blowing and blow molding) [1-7]. However, neat PLA exhibits slow crystallization and low heat resistance (low storage modulus at high temperature) and thermal stability [7] which limit its use in some applications. To overcome these challenges, one solution is the addition of reinforcements to improve the mechanical and thermal behavior of PLA, while maintaining its unique properties such as biocompatibility, biodegradability and transparency.

Among the different reinforcements, cellulose nanofibers (CNFs) have attracted considerable interest as potential reinforcement material for applications in automotive, construction, electronics, cosmetics, medical fields and food packaging [3, 8-11]. The excellent properties of CNFs, in particular their high modulus and strength, large surface area, high aspect ratio, abundance in nature, renewability, nontoxicity, biocompatibility, biodegradability, low cost, low density, non-abrasiveness to the processing equipment and the possibility to be incinerated while keeping CO_2 neutrality make them a good alternative to inorganic fillers such as carbon nanotubes, nanoclays, glass fibers and carbon fibers [2, 3, 5-15]. Thus, PLA/CNF should be preferable over other PLA/reinforcement systems, due to the entirely bio-based content of the final composites [7, 8, 15].

However, CNFs can form very strong particle–particle interactions due to their length, flexibility and strong hydrogen bonds. Therefore, agglomerates are likely to form and obtaining a uniform dispersion is challenging, especially when CNFs are incorporated in a nonpolar polymer matrix [2-5, 8, 11, 12, 14]. Good dispersion with minor agglomeration may be obtained by using a solvent, in which the CNFs are initially well dispersed; then, the polymer is added and finally the mixture is dried [5, 7, 8, 15]. In some cases, the product of this step might be mixed [7, 8] or diluted with the same or another polymer [5, 15] via a melt mixing process. However, finding an appropriate solvent remains a challenging issue when the polymer matrix is not hydrosoluble, mainly because of different polarities between the fibers and the matrix. In some cases, solvent exchange [5, 7] is required to obtain a uniform dispersion of the CNFs, which makes the preparation process even more tedious. Another method that can be used to favor good dispersion of CNFs within nonpolar polymer matrices is chemical modification to lower the hydrophilicity of the CNFs, which is also mainly conducted in solution. After drying, the modified CNFs can be directly mixed with the polymer in the molten state using an internal mixer or extruder [2, 4, 12]. However, modified CNFs may still have a tendency to agglomerate during the drying step. Thus, it would be difficult to re-disperse them within the polymer in the molten state.

The few attempts to prepare PLA/CNF composites with enhanced properties at low CNF loadings were not highly successful. Iwatake et al. [8] prepared PLA reinforced with micro-fibrillated cellulose (MFC) via a solution preparation method using acetone. The suspensions were dried and finally the samples were kneaded in the molten state. For the sake of comparison one sample was prepared by direct melt mixing. Uniform dispersion was observed for the solution-based sample,

while agglomerates persisted in the latter case. The mechanical properties of PLA were deteriorated for the melt-prepared sample, whereas they improved by 38% for the Young modulus and 33% for the tensile strength for solution-based samples with the addition of MFC up to 10 wt%, but for larger concentrations they decreased. Suryanegara et al. [7] incorporated up to 20 wt% of MFC into PLA using a solution method with dichloromethane, followed by drying and kneading in the molten state. The maximum enhancements were obtained at the highest MFC concentration: the Young modulus and tensile strength increased by ca. 42 and 14%, respectively; storage modulus at 20 and 80 °C improved by 37 and 220%, respectively, relative to those of the PLA. Jonoobi et al. [5] developed PLA/CNF composites via a masterbatch preparation in a mixture of acetone and chloroform. The resulting masterbatch, after drying and grinding, was diluted with PLA using a twin-screw extruder. Large agglomerates were observed in thin films of the resulting composites. The Young modulus and tensile strength of PLA increased by 24 and 21%, respectively, by incorporating 5 wt% CNFs. Kowalczyk et al. [15] employed a solution-based method in dichloromethane followed by melt mixing to prepare PLA/CNF composites containing 2 wt% nanofibers. Good dispersion of the CNFs within the PLA matrix was obtained. Slight increases in the storage modulus at 20 °C (14%) and the tensile strength at 25 °C (5%) were observed. Moreover, the CNFs did not show a nucleation effect. Wang and Sain [12] tried to modify hemp nanofibers (HPNs) by adding styrene maleic anhydride copolymer (SMA) to the fibers in aqueous suspension. After freeze-drying, the unmodified and modified fibers were used to prepare composites containing 5 wt% fibers using an internal mixer in the molten state. SMA reduced the entanglements of the nanofibers. However, the modified nanofibers were not uniformly dispersed in the PLA matrix and the presence of agglomerates was reported. The Young modulus and tensile strength increased slightly for PLA containing 5 wt% SMA-modified HPNs (SMA-HPNs), 10 and 9%, respectively, and the enhancement was lower for the unmodified composite. Frone et al. [2, 4] investigated the influence of silane-modified CNFs on properties of PLA. To this end, a mixture of ethanol/water containing 3-aminopropyltriethoxysilane (APS) was added to CNF aqueous suspension. Then, the composites were produced via melt mixing of dried modified and unmodified CNFs with PLA in an internal mixer. Better dispersion/distribution of the APS-modified CNFs (APS-CNFs) was observed in the matrix, as compared to the unmodified CNFs. The CNFs were reported to act as nucleating agents and a higher degree of crystallinity was achieved for the PLA containing unmodified CNFs compared to the composites with APS-CNFs [2]. The storage

modulus at 25 °C increased by 18% for both composites containing 2.5 wt% modified and unmodified fibers compared to that of PLA; however, the storage modulus at 80 °C decreased for both composites [4].

In the present work, a solution-based method was employed to produce PLA/CNF composites with the objective of achieving a uniform dispersion and, consequently, enhanced properties at low CNF loadings. Then, the effects of the CNFs on rheological and mechanical properties, transparency, crystallization, thermal stability and heat resistance of the PLA were investigated. Also, the Young modulus data were compared with predictions of the modified Halpin-Tsai and Krenchel models. The results from this study stress the substantial reinforcing potential of CNFs that could be imparted to PLA. This would enhance and extend applications of PLA, where slow crystallization, low heat resistance and thermal stability have raised challenges (e.g. in film blowing and blow molding). Moreover, good dispersion of CNFs within PLA can provide similar transparency to that of the neat matrix, which is favorable for many applications especially in optical [16-18] and optoelectronics [10, 17, 19], where several common nanofillers (e.g. carbon nanotubes and nanoclays) cannot be used because of the lack of transparency in the resulting composites.

5.3 Experimental section

5.3.1 Materials

A commercial grade polylactide (PLA) (Ingeo Biopolymer 3251D, NatureWorks, Minnetonka, MN, USA) with MFI of 35 g/10 min (190 °C/2.16 kg) and melting point of 155–170 °C was used as the matrix. N,N-dimethylformamide (DMF), anhydrous 99.8% (Sigma-Aldrich Canada Co., Oakville, ON, Canada) was used as received. The cellulose nanofiber (CNF) aqueous suspension (2.3 wt%) was kindly provided by the University of Toronto (Toronto, ON, Canada). The CNFs have a diameter smaller than 50 nm and their length is around several micrometers [18].

5.3.2 Sample preparation

The composite samples were produced via a solution mixing method. The CNF aqueous suspension was dried using a freeze-dryer (Labconco Freezone 2.5^{Plus}) for 48 h. The freeze-dried CNFs (0.1–2 g) were dispersed in 200 mL DMF using a water-bath sonicator (FS30 100 Watts Ultrasonic Cleaner, Fisher Scientific, Pittsburgh, PA, USA) for 1 h and, then, stirred with a magnetic stirrer

at 400 rpm for 1 more hour. The desired amount of PLA, dried at 80 °C for 24 h under vacuum, was added to the suspension and heated up to 70 °C while stirring at 400 rpm for 2 h until complete dissolution of the PLA pellets. Finally, the mixture was dried in a vacuum oven at 80 °C for 24 h. The product was then ground into small granules using a laboratory grinder (Janke & Kunkel A10S1 model, IKA WERK, Germany) and kept in a vacuum oven at 60 °C for 48 h. For the sake of comparison, the same procedure was used for the neat PLA sample. Thereafter, the samples were compression molded in a hot Carver press (12 Ton Manual Hydraulic Press, Carver, Inc., Wabash, IN, USA) for 10 min at 175 °C in the presence of nitrogen to prepare the test specimens. For film preparation, a desired amount of material for each sample was placed between two rectangular metal plaques without the use of any mold. The pressure was increased gradually from 0 to 29 kPa. After compression molding, the samples were cooled in the press at ambient temperature for 5 min under a 29 kPa load and, then, stored in a desiccator before subsequent testing. The composites containing nanofibers were coded according to their fiber content on weight percentage basis (0.25–5 wt%). For instance, PLA/0.25CNF denotes composite with 0.25 wt% CNFs, based on total weight of the composite.

5.3.3 Characterization

5.3.3.1 Microscopy

Scanning electron microscopy (SEM) was carried out on ultra-microtomed surfaces, coated with platinum. The microscope was a JEOL JSM 7600TFE instrument (JEOL USA, Inc., Peabody, MA, USA) operated at a voltage of 2 kV.

5.3.3.2 Rheology

The rheological properties of PLA and the corresponding composites were measured using a stress-controlled Anton Paar MCR 301 rheometer (Anton Paar, Austria) on disks of 25 mm diameter and 1 mm thickness. The experiments were conducted at 175 °C under nitrogen to avoid degradation of the samples. A cone-and-plate geometry was used with a cone truncation of 0.051 mm, cone angle of ca. 2° and a plate diameter of 25 mm. Measurements were performed in oscillatory mode in the linear viscoelastic region. To examine the thermal stability of the samples, time sweep tests were carried out at a frequency of 1 rad/s for 15 min. Frequency sweeps at a strain amplitude of 5% were conducted over 15 min.

5.3.3.3 Mechanical and thermal properties

Tensile properties of dog-bone shape type V (length of 63.5 mm, width of 9.5 mm and 1.6 mm thick) specimens of the samples were measured using an Instron 3365 (Instron, Norwood, MA, USA) at room temperature, according to standard ASTM D638 with a crosshead speed of 5 mm/min and a load cell of 5 kN. For each sample, a minimum of seven specimens were tested.

Dynamic mechanical thermal analysis (DMTA) was performed using a DMA 2980 analyzer (TA Instruments, New Castle, DE, USA). The specimens, bars 1.6 mm thick, 12.2 mm wide and 60.5 mm long, were tested in the dual cantilever bending (flexion) mode at an amplitude of 30 μm, a frequency of 1 Hz and a heating rate of 2 °C/min from room temperature to 120 °C. A minimum of three replicates for each sample were tested.

Differential scanning calorimetry (DSC) was performed on PLA and the composites using a DSC Q1000 (TA Instruments, New Castle, DE, USA) on typically 10 mg samples, under a nitrogen atmosphere. The samples were heated from room temperature to 200 °C at a constant rate of 2 °C/min and held at that temperature for 3 min, then cooled to 20 °C with the same rate. The DSC tests were performed twice for each sample with a fresh specimen.

Thermogravimetric analysis (TGA) was performed using a TGA Q500 (TA Instruments, New Castle, DE, USA). The measurements were carried out in high-resolution mode at a heating rate of 10 °C/min from room temperature to 800 °C in a nitrogen atmosphere with a flow rate of 60 mL/min. The sample weight was approximately 15 mg and the test was performed twice for each sample.

5.3.3.4 Optical properties

Light transmittance of the various samples was determined quantitatively on corresponding 30 × 30 mm^2 films with an average thickness of 102 ± 6 μm, using a LAMBDA 1050 UV/Vis/NIR Spectrophotometers (PerkinElmer, Waltham, MA, USA) with 150 mm InGaAs Int.Sphere. The wavelength was varied between 250 and 800 nm with a scanning rate of 141 nm/min and a spectral bandwidth of 5 nm. Three replicates for each sample were characterized.

5.4 Results and discussion

5.4.1 Scanning electron microscopy (SEM)

Figure 5.1 presents SEM micrographs of the freeze-dried CNF aqueous suspension (0.1 wt%) and PLA containing 2 wt% CNFs. Figure 5.1a depicts a 3D entangled structure of individual and bundles of CNFs even when they are dispersed in water, which is known as the preferred medium to disperse the CNFs [20]. The SEM micrograph of PLA/2CNF, presented in Figure 5.1b, shows fair dispersion and distribution of the CNFs in the PLA matrix. Considering the lower affinity of the CNFs with PLA in comparison with water, the presence of some bundles of fibers in PLA/2CNF was expected. The good dispersion and distribution of the CNFs for PLA/CNF composites can be ascribed to the efficiency of the solution preparation method employed in the present work.

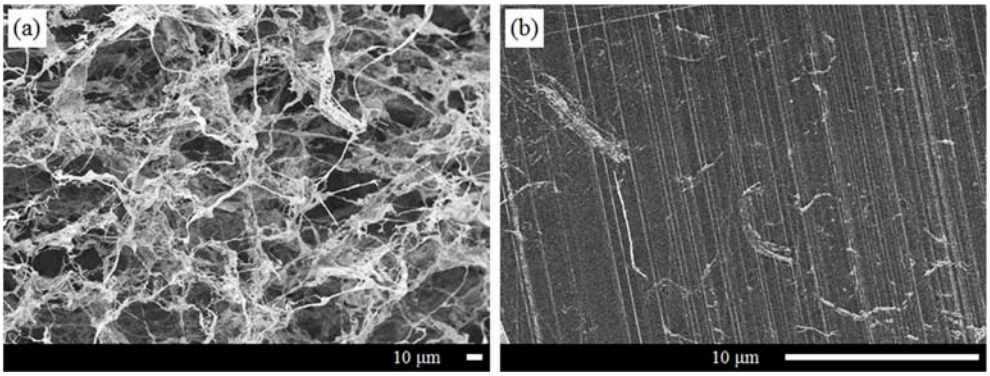

Figure 5.1: SEM micrographs of (a) freeze-dried CNF aqueous suspension (0.1 wt%) and (b) PLA/2CNF.

5.4.2 Rheology

Rheology has been used to investigate the quality of the dispersion and distribution of CNFs within the PLA. All the samples exhibited stable rheological properties in time-sweep tests, with changes less than 7% in the time limit of the experiments (15 min). Figure 5.2 presents the complex viscosity, η^*, and storage modulus, G', as functions of the frequency, ω, for all samples. The PLA exhibits a plateau with a slight shear-thinning behavior at high frequencies for the complex viscosity (Figure 5.2a), and a terminal zone with a slope of 2 on the plot of G' versus ω (Figure 5.2b), which is the typical behavior of molten polymers. By the incorporation of CNFs, the plateau

region of η^* disappears and shear-thinning is observed for the composites, mainly at low frequencies (Figure 5.2a). Also, the frequency dependency of G' becomes very weak at high loadings (Figure 5.2b). Large increases up to two orders of magnitude for the η^* and five orders of magnitude for the G' of the composites are observed, mainly at low frequencies in comparison with the neat PLA (extrapolating the G' data for the PLA). This suggests the presence of a strong CNF network attributed to their good dispersion/distribution in the PLA matrix, which results in a transition from liquid- to solid-like behavior, with a viscosity upturn and a plateau in G' at low frequencies, indicative of an apparent yield stress.

The apparent yield stress, σ_y, can also be quantified by using the modified Carreau-Yasuda model [21]:

$$\eta^* = \sigma_y/\omega + \eta_0(1 + (\lambda\omega)^a)^{(n-1/a)} \qquad (5.1)$$

where η_0 is zero shear viscosity, λ is time constant, n is the flow index and a is Yasuda parameter. The fits of the modified Carreau-Yasuda model are represented by the solid lines in Figure 5.2a, and Table 5.1 presents the parameters of the modified Carreau-Yasuda model. The model is shown to fit very well the data for all samples. It is difficult to justify the variations of all these five parameters with the CNF concentration, but as expected the apparent yield stress increases drastically with the CNF content while n decreases, characteristic of more shear-thinning behavior. Also, large increases in zero-shear viscosity of the composites are observed compared to the PLA, especially in the presence of higher contents of CNFs, i.e., 1–5 wt%. Furthermore, the time constant, λ, significantly increases with the incorporation of CNFs. These are the results of stronger CNF–CNF and/or polymer–CNF interactions and, consequently, more restriction to PLA chain mobility. However, for the composites containing 0.25 and 0.5 wt% CNFs, the predicted apparent yield stresses are negligible. Therefore, the rheological percolation threshold is estimated to occur at a CNF concentration between 0.5 and 1 wt%. Similar rheological behavior has been reported for other polymer composites containing organoclays [22, 23], carbon nanotubes [24] and cellulose nanocrystals [21, 25, 26].

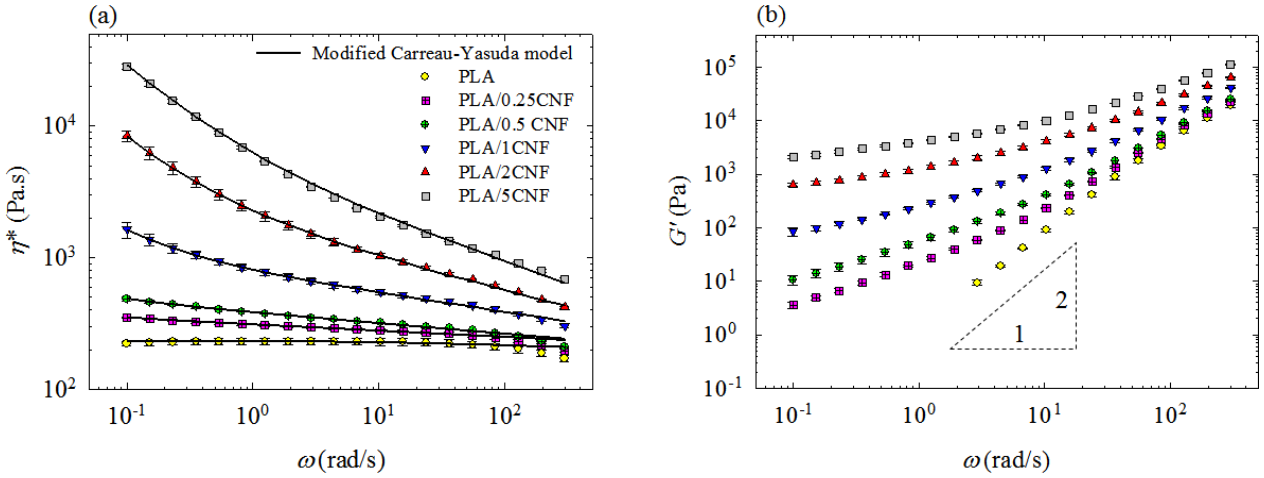

Figure 5.2: Complex viscosity (a) and storage modulus (b) vs frequency for PLA and PLA/CNF composites at 175 °C and strain amplitude of 5%. The fits of the modified Carreau-Yasuda model, Eq. 5.1, are shown by the solid lines in (a).

Table 5.1: Parameters of the modified Carreau-Yasuda model, Eq. 5.1.

Sample	n	σ_y (Pa)	λ (s)	η_0 (Pa.s)	a
PLA	0.97	0.00	0.100	232	0.99
PLA/0.25CNF	0.95	1.00	321	417	0.36
PLA/0.5CNF	0.92	3.00	405	617	0.75
PLA/1CNF	0.85	58.0	539	1890	0.94
PLA/2CNF	0.75	531	777	9170	0.87
PLA/5CNF	0.66	1990	963	43600	0.78

5.4.3 Tensile properties

Figure 5.3 presents typical stress-strain curves for different samples and the normalized values of the Young modulus, E/E_m, tensile strength, σ/σ_m, and elongation at break, $\varepsilon/\varepsilon_m$, where subscript m refers to the matrix (PLA), are reported in Figure 5.4. The composite samples present a brittle behavior, similar to the PLA. The Young modulus and tensile strength significantly increase with the CNF content, but the elongation at break decreases (Figure 5.3). The Young modulus of PLA is raised from 2.96 to 4.44 GPa with the addition of 5 wt% CNFs, which corresponds to a 50% increase (Figure 5.4a). Similarly, the tensile strength of PLA (66.3 MPa) is increased by 31% for

PLA/5CNF (Figure 5.4b), possibly due to good interactions between PLA and CNFs, which enhances the stress transfer from the matrix to the fibers when a load is applied [5, 27]. Also, the presence of a strong CNF network is beneficial for load transfer from a fiber to another. Smaller improvements of the mechanical properties of PLA reinforced with cellulosic fibers were reported by other investigators. Kowalczyk et al. [15] obtained an increase of 5% in the tensile strength of PLA in the presence of 2 wt% of CNFs. The Young modulus and tensile strength increased by 10 and 9%, respectively, in comparison with the matrix for PLA containing 5 wt% SMA-HPNs in the work of Wang and Sain [12]; the enhancement was less for the sample containing 5 wt% unmodified CNFs. Jonoobi et al. [5] obtained 24% improvement for the Young modulus and 21% for the tensile strength of PLA containing 5 wt% CNFs compared to those of PLA. For a PLA/10MFC composite, Iwatake et al. [8] reported 38 and 33% increases in the Young modulus and tensile strength of PLA, respectively. However, no improvement for PLA/3MFC was achieved. In another investigation, the addition of 20 wt% MFC increased the tensile modulus and strength of PLA by 42 and 14%, respectively [7].

Figure 5.4c presents the normalized values of elongation at break for the PLA and PLA/CNF composites. The elongation at break of PLA is 4% and decreases down to ca. 50% when the largest content of CNFs is added, which is generally the case for composite materials, due to the reduction of chain mobility caused by the fillers [28]. Similar results for elongation at break have been reported in the case of PLA reinforced with cellulosic fibers [5, 7, 8, 15].

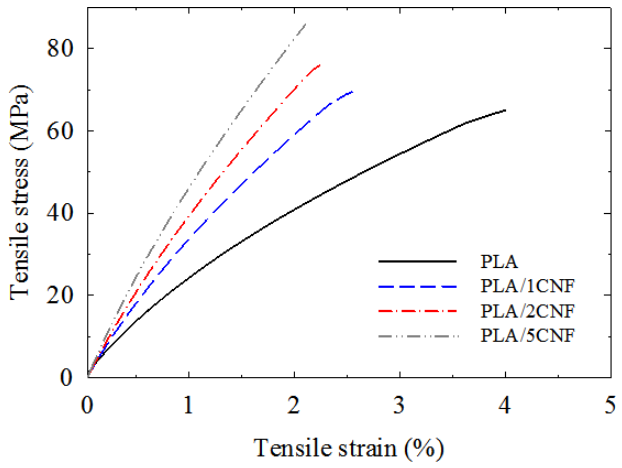

Figure 5.3: Typical stress-strain curves behavior for different samples.

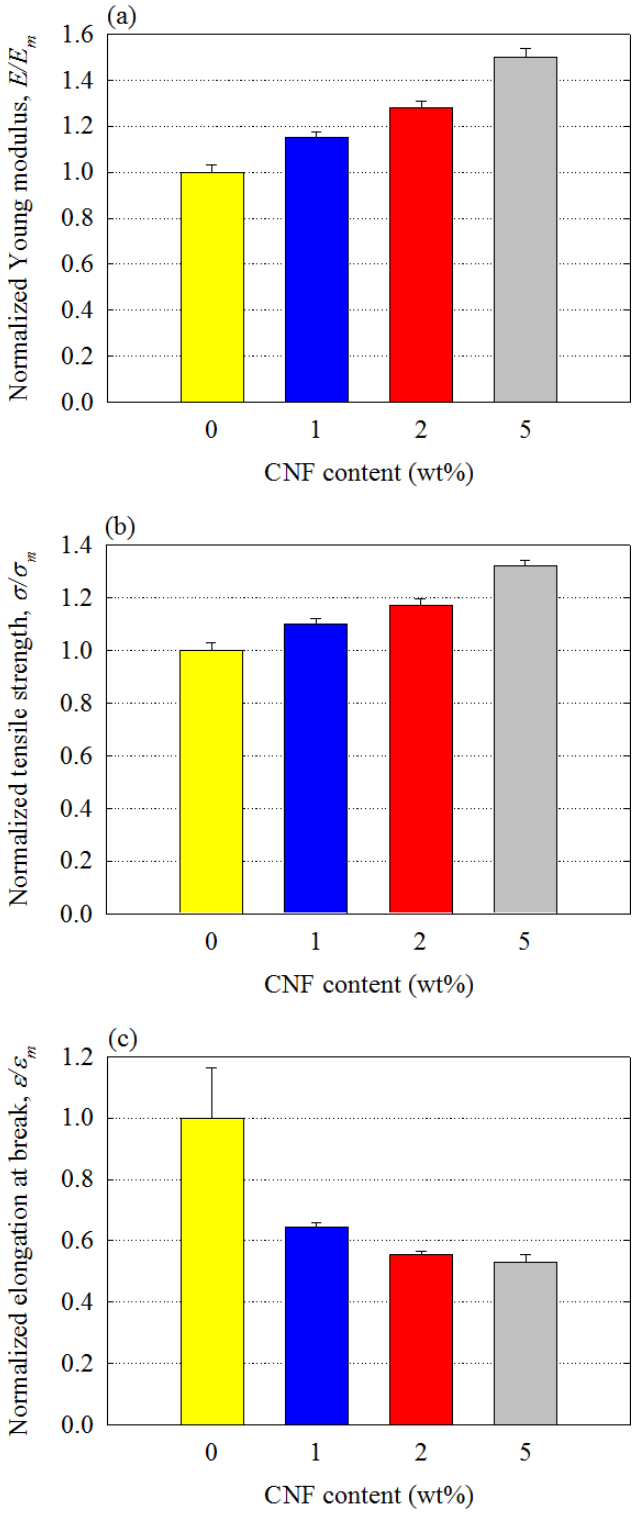

Figure 5.4: Normalized values of the Young modulus (a), tensile strength (b) and elongation at break (c) of the PLA and its composites with different CNF contents.

The Young modulus of fiber-reinforced composites, E, can be described by models developed by Halpin-Tsai [29, 30] and Krenchel [5]. For fibers with length l and diameter d, the modulus of a composite, E, based on the modified Halpin-Tsai model is given by [29]

$$E = E_m(1 + \xi\Psi\varphi_f)/(1 - \Psi\varphi_f) \qquad (5.2)$$

with

$$\Psi = (\alpha E_f/E_m - 1)/(\alpha E_f/E_m + \xi) \qquad (5.3)$$

where E_m and E_f are the Young moduli of the matrix and the fibers, respectively, $\xi = 2l/d$ is a shape parameter, φ_f is the fiber volume fraction and α is the orientation factor, which is equal to 1/3 for planar random orientation.

For 3D random orientation of fibers, the modified Halpin-Tsai model is expressed by [30]:

$$\frac{E}{E_m} = \frac{3}{8}\left[\frac{1+\xi\Psi_L\varphi_f}{1-\Psi_L\varphi_f}\right] + \frac{5}{8}\left[\frac{1+2\Psi_T\varphi_f}{1-\Psi_T\varphi_f}\right] \qquad (5.4)$$

where

$$\Psi_L = (E_f/E_m - 1)/(E_f/E_m + \xi) \qquad (5.5)$$

and

$$\Psi_T = (E_f/E_m - 1)/(E_f/E_m + 2) \qquad (5.6)$$

Another model that has also been used for carbon nanotube and CNF composites is the Krenchel model [5]:

$$E = E_m\left(1 - \varphi_f\right) + \Psi_l\Psi_o E_f\varphi_f \qquad (5.7)$$

where the orientation factor, Ψ_o, is equal to 3/8 under the assumption of planar random orientation and Ψ_l is the length factor, which can be calculated from

$$\Psi_l = 1 - (\tan h(\beta l/2)/(\beta l/2)) \qquad (5.8)$$

with

$$\beta = 1/r\,(E_m/2E_f\,\ln(R/r))^{1/2} \qquad (5.9)$$

where r is the fiber radius and R/r is taken to be $(K_r/\varphi_f)^{1/2}$, with K_r equals $\pi/4$ for square packing of fibers.

For the calculation of E, the following values were considered: E_m = 2.96 GPa, E_f = 150 GPa [31], ρ_m = 1.25 g/cm^3, ρ_f = 1.58 g/cm^3 [5, 12], d = 50 nm [18], and l is ca. 20 µm. The predictions of the modified Halpin-Tsai and Krenchel models are compared with experimental data in Figure 5.5. Reasonable agreement between the predictions (mainly those of the Krenchel model) and experimental data is observed for the composites containing 1 and 2 wt% CNFs. The lower experimental value for PLA/5CNF compared to the predictions is probably due to the presence of more bundles of fibers [5] than the two other composites, and the decrease in crystalline content of PLA in the presence of CNFs, which are not accounted for by the models. It is worth mentioning that negligible differences (less than 3%) in the predictions of the models were calculated for shorter CNF lengths, from 20 µm down to a value of 5 µm. These calculations were done to verify that a possible size reduction of the nanofibers due to grinding of the samples could not significantly affect the model predictions.

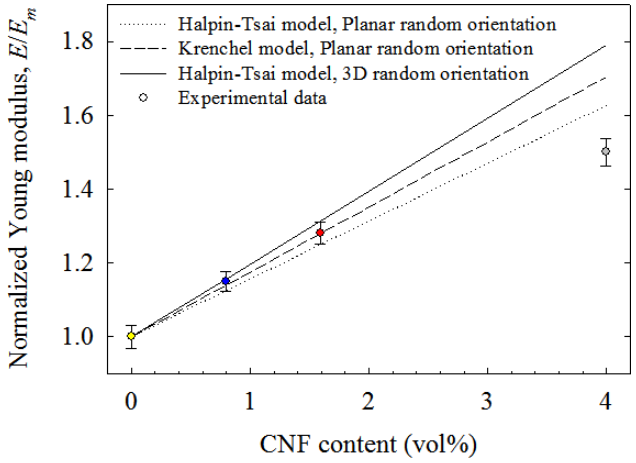

Figure 5.5: Comparison of the experimental data of the normalized Young's modulus of the PLA/CNF composites and predictions of the modified Halpin-Tsai and Krenchel models, Eqs. 5.2, 5.4 and 5.7, respectively.

5.4.4 Dynamic mechanical thermal analysis (DMTA)

Figure 5.6 presents the storage modulus in flexion, E', and loss tangent, $\tan\delta$ where δ is the phase angle, for the PLA and PLA/CNF composites over a wide range of temperatures. For all samples,

above the glass transition temperature the storage modulus increases until reaches a constant value at higher temperatures. These increases are explained by cold crystallization of PLA that occurred during the test. Similar results have been reported in other investigations [28, 32]. The storage modulus of PLA increases in both glassy and rubbery regions with the incorporation of the CNFs; larger increases are observed at higher CNF contents (Figure 5.6a). The $\tan\delta$ peak, which corresponds to the glass transition temperature, T_g, of the samples is shifted to higher temperatures with increasing CNF content (Figure 5.6b). The values of T_g for the different samples are reported in Table 5.2. The peak for PLA occurs at 59 °C and increases to 64 °C for the composite containing 5 wt% CNFs. Additionally, Figure 5.6b shows that the area under the $\tan\delta$ peak of PLA decreases with the incorporation of nanofibers and this decrease is larger for higher CNF contents. The normalized area under the $\tan\delta$ peak decreases from 1, for PLA, to 0.62 for the composite sample containing 5 wt% CNFs. This indicates that the PLA chains are restricted by the nanofibers, due to good dispersion of the fibers that leads to a large interfacial area and suppresses the energy dissipated by the segmental motion of the PLA chains in this transition. We ascribe the increase in modulus, together with the positive shift in T_g and the smaller area under $\tan\delta$ peak compared to those of the neat PLA, to interactions/restrictions caused by the incorporation of the CNFs [33]. Similar results were obtained by Jonoobi et al. [5]; however, in other investigations, T_g was not affected by the presence of the CNFs [4, 15].

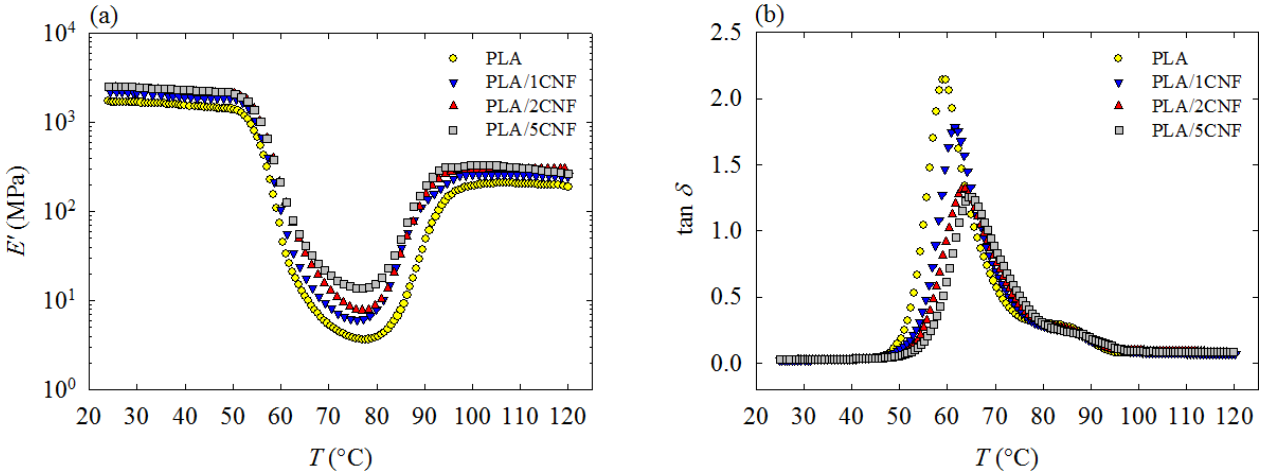

Figure 5.6: Storage modulus in flexion (a) and $\tan\delta$ (b) of the PLA and its composites.

Figure 5.7 compares the normalized storage modulus in flexion, E'/E'_m, at 25 and 70 °C for all samples. Significant improvement is observed by incorporating the CNFs into PLA, particularly at temperatures higher than T_g, here at 70 °C, due to the good dispersion and strong entangled network of the cellulosic fibers within the polymer matrix [5, 34]. The storage modulus of PLA, 1.71 GPa, increases by 51% for PLA/5CNF at 25 °C (Figure 5.7a). On the other hand, a 264% increase in the storage modulus of PLA (5.6 MPa) is observed for the sample containing 5 wt% CNFs at 70 °C (Figure 5.7b). In fact, when the matrix goes through the rubbery region its modulus decreases significantly and the reinforcement effect of the nanofibers becomes more evident at high temperatures [7]. This can result in extending the applications of PLA, particularly for products exposed to high temperature. In other investigations, smaller increases in the storage modulus of PLA reinforced with cellulosic fibers were reported. Kowalczyk et al. [15] obtained an increase of 14% in the storage modulus of PLA at 20 °C in the presence of 2 wt% of CNFs. Frone et al. [4] reported a 18% improvement for the storage modulus of PLA containing 2.5 wt% unmodified and APS-CNFs at 25 °C, compared to that of PLA. However, the storage modulus at 80 °C decreased for both composites. In another investigation, the addition of 20 wt% MFC increased the storage modulus of PLA by 37 and 220% at 20 and 80 °C, respectively [7].

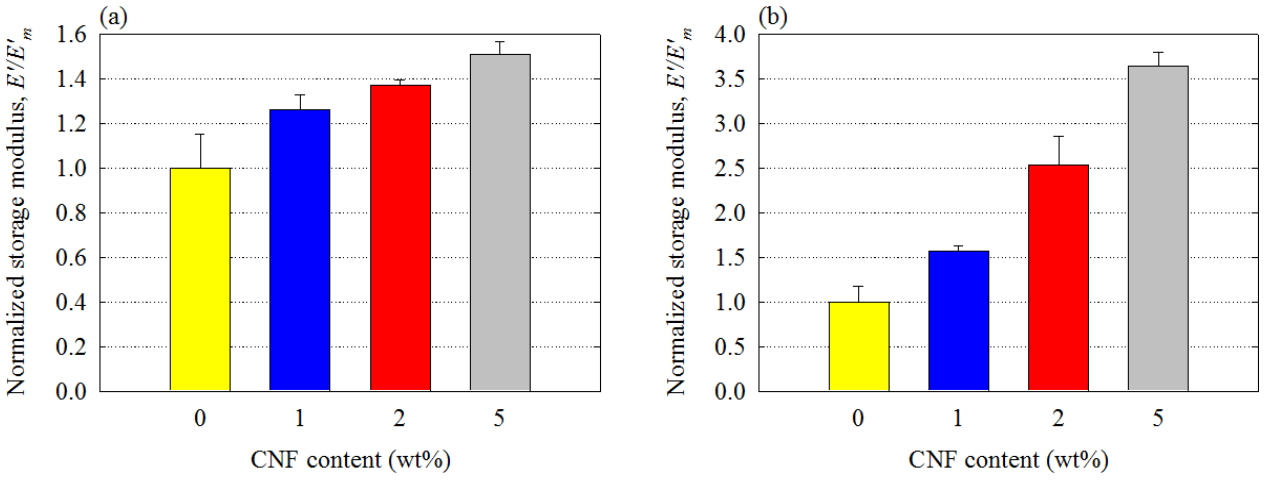

Figure 5.7: Normalized storage modulus in flexion at 25 °C (a) and 70 °C (b) for various samples.

5.4.5 Differential scanning calorimetry (DSC)

Figure 5.8 depicts DSC thermograms of first heating and first cooling sequences for the neat PLA and PLA/CNF composites. All composites exhibit a cold crystallization peak with no significant shift as compared to that of PLA in the first heating scans (Figure 5.8a); however, the peak sharpens

with the incorporation of CNFs. Melting peaks also show up with a similar shape to that of the PLA matrix and at the same temperature. First cooling scans are presented in Figure 5.8b. Neat PLA exhibits a broad peak corresponding to its crystallization upon cooling; however, in the presence of CNFs, the offset of the crystallization peak is observed at higher temperatures. The details of DSC measurements are presented in Table 5.2. The crystalline contents of the samples upon heating and cooling sequences, $X_c^{heating}$ and $X_c^{cooling}$, reported in Table 5.2 were calculated from [22]:

$$X_c^{heating} = (\Delta H_m - \Delta H_{cc}) \times 100/(w_m \Delta H_m^0) \qquad (5.10)$$

$$X_c^{cooling} = \Delta H_c \times 100/(w_m \Delta H_m^0) \qquad (5.11)$$

where ΔH_m, ΔH_{cc} and ΔH_c are the enthalpies of melting, cold crystallization and crystallization, respectively; w_m is the weight fraction of the PLA phase of the sample and ΔH_m^0 is the melting enthalpy of the 100% crystalline PLA (taken as 93 J/g [35]).

Both the total amount of nuclei and mobility of polymer chains affect the overall crystalline content. The incorporation of nanofibers is expected to enhance nucleation, while restricting the mobility. Hence, in some cases, the crystalline content of the composites is similar to that of the polymer matrix. Here, the addition of 1 wt% CNFs slightly increases the total crystalline content of PLA in the heating sequence, probably due to predominance of the nucleation effect of the CNFs. However, the crystalline content decreases at higher CNF concentrations, which may be attributed to the restriction of the mobility of the PLA chains. In fact, the samples for DSC measurements were cut from specimens used for tensile tests. Since the measured crystallinity in the heating sequence of the samples containing 1 and 2 wt% CNFs is effectively the same as that of the unfilled PLA, it would appear that reinforcement by CNFs, rather than crystallinity, is the main factor influencing the mechanical properties. On the other hand, the effect of the decrease in crystalline content of PLA at 5 wt% CNFs on the mechanical properties is compensated by the presence of a strong network of CNFs within the PLA matrix. Cold crystallization temperature, T_{cc}, and melting temperature, T_m, for the composite samples are close to those of PLA. However, the crystallization temperature during the cooling sequence, T_c, is shifted to higher temperatures, due to the nucleation effect of the CNFs. Therefore, CNFs could facilitate the crystallization of PLA. In contrast, Frone et al. [2] observed that T_c of PLA remained unchanged for the composites containing 2.5 wt%

CNFs. Kowalczyk et al. [15] have also found no significant influence of the CNFs when they were added in small quantity (i.e., 2 wt%).

As observed in Table 5.2, $X_c^{cooling}$ for the composite samples increases up to 18% with the addition of CNFs, compared to the neat PLA. This shows the ability of the CNFs to act as nucleation agents for the crystallization of PLA chains when they are well dispersed/distributed, and, consequently, contribute to the rise of crystalline content.

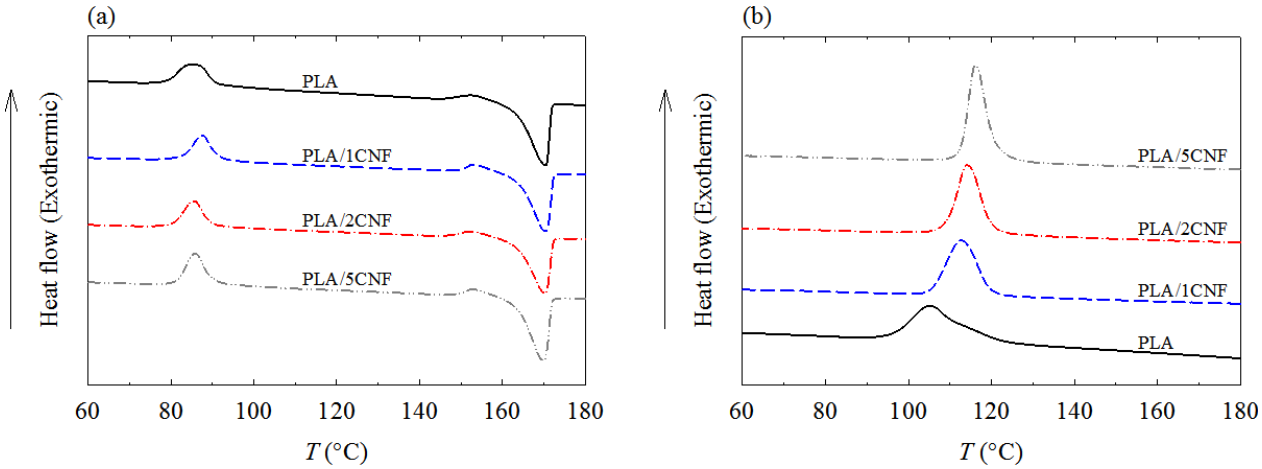

Figure 5.8: DSC thermograms of first heating (a) and first cooling (b) sequences for all samples.

Table 5.2: DSC results for first heating and first cooling sequences.

Sample	T_g^* (°C)	T_{cc} (°C)	T_c (°C)	T_m (°C)	$X_c^{heating}$ (%)	$X_c^{cooling}$ (%)
PLA	59.4 ± 0.4	85.2 ± 0.3	105.2 ± 0.2	170.3 ± 0.3	29.1 ± 0.2	38.4 ± 0.1
PLA/1CNF	61.8 ± 0.2	87.6 ± 0.3	112.7 ± 0.3	170.4 ± 0.5	31.3 ± 0.1	46.4 ± 0.2
PLA/2CNF	63.2 ± 0.4	85.6 ± 0.5	114.1 ± 0.3	170.4 ± 0.4	29.4 ± 0.4	45.4 ± 0.1
PLA/5CNF	64.3 ± 0.1	85.9 ± 0.1	116.0 ± 0.1	170.0 ± 0.1	24.4 ± 0.5	45.4 ± 0.5

All temperatures indicate the values at the corresponding peak.
* The T_g data have been extracted from the DMTA tests.

5.4.6 Thermogravimetric analysis (TGA)

Thermal stability of samples was investigated by TGA and first derivative of TGA (DTG). Figure 5.9a presents TGA results for freeze-dried CNFs, PLA and PLA/5CNF. The temperature at which the samples lose 5% of their weight after evaporation of the absorbed moisture increases negligibly from 327 °C for PLA to 329 °C for PLA/5CNF, while, this temperature for CNFs is 306 °C. Figure

5.9b depicts that the DTG peak temperature increases from 330 °C for PLA to 335 °C for PLA/5CNF, whereas CNFs exhibit a peak temperature of 340 °C. The onset temperatures of degradation for CNFs and PLA are 317 and 324 °C, respectively, (Figure 5.9b). However, the onset temperature for PLA/5CNF is 329 °C. Consequently the CNFs have no detrimental effect on the thermal stability of PLA but also result in a slight improvement in stability of the composites, which is indeed favorable for PLA applications at elevated temperatures [36]. This increase can be ascribed to a restriction of the polymer chain mobility due to the good dispersion/distribution of CNFs in the PLA [37].

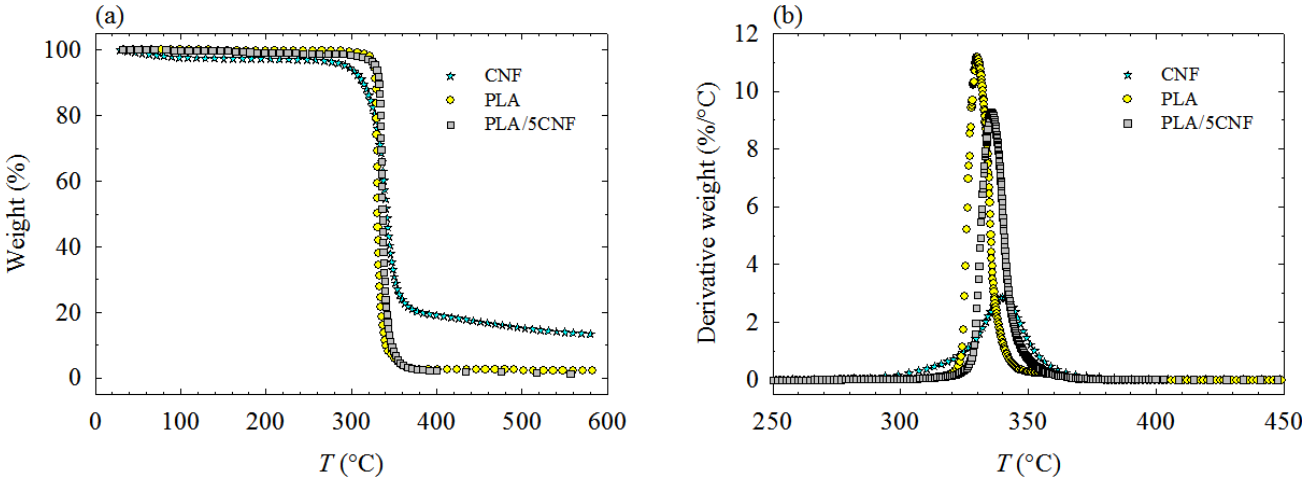

Figure 5.9: TGA (a) and DTG (b) curves of freeze-dried CNFs, PLA and PLA/5CNF.

5.4.7 Optical properties

High transparency of composite films is an important factor for many applications. The quality of the filler dispersion allows the films to maintain the original transparency of the polymer [20]. Hence, light transmittance of the samples was determined as an indicator of the dispersion quality of CNFs. Generally, light transmittance greater than 75% is considered as good transparency [35]. Figure 5.10 presents the light transmittance values for PLA and PLA/5CNF films over a wide range of wavelength, λ. The highest concentration of CNFs in PLA (i.e., 5 wt%) does not compromise significantly the optical properties of the matrix in the wavelength range of 390 to 700 nm, which corresponds to the limit of visible light; for example, the transparency of PLA film decreases by only ca. 5% at λ = 390 nm, where the highest difference between the two sets of data is seen. This suggests good dispersion/distribution of CNFs in PLA [13] that is an improved result over other investigations where white spots or visible CNF agglomerates were observed while assessing

qualitatively the transparency of PLA filled samples [5, 11], due to poorer dispersion/distribution of CNFs. Adequate light transmittance of PLA/CNF composites, as demonstrated in the present study, opens up opportunities for their uses in optical [16-18] and optoelectronic [10, 17, 19] applications, where other nano-reinforcements (carbon nanotubes and nanoclays) cannot be used due to the lack of transparency of the resulting composites [16].

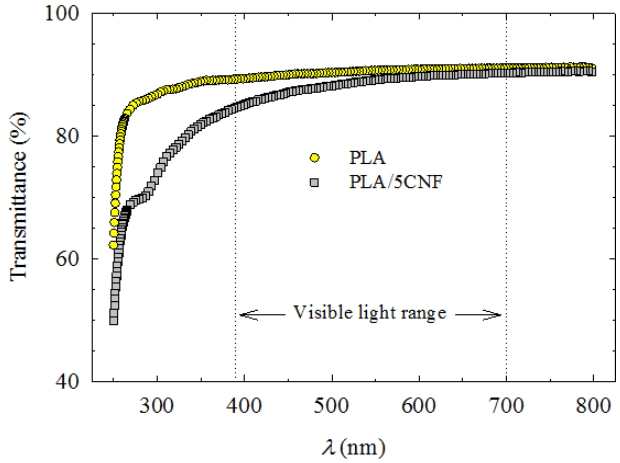

Figure 5.10: Light transmittance of PLA and PLA/5CNF films.

5.5 Concluding remarks

The effects of incorporating different contents of CNFs on the rheological, mechanical, thermal and optical properties of PLA were investigated. To this end, a solvent-casting method was employed to prepare the PLA/CNF composites. The SEM micrograph showed a uniform dispersion of the CNFs within PLA, without the presence of large bundles of fibers. The addition of CNFs resulted in substantial increases in the storage modulus and complex viscosity in the molten state, and the rheological percolation threshold was estimated to occur in the range of 0.5 and 1 wt% CNFs. Significant enhancements of the Young modulus and tensile strength of PLA were achieved, up to 50 and 31%, respectively, in presence of 5 wt% CNFs. The modified Halpin-Tsai and Krenchel models were used to predict the Young moduli of composites and good agreement to the experimental data was observed for lower concentrations of CNFs, especially with the predictions of Krenchel model. Also, solid-state flexural storage modulus in DMTA increased over a wide range of temperatures, especially in the rubbery region; the storage modulus of PLA at 25 and 70 °C was enhanced by 51 and 264%, respectively, for the PLA/5CNF composite. The T_g of the PLA was shifted to higher temperatures and the area under the $\tan\delta$ peak decreased by the addition of

the CNFs. DSC measurements indicated that the enhancement in the mechanical properties was mainly attributed to the reinforcement effect of CNFs, rather than to the nucleating/crystallization effect. However, the nucleation effect of the CNFs caused a shifting of T_c to higher values, up to 11 °C, in the cooling sequence and the crystallization of PLA was accelerated in the presence of CNFs. The thermal stability of PLA also increased by incorporating the CNFs. The transparency of the composite films in the visible light range remained comparable to that of the neat PLA due to the good dispersion of CNFs within the host matrix. The results presented in this work demonstrate that the incorporation of CNFs can extend the applications of PLA where transparency and good mechanical properties over a wide range of temperatures and thermal properties are of utmost importance. Also, the observed improvement of PLA behavior points out to the important advantage of the preparation method employed in this work, which favors good dispersion/distribution of the hydrophilic CNFs within the hydrophobic PLA matrix.

5.6 Acknowledgments

The authors wish to thank Prof. Mohini M. Sain of the University of Toronto for providing the CNFs.

5.7 References

[1] Zhou C, Shi Q, Guo W, Terrell L, Qureshi AT, Hayes DJ, Wu Q. Electrospun Bio-Nanocomposite Scaffolds for Bone Tissue Engineering by Cellulose Nanocrystals Reinforcing Maleic Anhydride Grafted PLA. ACS Applied Materials and Interfaces. 2013;5(9):3847-3854.

[2] Frone AN, Berlioz S, Chailan JF, Panaitescu DM. Morphology and Thermal Properties of PLA-Cellulose Nanofibers Composites. Carbohydrate Polymers. 2013;91(1):377-84.

[3] Nakagaito AN, Fujimura A, Sakai T, Hama Y, Yano H. Production of Microfibrillated Cellulose (MFC)-Reinforced Polylactic Acid (PLA) Nanocomposites from Sheets Obtained by a Papermaking-Like Process. Composite Science and Technology. 2009;69(7–8):1293-1297.

[4] Frone AN, Berlioz S, Chailan JF, Panaitescu DM, Donescu D. Cellulose Fiber-Reinforced Polylactic Acid. Polymer Composites. 2011;32(6):976-985.

[5] Jonoobi M, Harun J, Mathew AP, Oksman K. Mechanical Properties of Cellulose Nanofiber (CNF) Reinforced Polylactic Acid (PLA) Prepared by Twin Screw Extrusion. Composite Science and Technology. 2010;70(12):1742-1747.

[6] Sanchez-Garcia M and Lagaron J. On the Use of Plant Cellulose Nanowhiskers to Enhance the Barrier Properties of Polylactic Acid. Cellulose. 2010;17(5):987-1004.

[7] Suryanegara L, Nakagaito AN, Yano H. The Effect of Crystallization of PLA on the Thermal and Mechanical Properties of Microfibrillated Cellulose-Reinforced PLA Composites. Composite Science and Technology. 2009;69(7-8):1187-1192.

[8] Iwatake A, Nogi M, Yano H. Cellulose Nanofiber-Reinforced Polylactic Acid. Composite Science and Technology. 2008;68(9):2103-2106.

[9] Brown EE and Laborie MPG. Bioengineering Bacterial Cellulose/Poly(ethylene oxide) Nanocomposites. Biomacromolecules. 2007;8(10):3074-3081.

[10] Tercjak A, Gutierrez J, Barud HS, Domeneguetti RR, Ribeiro SJL. Nano- and Macroscale Structural and Mechanical Properties of in Situ Synthesized Bacterial Cellulose/PEO-b-PPO-b-PEO Biocomposites. ACS Applied Materials and Interfaces. 2015;7(7):4142-4150.

[11] Tingaut P, Zimmermann T, Lopez-Suevos F. Synthesis and Characterization of Bionanocomposites with Tunable Properties from Poly(lactic acid) and Acetylated Microfibrillated Cellulose. Biomacromolecules. 2010;11(2):454-464.

[12] Wang B and Sain M. The Effect of Chemically Coated Nanofiber Reinforcement on Biopolymer Based Nanocomposites. Bioresources. 2007;2(3):371-388.

[13] Petersson L and Oksman K. Biopolymer Based Nanocomposites: Comparing Layered Silicates and Microcrystalline Cellulose as Nanoreinforcement. Composite Science and Technology. 2006;66(13):2187-2196.

[14] Xu X, Wang H, Jiang L, Wang X, Payne SA, Zhu JY, Li R. Comparison between Cellulose Nanocrystal and Cellulose Nanofibril Reinforced Poly(ethylene oxide) Nanofibers and Their Novel Shish-Kebab-Like Crystalline Structures. Macromolecules. 2014;47(10):3409-3416.

[15] Kowalczyk M, Piorkowska E, Kulpinski P, Pracella M. Mechanical and Thermal Properties of PLA Composites with Cellulose Nanofibers and Standard Size Fibers. Composites Part A: Applied Science and Manufturing. 2011;42(10):1509-1514.

[16] Xu X, Liu F, Jiang L, Zhu JY, Haagenson D, Wiesenborn DP. Cellulose Nanocrystals vs. Cellulose Nanofibrils: A Comparative Study on Their Microstructures and Effects as Polymer Reinforcing Agents. ACS Applied Materials and Interfaces. 2013;5(8):2999-3009.

[17] Kalia S, Boufi S, Celli A, Kango S. Nanofibrillated Cellulose: Surface Modification and Potential Applications. Colloid and Polymer Science. 2014;292(1):5-31.

[18] Janardhnan S and Sain M. Bio-Treatment of Natural Fibers in Isolation of Cellulose Nanofibres: Impact of Pre-Refining of Fibers on Bio-Treatment Efficiency and Nanofiber Yield. Journal of Polymers and the Environment. 2011;19(3):615-621.

[19] Siró I and Plackett D. Microfibrillated Cellulose and New Nanocomposite Materials: a Review. Cellulose. 2010;17(3):459-494.

[20] Eichhorn SJ, Dufresne A, Aranguren M, Marcovich NE, Capadona JR, Rowan SJ, Weder C, Thielemans W, Roman M, Renneckar S, Gindl W, Veigel S, Keckes J, Yano H, Abe K, Nogi M, Nakagaito AN, Mangalam A, Simonsen J, Benight AS, Bismarck A, Berglund LA, Peijs, T. Review: Current International Research into Cellulose Nanofibres and Nanocomposites. Journal of Materials Science. 2010;45(1):1-33.

[21] Kamal MR and Khoshkava V. Effect of Cellulose Nanocrystals (CNC) on Rheological and Mechanical Properties and Crystallization Behavior of PLA/CNC Nanocomposites. Carbohydrate Polymers. 2015;123:105-14.

[22] Ghanbari A, Heuzey MC, Carreau PJ, Ton-That MT. A Novel Approach to Control Thermal Degradation of PET/Organoclay Nanocomposites and Improve Clay Exfoliation. Polymer. 2013;54(4):1361-1369.

[23] Ghanbari A, Heuzey MC, Carreau PJ, Ton-That MT. Morphological and Rheological Properties of PET/Clay Nanocomposites. Rheologica Acta. 2013;52(1):59-74.

[24] Abbasi S, Carreau PJ, Derdouri A, Moan M. Rheological Properties and Percolation in Suspensions of Multiwalled Carbon Nanotubes in Polycarbonate. Rheologica Acta. 2009;48(9):943-959.

[25] Bagheriasl D, Carreau PJ, Riedl B, Dubois C, Hamad WY. Shear Rheology of Polylactide (PLA)–Cellulose Nanocrystal (CNC) Nanocomposites. Cellulose. 2016;23(3):1885-1897.

[26] Khoshkava V and Kamal MR. Effect of Cellulose Nanocrystals (CNC) Particle Morphology on Dispersion and Rheological and Mechanical Properties of Polypropylene/CNC Nanocomposites. ACS Applied Materials and Interfaces. 2014;6(11):8146-8157.

[27] Miao C and Hamad WY. Cellulose Reinforced Polymer Composites and Nanocomposites: A Critical Review. Cellulose. 2013;20(5):2221-2262.

[28] Arias A, Heuzey MC, Huneault M. Thermomechanical and Crystallization Behavior of Polylactide-Based Flax Fiber Biocomposites. Cellulose. 2013;20(1):439-452.

[29] Gómez-del Río T, Poza P, Rodríguez J, García-Gutiérrez MC, Hernández JJ, Ezquerra TA. Influence of Single-Walled Carbon Nanotubes on the Effective Elastic Constants of Poly(ethylene terephthalate). Composite Science and Technology. 2010;70(2):284-290.

[30] Coleman JN, Khan U, Blau WJ, Gun'ko YK. Small but Strong: A Review of the Mechanical Properties of Carbon Nanotube–Polymer Composites. Carbon. 2006;44(9):1624-1652.

[31] Wang S, Cheng Q, Rials TG, Lee SH. "Cellulose Microfibril/Nanofibril and Its Nanocompsites" in *The 8th Pacific rim bio-based composites symposium*, Kuala Lumpur, Malaysia, 2006, pp. 301-308.

[32] Oksman K, Skrifvars M, Selin JF. Natural Fibres as Reinforcement in Polylactic Acid (PLA) Composites. Composite Science and Technology. 2003;63(9):1317-1324.

[33] Bagheriasl D, Carreau PJ, Dubois C, Riedl B. Properties of Polypropylene and Polypropylene/Poly(ethylene-co-vinyl alcohol) Blend/CNC Nanocomposites. Composite Science and Technology. 2015;117:357-363.

[34] Azizi Samir MAS, Alloin F, Paillet M, Dufresne A. Tangling Effect in Fibrillated Cellulose Reinforced Nanocomposites. Macromolecules. 2004;37(11):4313-4316.

[35] Ambrosio-Martín J, Fabra MJ, Lopez-Rubio A, Lagaron JM. Melt Polycondensation to Improve the Dispersion of Bacterial Cellulose into Polylactide via Melt Compounding: Enhanced Barrier and Mechanical Properties. Cellulose. 2015;22(2):1201-1226.

[36] Li ZQ, Zhou XD, Pei CH. Preparation and Characterization of Bacterial Cellulose/Polylactide Nanocomposites. Polymer-Plastics Technology and Engineering. 2010;49(2):141-146.

[37] Ramezani Kakroodi A, Cheng S, Sain M, Asiri A. Mechanical, Thermal, and Morphological Properties of Nanocomposites Based on Polyvinyl Alcohol and Cellulose Nanofiber from Aloe vera Rind. Journal of Nanomaterials. 2014;2014:1-7.

CHAPTER 6 ARTICLE 2 : ENHANCED PROPERTIES OF POLY(ETHYLENE OXIDE)/CELLULOSE NANOFIBER BIOCOMPOSITES[2]

Fatemeh Safdari[a], Pierre J. Carreau[a*], Marie C. Heuzey[a], Musa R. Kamal[b], Mohini M. Sain[c,d]

[a] *Research Center for High Performance Polymer and Composite Systems (CREPEC), Chemical Engineering Department, Polytechnique Montreal, Montreal, Quebec H3C 3A7, Canada*

[b] *CREPEC, Chemical Engineering Department, McGill University, Montreal, Quebec H3A 0C5, Canada*

[c] *Faculty of Forestry, University of Toronto, Toronto, Ontario M5S 3B3, Canada*

[d] *Department of Chemical Engineering and Applied Chemistry, University of Toronto, Toronto, Ontario M5S 3E5, Canada*

Parts of this chapter have been presented at the:

- *CREPEC Student Conference*, Montreal, Canada (June 2016)
- *Canadian Chemical Engineering Conference*, Quebec City, Canada (October 2016)

[2] Published in *Cellulose*; DOI 10.1007/s10570-016-1137-1.

6.1 Abstract

Poly(ethylene oxide) (PEO)/cellulose nanofiber (CNF) biocomposites were developed using a simple aqueous solution technique. A PEO/CNF composite was also produced in the molten state to compare different preparations. The effects of nanofibers on different properties of PEO including rheological, thermal, mechanical and optical were investigated. For the sample prepared in the molten state, no change in properties was observed as compared to the neat matrix. On the other hand, for the solution-based samples, scanning electron microscopy revealed good dispersion/distribution of nanofibers in the PEO, which resulted in a significant increase of the rheological properties and also a notable shear-thinning behavior. A liquid- to solid-like behavior transition along with the observation of apparent yield stress suggested the formation of a strong CNF 3D network. The Young modulus and tensile strength of PEO with 3 wt% CNFs were enhanced by 49 and 35%, respectively, compared to the neat PEO. The storage modulus of PEO was significantly improved for all tested temperatures in the dynamic mechanical thermal analysis; at room temperature that corresponds to the rubbery region, a 47% enhancement was observed by incorporating 3 wt% nanofibers. Also, PEO/CNF composites demonstrated good optical transmittance, which is generally not the case with many reinforcements. These results show that PEO/CNF biocomposites with good mechanical and optical properties can be fabricated via a simple aqueous solution technique.

Keywords: *Biocomposites*, *Poly(ethylene oxide) (PEO)*, *Cellulose nanofibers (CNFs)*, *Rheology*, *Crystallinity*, *Mechanical properties*, *Transparency*

6.2 Introduction

Cellulose nanofibers (CNFs) as a potential reinforcing agent show interesting physical and mechanical properties and exhibit many advantages, which make them preferable over inorganic reinforcements [1-9]. They have attracted considerable interest for applications in the automotive, aircraft, railway, and furniture industries as well as sport items, irrigation systems, electrochemicals, etc. [1, 2, 4, 6, 10, 11]. However, CNFs form very strong particle–particle interactions with notable potential for entanglement and agglomeration since they are long and flexible and form hydrogen bonds. Thus, uniformly dispersing the CNFs within polymer matrices is a challenge [6, 12-17].

The use of more environmentally friendly materials such as biocomposites has been the subject of many studies since they are biodegradable and biocompatible products comprising components from renewable sources, all or in parts. Among different biopolymers, poly(ethylene oxide) (PEO) is a nontoxic, highly hydrophilic, semi-crystalline, thermoplastic polymer [4, 9, 18]. It has already found applications in the medical and biomedical fields, tissue engineering, energy storage [5, 9, 18-20], and the electrochemical field as electrolyte in lithium polymer cells [2, 10, 11, 18]. It has also been used as hydrogel, dispersant, surfactant, flocculating agent and rheology modifier [18, 21]. However, neat PEO exhibits low mechanical and thermal properties and high crystallinity, which makes it unsuitable for many applications. Thermal and mechanical properties of PEO can be improved by incorporating reinforcements while retaining its advantageous properties including high biocompatibility, biodegradability [18, 20, 21] and transparency [22, 23].

In view of the above considerations, CNF-reinforced PEO should be an interesting system due to the biocompatibility and biodegradability of the all both key components and final composites. In some studies, to develop enhanced PEO/CNF composites electrospinning [17, 24], which is a slow method for composite preparation and is aimed at special applications, and solution casting [5, 20] have been used. To prepare PEO/CNF composites, Brown and Laborie [20] incorporated PEO in a culture medium of *acetobacter xylinum* (used for bacterial cellulose nanofiber (BCNF) culture). They reported no change in melting temperature of PEO, and a decrease in the crystalline content (from 67% for PEO to 49% for the composite), in the presence of 15 wt% BCNFs. Xu et al. [5] prepared PEO/CNF composite films by solution casting. A CNF hydrogel was mixed with a PEO solution, allowing PEO molecules to penetrate in the CNF network. They reported a 4 °C decrease in the melting temperature and also a small decrease in the crystalline content of PEO (from 82 to 79%) by adding 4 wt% CNFs; a 46% improvement in the yield strength and a 31% enhancement in the Young modulus of PEO were also reported. However, the solution-based approach is unlikely to be used commercially, as it requires a further step for solvent evaporation, including the use of toxic solvents for polymers not soluble in water. In this regard, other approaches such as the one described by Iyer et al. [25] comprising a non-solvent-based processing method, solid-state shear pulverization, can be used. Despite this, it is worth mentioning that there are some solution-based techniques such as *in-situ* polymerization that require the use of organic solvents and are nevertheless used in industry [26].

In our recent work [6], solvent casting was employed to incorporate CNFs into polylactide (PLA) as a widely-used biopolymer to overcome some of its drawbacks, e.g. slow crystallization, low thermal stability and heat resistance, which could successfully improve the properties in different aspects without affecting the transparency of the matrix. A 50% increase in Young's modulus and storage modulus at 25 °C, a 264% enhancement in the storage modulus at 70 °C and a 31% increase in the tensile strength of the matrix were achieved for the composite containing 5 wt% CNFs. Moreover, an increase of 11 °C of the crystallization temperature was achieved with 5 wt% CNFs and the composites showed improved thermal stability over PLA. In the current study, a simple aqueous solution technique was used to prepare enhanced PEO/CNF composites with low nanofiber contents. Since there is a lack of information on light transparency and the molten-state rheological behavior of CNF-filled composites in the literature, we present novel data regarding the effect of CNFs on these properties of PEO. Moreover, the CNF-reinforced PEO biocomposites were characterized in terms of crystallization, mechanical properties, heat resistance and thermal stability. To our knowledge, such a full characterization of PEO/CNF composites has not been reported in the literature. The results of this study point out the great potential of CNFs to reinforce PEO and, thus, to extend the applications of PEO.

6.3 Experimental section

6.3.1 Materials

Poly(ethylene oxide) (PEO) in powder form (Sigma-Aldrich Canada Co., Oakville, ON, Canada) with melting point of 65 °C and a viscosity-average molecular weight of 100,000 g/mol was used as the matrix. An aqueous suspension of cellulose nanofibers (CNFs), several micrometers long and less than 50 nm in diameter, was prepared by Janardhnan and Sain following the methodology described in [27]. The concentration of nanofibers in the suspension was 2.3 wt%.

6.3.2 Sample preparation

The desired amount of CNF aqueous suspension (containing 0.2–0.6 g solid content) was diluted with distilled water for a total volume of 60 mL and stirred for 1 h at the speed of 600 rpm using a magnetic stirrer. At the same time, a solution of the desired amount of PEO in 140 mL distilled water was prepared using a magnetic stirrer under the same conditions. Thereafter, the diluted CNF

suspension was added to the PEO solution while stirring for 1 h. A similar procedure was followed for the neat PEO sample. Then, a vacuum oven was utilized to dry the mixture for 48 h at 50 °C. The composites containing nanofibers were referred to as PLA/xCNF, while x (equals to 1, 2, or 3) represents the fiber wt% according to the overall composite weight. For instance, PEO/1CNF denotes that 1% of the overall composite weight consists of CNFs.

To assess the adequacy of the aqueous solution technique in improving the properties, neat PEO and a composite sample containing 3 wt% CNFs were also prepared in melt via an internal batch mixer, DDRV501 Brabender (C. W. Brabender Instruments Inc., NJ, USA). These samples were coded as PEO (M) and PEO/3CNF (M), respectively, where (M) refers to melt preparation. To do so, the as-received PEO was vacuum dried at 50 °C for 24 h. The aqueous suspension of nanofibers was also freeze-dried in a Labconco Freezone 2.5^{Plus} for 48 h to be directly melt-compounded with PEO at 85 °C and 100 rpm for 7 min under nitrogen atmosphere.

Then, the products of both solution and melt methods were molded in a manual hydraulic press (Carver, Inc., Wabash, IN, USA) at 85 °C for 10 min under a nitrogen atmosphere to produce disks, dumb-bells, bars and films for testing. Thereafter, cooling of the samples was done using the press for 5 min at room temperature. The samples were kept under vacuum until characterization.

6.3.3 Characterization

6.3.3.1 Microscopy

Gold-coated cryo-fractured surfaces of samples were observed by scanning electron microscopy (SEM) using a JEOL JSM 7600TFE instrument (JEOL USA, Inc., Peabody, MA, USA) with an operating voltage of 2 kV.

6.3.3.2 Rheology

Rheology tests were performed on sample disks of 25 mm diameter and 1 mm thickness, using a stress-controlled Anton Paar MCR 301 rheometer (Anton Paar, Austria). The experiments were conducted at 85 °C in the presence of nitrogen to prevent degradation of the samples. A cone-and-plate geometry with a plate diameter of 25 mm, a cone truncation of 0.051 mm and cone angle of ca. 2° was used to perform measurements in the linear viscoelastic region in the small amplitude oscillatory shear mode. Frequency sweeps were carried out for 85 min at a strain amplitude of 0.05.

Prior to the frequency sweep tests, time sweeps were conducted for 85 min at a frequency of 1 rad/s to verify the thermal stability; all the rheological properties of the samples were stable, with increases less than 7%.

6.3.3.3 Mechanical and thermal properties

Differential scanning calorimetry (DSC) was performed using a DSC Q1000 (TA Instruments, New Castle, DE, USA) under nitrogen. The samples, typically 10 mg, were heated at a rate of 2 °C/min and held at 100 °C for 3 min. Thereafter, they were cooled (2 °C/min) to 20 °C. The characterization was performed twice for each sample.

Tensile tests were performed on specimens (63.5 mm long, 9.5 mm wide and 1.6 mm thick) with dumb-bell shape type V (standard ASTM D638) using an Instron 3365 (Instron, Norwood, MA, USA). The tests were performed at room temperature with a load cell of 500 N and a crosshead speed of 5 mm/min. At least seven specimens per sample were tested.

Dynamic mechanical thermal analysis (DMTA) was carried out using a DMA 2980 analyzer (TA Instruments, New Castle, DE, USA). The specimens, rectangular bars of 1.6 mm thickness, 12.2 mm width and 60.5 mm length, were tested in a dual cantilever bending mode at 1 Hz frequency with 30 μm amplitude and a heating rate of 2 °C/min. The measurements were conducted in the range of -100 to 50 °C with a span length of 35 mm on at least three specimens for each sample.

For thermogravimetric analysis (TGA), a TGA Q500 (TA Instruments, New Castle, DE, USA) was used in high-resolution mode. The samples were heated to 800 °C with a rate of 10 °C/min and a nitrogen flow rate of 60 mL/min. The tests were performed twice on typically 15 mg specimen for each sample.

6.3.3.4 Optical properties

Optical properties were determined using a LAMBDA 1050 UV/Vis/NIR Spectrophotometer (PerkinElmer, Waltham, MA, USA) with 150 mm InGaAs Int.Sphere. The light transparency of the samples was determined quantitatively by the assessment of the corresponding 30 × 30 mm^2 films of 145 ± 18 μm thickness and used as a measure of the CNF dispersion quality. The wavelength range of 250–800 nm was tested with a 5 nm bandwidth and the rate of 141 nm/min. The characterization was conducted three times for each sample.

6.4 Results and discussion

6.4.1 SEM

SEM micrographs of the CNFs (freeze-dried from a suspension of 0.1 wt% nanofibers in water) and PEO containing 3 wt% CNFs prepared in solution and melt are presented in Figure 6.1. A web-like structure comprising single fibers and CNF bundles is illustrated in Figure 6.1a. It is worth mentioning that even in the preferred medium to disperse CNFs (i.e., water) [28] the presence of fiber entanglements and bundles is evident (Figure 6.1a). The SEM micrographs of PEO/3CNF (Figure 6.1b and c) show quite a good dispersion/distribution of the nanofibers in the PEO matrix without obvious fiber bundles; however, a very large agglomerate is evident in Figure 6.1d for the composite sample prepared in the molten state, i.e., PEO/3CNF (M). Also, the presence of some fiber bundles has been observed in our previous investigation on hydrophobic polymer, PLA, CNF composites [6]. The good dispersion/distribution of the nanofibers within PEO is attributed to the efficient aqueous solution technique utilized in the current study.

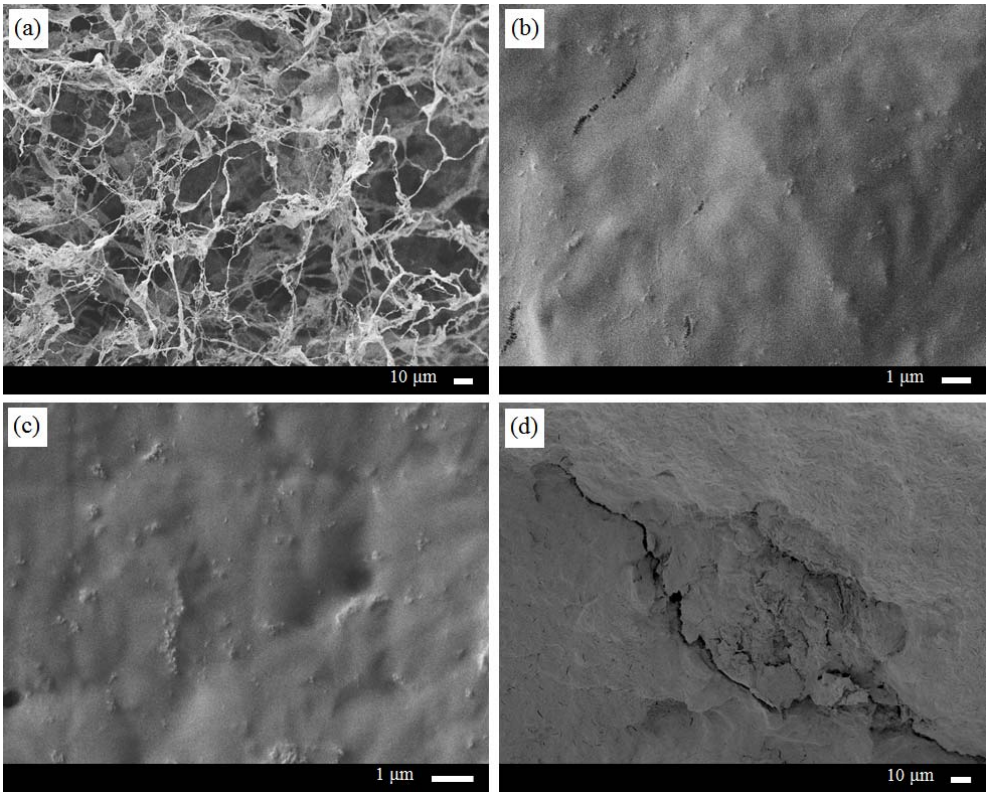

Figure 6.1: SEM micrographs of (a) freeze-dried CNFs, (b and c) PEO/3CNF for two different samples, and (d) PEO/3CNF (M).

6.4.2 Rheology

To verify qualitatively the dispersion/distribution of the nanofibers in the matrix, rheological measurements were performed. Figure 6.2 illustrates the complex viscosity, η^*, and storage and loss moduli, G' and G'', as functions of the frequency, ω, for the solution-prepared samples. For the neat PEO, a short plateau followed by a shear-thinning behavior on the plot of η^* versus ω (Figure 6.2a), and a low-frequency region with a slope of 1.17 for G' (Figure 6.2b) are observed, indicating that the terminal zone was not reached at the lowest frequency. By the incorporation of CNFs, the shear-thinning behavior of the composites becomes more evident, mainly at low frequencies (Figure 6.2a). Moreover, G' for the composites becomes less frequency dependent at high loadings (Figure 6.2b); a low-frequency slope of 0.11 is obtained for PEO/3CNF. The same trend is observed for G'' (Figure 6.2b), while the storage modulus is more sensitive to the presence of CNFs. Also, Figure 6.2b shows that G' and G'' for PEO/1CNF cross at a frequency lower than that for PEO. It is interesting that for composites containing higher loadings of CNFs, the loss modulus is lower than the storage modulus for the whole range of frequencies tested here. Significant increases up to two, three and two orders of magnitude are observed at low frequencies for η^*, G' and G'' of the composites, respectively, in comparison with the properties of the neat PEO. Likewise, the increases relative to the PLA properties were of two orders of magnitude for η^*, five for G' and two for G'' in the case of the PLA/CNF composite containing 5 wt% nanofibers [6]. These are indicators of a strong nanofiller network along with the interactions between the nanofibers and possibly polymer chains with nanofibers [29]. Hence, a liquid- to a solid-like behavior transition is observed, with an upturn in viscosity and plateaus at the low-frequency region for G' and G'' along with an apparent yield stress, σ_0, that can be obtained via the modified Herschel-Bulkley model [6, 30]:

$$\eta^* = G_0^*/\omega + k(\gamma^0\omega)^{n-1} \qquad (6.1)$$

and

$$\sigma_0 = G_0^* \gamma^0 \qquad (6.2)$$

where G_0^* is the magnitude of the complex modulus at the lowest frequency, k is a constant, γ^0 is the strain amplitude (0.05) and n is the flow index. The solid lines in Figure 6.2a represent the fits of the modified Herschel-Bulkley model. The model is shown to fit very well the data for the

composites containing 2 and 3 wt% CNFs with apparent yield stress values of 279 and 1330 Pa, respectively; however, for the composite containing 1 wt% CNFs, due to the lack of good fit at low frequencies, a yield stress of zero was assumed and a good fit could be achieved using the second term of Eq. 6.1, i.e., $\eta^* = k(\gamma^0\omega)^{n-1}$. As expected, n decreases with the CNF content, from 0.54 for PEO/1CNF to 0.48 for PEO/2CNF and 0.44 for PEO/3CNF. A similar behavior has been observed for other polymer composites such as PLA/CNF [6, 31], PLA/cellulose nanocrystal (CNC) [30, 32], polypropylene/CNC [33], polyethylene terephthalate/organoclay [34, 35] and polycarbonate/carbon nanotube [36].

It is also believed that the apparent yield stress is observed for concentrations above the rheological percolation threshold. Here, as the composite samples containing 2 and 3 wt% CNFs exhibit large apparent yield stresses, the percolation is considered to occur at a CNF concentration between 1 and 2 wt%. A percolation concentration in the range of 0.5–1 wt% CNFs and CNCs in a PLA matrix has been previously reported by Safdari et al. [6] and Bagheriasl et al. [32], respectively.

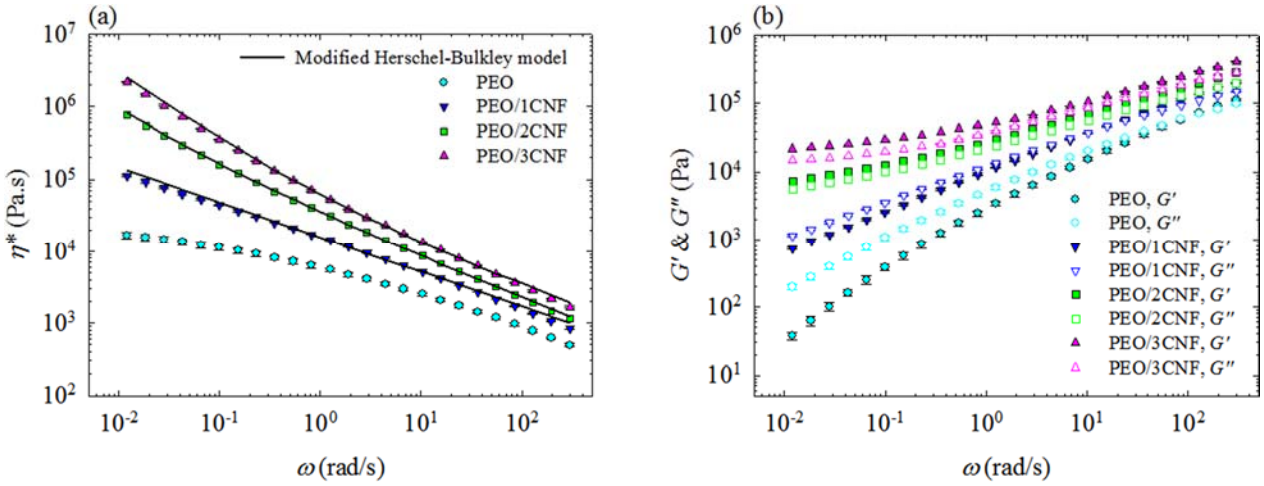

Figure 6.2: Plots of (a) complex viscosity, and (b) storage and loss moduli as functions of frequency at 85 °C and strain amplitude of 0.05 for solution-prepared samples. The solid lines in (a) represent the fits of the modified Carreau-Yasuda model, Eq. 6.1, for all samples.

Figure 6.3 compares η^* and G' as functions of ω, for the matrix and PEO/CNF composites containing 3 wt% CNFs prepared in both solution and melt. PEO and PEO (M) show similar rheological properties. In contrast to the results obtained for the solution-prepared samples, the complex viscosity and storage modulus of PEO/3CNF (M) do not increase compared to those of

the neat PEO (M). This emphasizes that dispersing the CNFs even within a polar matrix is quite challenging in direct melt mixing because of the highly entangled structure of the fibers. Hence, the solution technique is better in dispersing the fibers more efficiently in PEO.

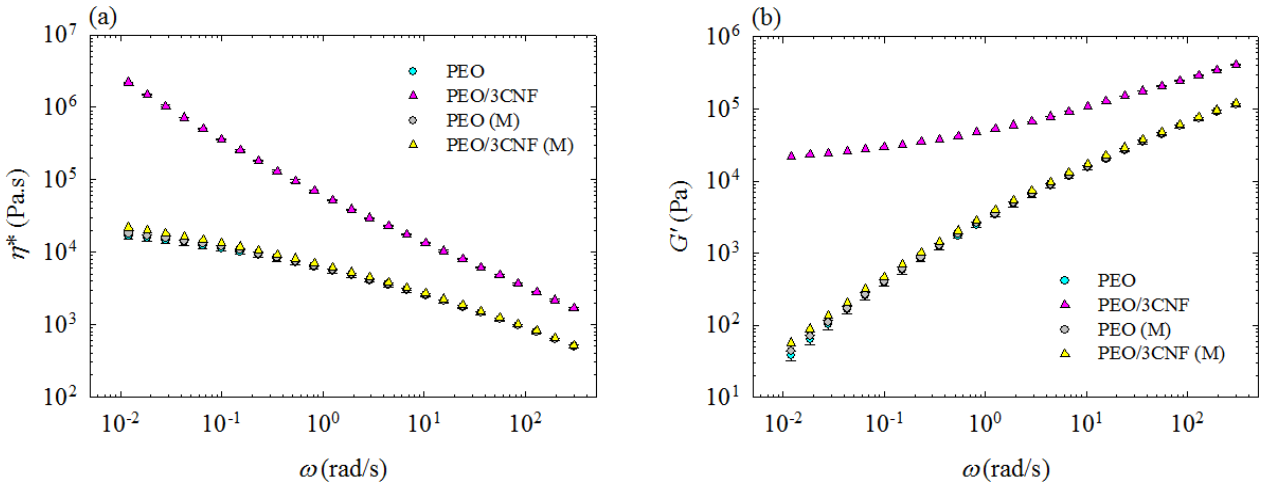

Figure 6.3: Plots of (a) complex viscosity and (b) storage modulus as functions of frequency at 85 °C and strain amplitude of 0.05 for PEO and PEO/CNF composites containing 3 wt% CNFs prepared in both solution and melt.

6.4.3 DSC

Table 6.1 presents the results of DSC measurements during the first heating and cooling cycles for various samples. To calculate the crystalline contents, $X_c^{heating}$ and $X_c^{cooling}$, the following equations were used

$$X_c^{heating} = \Delta H_m \times 100/(w_m \Delta H_m^0) \qquad (6.3)$$

$$X_c^{cooling} = \Delta H_c \times 100/(w_m \Delta H_m^0) \qquad (6.4)$$

where ΔH_m and ΔH_c are the enthalpies of melting and crystallization, respectively; w_m is the weight fraction of the PEO in each sample and ΔH_m^0 is the melting enthalpy of the 100% crystalline PEO (201.2 J/g [20]).

The total crystalline content depends on both the number of nuclei and the mobility of polymer chains. By incorporating nanofibers, nucleation would enhance while the polymer chain mobility could be restricted. Here, the overall crystalline content of PEO decreases in both heating and cooling sequences that can be ascribed to the hindrance effect of the CNFs on PEO chain mobility,

suppressing their participation into ordered structures that results in smaller and less stable crystals [9, 20]. Lowering the large crystalline content of PEO can be beneficial for some applications [2, 10, 11]. Furthermore, the crystallization temperature, T_c, and the melting temperature, T_m, for the composite samples are similar to those of PEO (Table 6.1). Brown and Laborie [20] also reported no change in the melting temperature of PEO and a decrease in the crystalline content of PEO (from 67 to 49%) for the sample containing 15 wt% BCNFs. Xu et al. [5] reported a 4 °C decrease in the melting temperature of PEO and a decrease (from 82 to 79%) in the crystalline content of PEO by incorporating 4 wt% CNFs. Safdari et al. [6] also found no change in the melting temperature, up to 11 °C increase in the crystallization temperature and 18% increase in the $X_c^{cooling}$ of the PLA due to the predominance of the nucleating effect of the CNFs for PLA/5CNF.

Table 6.1: Results of DSC tests for the first heating and cooling cycles.

Sample	T_c (°C)	T_m (°C)	$X_c^{heating}$ (%)	$X_c^{cooling}$ (%)
PEO	50.3 ± 0.1	63.1 ± 0.1	65.4 ± 0.1	65.3 ± 0.1
PEO/1CNF	48.9 ± 0.2	63.0 ± 0.2	61.6 ± 0.1	62.7 ± 0.2
PEO/2CNF	49.8 ± 0.1	63.3 ± 0.1	58.7 ± 0.2	59.2 ± 0.1
PEO/3CNF	49.3 ± 0.2	63.2 ± 0.6	54.6 ± 0.2	55.6 ± 0.3

The data for all temperatures are based on the position of the corresponding peaks.

6.4.4 Tensile properties

Figure 6.4 reports the normalized Young's modulus, E/E_m, tensile strength, σ/σ_m, and elongation at break, $\varepsilon/\varepsilon_m$, for all samples ($m$ stands for the matrix, i.e., PEO). For the solution-prepared samples, the Young modulus increases with CNF content (Figure 6.4a). For PEO/3CNF the modulus is 1.021 GPa, which corresponds to a 49% increase compared to that of PEO (686.8 MPa). For DSC measurements, the specimens were cut from the samples of tensile tests. Since in the heating sequence the composites show a lower crystallinity compared with the neat PEO (Table 6.1), their modulus should decrease. However, this negative effect on the modulus of the composites is compensated by the reinforcement effect and/or a strong nanofiber network in the PEO. Figure 6.4b shows the same trend for tensile strength; an increase of 35% in comparison with PEO (15 MPa) is observed for the solution-prepared composite containing 3 wt% CNFs. This could possibly be ascribed to the enhanced stress transfer from the matrix to the fibers due to a good

interaction between the polymer matrix and CNFs [4, 6, 14]. This strong nanofiber network is also advantageous for transferring the load between the fibers [6]. Xu et al. [5] reported a 31% increase in the Young modulus and 46% increase in the yield strength of PEO by adding 4 wt% CNFs. Safdari et al. [6] observed 50 and 31% enhancements in the Young modulus and tensile strength of PLA by adding 5 wt% CNFs. Figure 6.4c presents the elongation at break for the samples, showing a decrease by ca. 25% for the composite with the largest CNF loading compared with the neat PEO (6.5%). This is the result of reduced chain mobility due to the presence of the filler that generally happens in composite systems [6, 37]. No enhancement in the Young modulus and tensile strength is observed for the composite sample prepared in the molten state, PEO/3CNF (M), possibly due to the presence of large agglomerates and low content of CNFs. Another probable reason is PEO degradation (reduction of its molecular weight) when the composite was prepared in the molten state at 85 °C and 100 rpm via the internal mixer. Similar results have been reported earlier [38, 39]. As the elongation at break of the neat PEO is already quite low, i.e., 6.5%, the marginally larger value for PEO/3CNF (M) compared to PEO/3CNF cannot provide meaningful information on the relative dispersion of CNFs in these two samples; we also note that the tensile strength values show exactly the reverse trend. Thus, further investigations were only performed on solution-prepared samples.

The Young modulus for fiber-reinforced composites can be predicted using the model developed by Halpin and Kardos [40]. The modulus of a 3D randomly-oriented fiber composite, E, is given by

$$\frac{E}{E_m} = 0.184\left[\frac{1+\xi\Psi_L\varphi_f}{1-\Psi_L\varphi_f}\right] + 0.816\left[\frac{1+2\Psi_T\varphi_f}{1-\Psi_T\varphi_f}\right] \qquad (6.5)$$

where

$$\Psi_L = (E_f/E_m - 1)/(E_f/E_m + \xi) \qquad (6.6)$$

and

$$\Psi_T = (E_f/E_m - 1)/(E_f/E_m + 2) \qquad (6.7)$$

where E_m and E_f are the Young moduli of the matrix and the fibers, respectively, φ_f is the fiber volume fraction, ξ is a shape parameter, which is equal to $0.5\ l/d$ for high aspect ratio fibers with diameter and length of d and l, respectively [5].

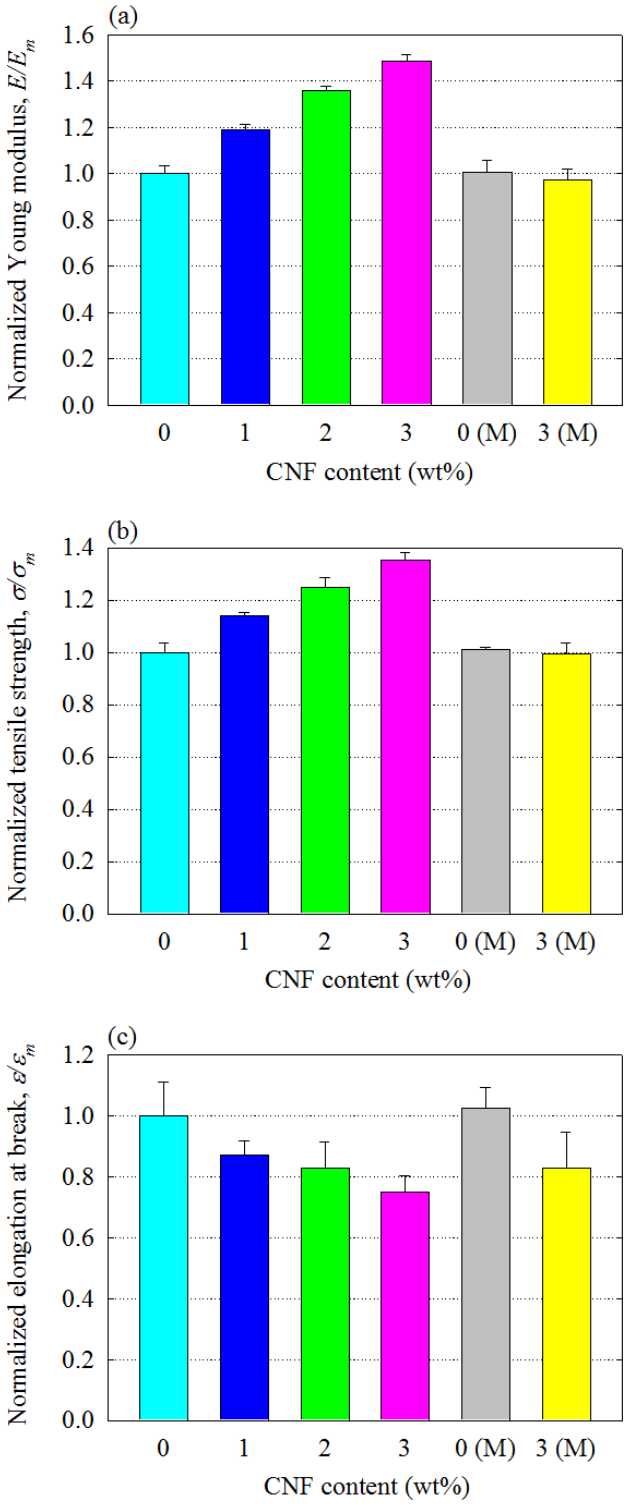

Figure 6.4: Normalized Young's modulus (a), tensile strength (b) and elongation at break (c) for PEO/CNF samples containing different CNF loadings prepared in both solution and melt. For the neat PEO values of 686.8 MPa, 15 MPa and 6.5% for the Young modulus, tensile strength and elongation at break, respectively, were obtained.

To calculate E, the following values were used: E_m = 686.8 MPa, E_f = 150 GPa [6, 41], ρ_m = 1.13 g/cm^3, ρ_f = 1.58 g/cm^3 [6, 13, 14], d = 50 nm [27] and l is ca. 20 µm. Figure 6.5 compares the experimental data with the predictions of the Halpin-Kardos model for l/d = 400, as initially estimated. The model is shown to slightly under-predict the data. Since the nanofibers are highly entangled and form a 3D structure, it is quite hard to estimate the length of the nanofibers. In this regard, a very good fit for the composites of lower CNF contents could be obtained by using a slightly larger aspect ratio, l/d of 553.

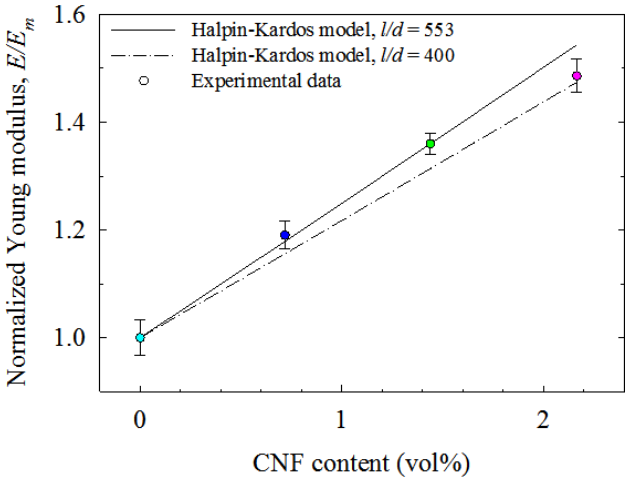

Figure 6.5: Predicted values based on the Halpin-Kardos model, Eq. 6.5 using two aspect ratios for the CNFs, and the experimental data for the normalized Young's modulus of different composite samples.

6.4.5 DMTA

The storage modulus, E', and loss tangent, $\tan\delta$ where δ is the phase angle, for the samples over a wide range of temperatures are presented in Figure 6.6. The composites show larger values of the storage modulus compared to the neat PEO in both glassy and rubbery regions (Figure 6.6a). Moreover, the area under the peak of $\tan\delta$ decreases for the PEO/CNF composites compared to the PEO; the decrease is more important at larger CNF loadings. The normalized area, A/A_m, is equal to 0.55 for the highest CNF loading (i.e., 3 wt%). This is an indicator of the reduction of PEO chain mobility due to good dispersion of the fibers [6, 42]. A lower decrease in A/A_m, from 1 to 0.62, was reported in our previous study for PLA containing 5 wt% CNFs [6].

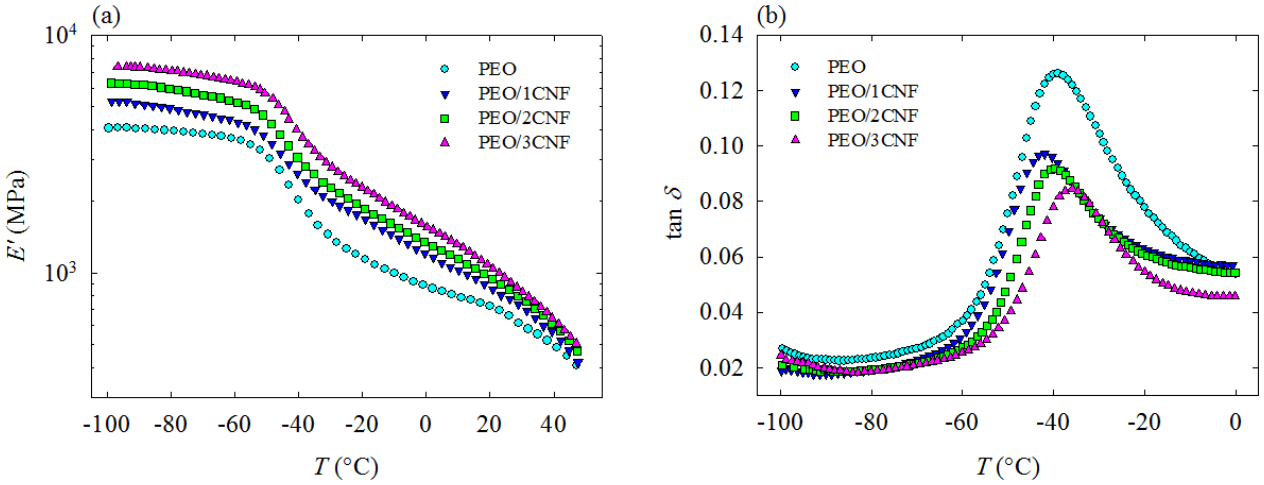

Figure 6.6: Plots of (a) storage modulus and (b) tan δ of the neat PEO and PEO/CNF composites.

The normalized storage moduli, E'/E'_m, at 20 °C of all samples are compared in Figure 6.7. Incorporation of the CNFs into the PEO leads to a significant improvement of the storage modulus due to the good dispersion and reinforcement effect and/or strong entangled network of the cellulosic fibers [6, 14, 43]. It is worth mentioning that the storage modulus data presents a similar trend as the Young modulus (Figure 6.4a). The storage modulus of PEO at 20 °C, 725.2 MPa, increases by 47% for PEO/3CNF (1.064 GPa). Safdari et al. [6] reported a 51% increase in storage modulus of PLA at 25 °C for PLA/5CNF.

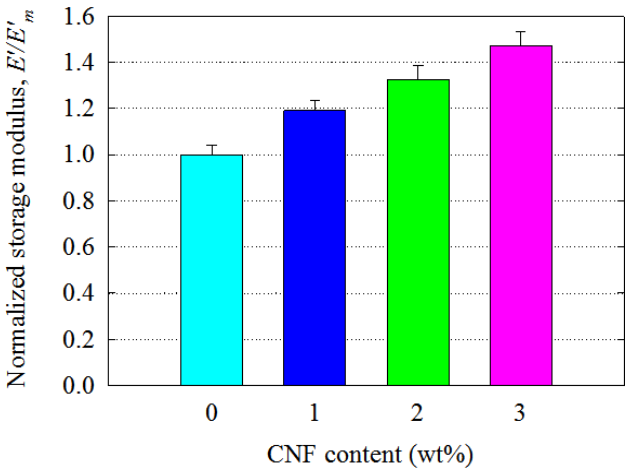

Figure 6.7: Normalized values of the storage modulus at 20 °C for various samples. The storage modulus of the neat PEO at 20 °C is 725.2 MPa.

6.4.6 TGA

Figure 6.8a illustrates TGA data and Figure 6.8b depicts the first derivative of TGA (DTG) for freeze-dried CNFs, PEO and PEO/3CNF. In addition to moisture evaporation (up to 100 °C), PEO and CNF lose 5% of their weight at 380 and 306 °C, respectively, while this temperature is increased to 388 °C for PEO/3CNF. Also, the inflection temperature of PEO increases in the presence of 3 wt% CNFs, while this temperature for CNF is at an even lower temperature. The DTG peak temperature increases for PEO/3CNF compared to the neat PEO (from 384 to 392 °C), while CNF exhibits a peak temperature of 340 °C (Figure 6.8b). The degradation for CNF and PEO starts at 317 and 378 °C (onset temperatures), respectively, (Figure 6.8b); however, it occurs at 387 °C for PEO/3CNF. The same trend exists for the offset temperature of degradation. Consequently, by the addition of CNFs, the thermal stability of PEO does not deteriorate and slightly improves, as it has been previously reported in other investigations [6]. This can be attributed to restricted polymer chains as a result of the good dispersion and distribution of the nanofibers in the PEO [6, 44].

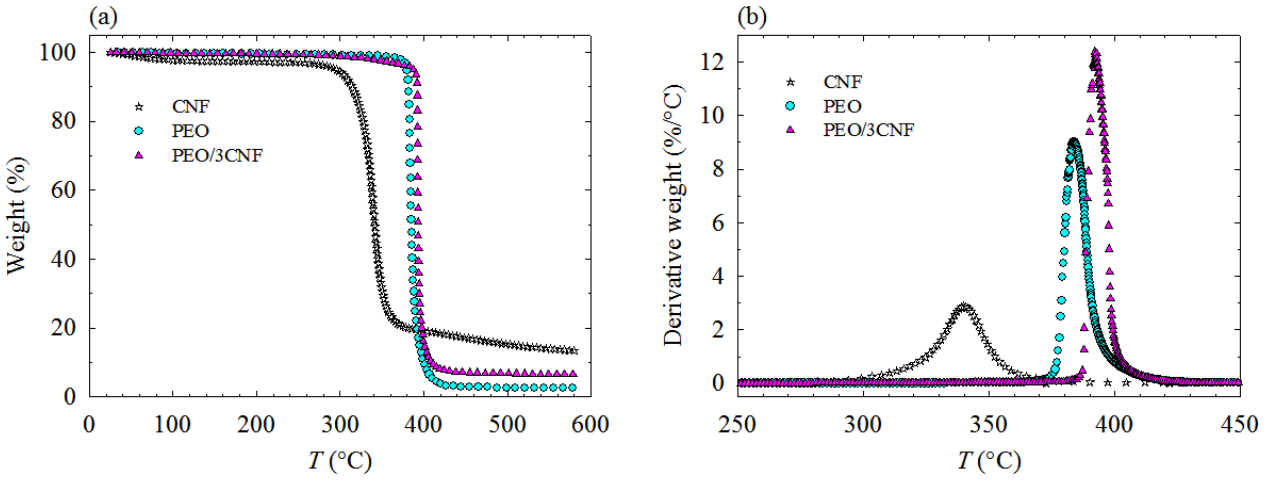

Figure 6.8: Plots of (a) TGA and (b) DTG for freeze-dried CNFs, PEO and PEO/3CNF.

6.4.7 Optical properties

High transparency of composites for many applications is an asset. A good state of dispersion/distribution of filler in the composite film could help maintaining the original transparency of the neat polymer matrix [6, 28]. In most cases, films with acceptable transparency should show values greater than 75% in optical transmittance; lower transmittance values

correspond to more opaque films [6, 45]. The light transmittance versus wavelength, λ, is compared in Figure 6.9 for the neat PEO and PEO/3CNF films. Over the range of visible light (i.e., λ = 390–700 nm), the transparencies of both films are quite similar and the addition of CNFs did not compromise the optical properties of PEO, suggesting good dispersion/distribution of CNFs in PEO [6, 46]. Moreover, a visual comparison of three different films is presented in Figure 6.10. The pictures of PEO and PEO/3CNF films (Figure 6.10a and b, respectively) qualitatively show equivalent transparency, whereas for the PEO/3CNF (M) film (Figure 6.10c) CNF agglomerates, in the form of white particles, are easily observable on the left side of the picture, indicating inadequate dispersion of nanofibers in this sample. Safdari et al. [6] also observed that PLA and PLA/5CNF films show similar transparencies; a decrease of only ca. 5% was reported in transmittance values of PLA film by incorporating 5 wt% CNFs. This provides the opportunity for optical and optoelectronic applications [5, 6, 21, 27, 47, 48], where other reinforcing agents (nanoclays and carbon nanotubes) deteriorate the transparency of the final products [5, 6].

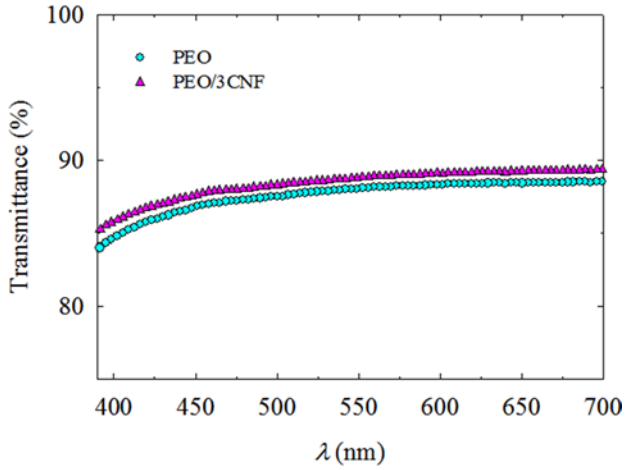

Figure 6.9: Light transmittance of PEO and PEO/3CNF films of 145 ± 18 µm thickness.

Figure 6.10: Visual comparison of (a) PEO, (b) PEO/3CNF, and (c) PEO/3CNF (M) films (thickness of 145 ± 18 µm).

6.5 Concluding remarks

A simple aqueous solution technique was used to prepare composites based on PEO and CNFs. The nanofibers were uniformly dispersed within PEO and no large fiber bundles were observed in SEM micrographs. The rheological behavior of the PEO significantly changed in the presence of nanofibers with the percolation threshold being in the range of 1 and 2 wt% CNFs. DSC results confirmed that reinforcing by the CNFs is the main reason for the enhancement of the mechanical properties since the crystalline content of PEO decreased in the presence of nanofibers. The Young modulus and tensile strength of PEO improved for the composites with the CNF content, up to 49 and 35%, respectively, for the composite sample containing only 3 wt% nanofibers. To predict the Young moduli of composites, the Halpin-Kardos model was employed and good agreement between experimental data and the predictions was observed. The storage modulus in DMTA was improved for all tested temperatures and the area under the peak of $\tan\delta$ decreased by incorporating the nanofibers; a 47% enhancement in storage modulus of PEO at 20 °C was achieved for PEO/3CNF. Furthermore, considerably larger storage modulus values of the composites compared with the neat PEO were observed at lower temperatures. Moreover, incorporating CNFs enhanced the thermal stability of PEO. The neat PEO and composite films showed similar transparency in the range of visible light.

The composite sample prepared using a melt mixing process did not exhibit any increases in rheological and mechanical properties of the matrix. This shows that dispersing highly entangled CNFs within a polar matrix, such as PEO, is quite challenging and not very easy to achieve via conventional direct melt mixing techniques. Hence, although melt processing is preferable from an industrial point of view, the solution-based preparation method is more efficient to prepare PEO/CNF composites with well-dispersed/distributed structure.

From the results presented in this work, it can be concluded that the reinforcement effect of nanofibers can expand the applications of PEO to cases where good thermal properties, enhanced mechanical properties in a wide temperature range and transparency are important factors. Also, the observed improvements for the PEO/CNF composites compared to PEO point out the importance of the solution technique used in this investigation to finely disperse and distribute CNFs within the PEO matrix.

6.6 Acknowledgments

The authors are greatly thankful for the financial support from the Natural Sciences and Engineering Research Council of Canada (NSERC) and Network for Innovative Plastic Materials and Manufacturing Processes (NIPMMP). They also appreciated the reviewers' helpful comments.

6.7 References

[1] Azizi Samir MAS, Alloin F, Dufresne A. Review of Recent Research into Cellulosic Whiskers, Their Properties and Their Application in Nanocomposite Field. Biomacromolecules. 2005;6(2):612-626.

[2] Azizi Samir MAS, Alloin F, Sanchez JY, Dufresne A. Cellulose Nanocrystals Reinforced Poly(oxyethylene). Polymer. 2004;45(12):4149-4157.

[3] Kloser E and Gray DG. Surface Grafting of Cellulose Nanocrystals with Poly(ethylene oxide) in Aqueous Media. Langmuir. 2010;26(16):13450-13456.

[4] Miao C and Hamad WY. Cellulose Reinforced Polymer Composites and Nanocomposites: A Critical Review. Cellulose. 2013;20(5):2221-2262.

[5] Xu X, Liu F, Jiang L, Zhu JY, Haagenson D, Wiesenborn DP. Cellulose Nanocrystals vs. Cellulose Nanofibrils: A Comparative Study on Their Microstructures and Effects as Polymer Reinforcing Agents. ACS Applied Materials and Interfaces. 2013;5(8):2999-3009.

[6] Safdari F, Bagheriasl D, Carreau PJ, Heuzey MC, Kamal MR. Rheological, Mechanical, and Thermal Properties of Polylactide/Cellulose Nanofiber Biocomposites. Polymer Composites. 2016.

[7] Frenot A, Henriksson MW, Walkenström P. Electrospinning of Cellulose-Based Nanofibers. Journal of Applied Polymer Science. 2007;103(3):1473-1482.

[8] Alloin F, D'Aprea A, Dufresne A, El Kissi N, Bossard F. Poly(oxyethylene) and Ramie Whiskers Based Nanocomposites: Influence of Processing: Extrusion and Casting/Evaporation. Cellulose. 2011;18(4):957-973.

[9] Zhou C, Chu R, Wu R, Wu Q. Electrospun Polyethylene Oxide/Cellulose Nanocrystal Composite Nanofibrous Mats with Homogeneous and Heterogeneous Microstructures. Biomacromolecules. 2011;12(7):2617-2625.

[10] Azizi Samir MAS, Mateos AM, Alloin F, Sanchez JY, Dufresne A. Plasticized Nanocomposite Polymer Electrolytes Based on Poly(oxyethylene) and Cellulose Whiskers. Electrochimica Acta. 2004;49(26):4667-4677.

[11] Azizi Samir MAS, Chazeau L, Alloin F, Cavaillé JY, Dufresne A, Sanchez JY. POE-Based Nanocomposite Polymer Electrolytes Reinforced with Cellulose Whiskers. Electrochimica Acta. 2005;50(19):3897-3903.

[12] Nakagaito AN, Fujimura A, Sakai T, Hama Y, Yano H. Production of Microfibrillated Cellulose (MFC)-Reinforced Polylactic Acid (PLA) Nanocomposites from Sheets Obtained by a Papermaking-Like Process. Composite Science and Technology. 2009;69(7–8):1293-1297.

[13] Wang B and Sain M. The Effect of Chemically Coated Nanofiber Reinforcement on Biopolymer Based Nanocomposites. Bioresources. 2007;2(3):371-388.

[14] Jonoobi M, Harun J, Mathew AP, Oksman K. Mechanical Properties of Cellulose Nanofiber (CNF) Reinforced Polylactic Acid (PLA) Prepared by Twin Screw Extrusion. Composite Science and Technology. 2010;70(12):1742-1747.

[15] Iwatake A, Nogi M, Yano H. Cellulose Nanofiber-Reinforced Polylactic Acid. Composite Science and Technology. 2008;68(9):2103-2106.

[16] Tingaut P, Zimmermann T, Lopez-Suevos F. Synthesis and Characterization of Bionanocomposites with Tunable Properties from Poly(lactic acid) and Acetylated Microfibrillated Cellulose. Biomacromolecules. 2010;11(2):454-464.

[17] Xu X, Wang H, Jiang L, Wang X, Payne SA, Zhu JY, Li R. Comparison between Cellulose Nanocrystal and Cellulose Nanofibril Reinforced Poly(ethylene oxide) Nanofibers and Their Novel Shish-Kebab-Like Crystalline Structures. Macromolecules. 2014;47(10):3409-3416.

[18] Kaczmarek H, Bajer K, Gałka P, Kotnowska B. Photodegradation Studies of Novel Biodegradable Blends Based on Poly(ethylene oxide) and Pectin. Polymer Degradation and Stability. 2007;92(11):2058-2069.

[19] Cai Z and Kim J. Bacterial Cellulose/Poly (ethylene glycol) Composite: Characterization and First Evaluation of Biocompatibility. Cellulose. 2010;17(1):83-91.

[20] Brown EE and Laborie MPG. Bioengineering Bacterial Cellulose/Poly(ethylene oxide) Nanocomposites. Biomacromolecules. 2007;8(10):3074-3081.

[21] Siró I and Plackett D. Microfibrillated Cellulose and New Nanocomposite Materials: a Review. Cellulose. 2010;17(3):459-494.

[22] Park OH, Eo YJ, Choi YK, Bae BS. Preparation and Optical Properties of Silica-Poly(ethylene oxide) Hybrid Materials. Journal of Sol-Gel Science and Technology. 1999;16(3):235-241.

[23] Elimat ZM. Optical Characterization of Poly (ethylene oxide)/Zinc Oxide Thin Films. Radiation Effects and Defects in Solids. 2014;169(8):686-695.

[24] Fortunato G, Zimmermann T, Lübben J, Bordeanu N, Hufenus R. Reinforcement of Polymeric Submicrometer-sized Fibers by Microfibrillated Cellulose. Macromolecular Materials and Engineering. 2012;297(6):576-584.

[25] Iyer KA, Schueneman GT, Torkelson JM. Cellulose Nanocrystal/Polyolefin Biocomposites Prepared by Solid-State Shear Pulverization: Superior Dispersion Leading to Synergistic Property Enhancements. Polymer. 2015;56:464-475.

[26] Hamad WY and Miao C. "Nanocomposite Biomaterials of Nanocrystalline Cellulose (NCC) and Polylactic Acid (PLA)" US 8,829,110 B2, 2014, 2014.

[27] Janardhnan S and Sain M. Bio-Treatment of Natural Fibers in Isolation of Cellulose Nanofibres: Impact of Pre-Refining of Fibers on Bio-Treatment Efficiency and Nanofiber Yield. Journal of Polymers and the Environment. 2011;19(3):615-621.

[28] Eichhorn SJ, Dufresne A, Aranguren M, Marcovich NE, Capadona JR, Rowan SJ, Weder C, Thielemans W, Roman M, Renneckar S, Gindl W, Veigel S, Keckes J, Yano H, Abe K, Nogi M, Nakagaito AN, Mangalam A, Simonsen J, Benight AS, Bismarck A, Berglund LA, Peijs, T. Review: Current International Research into Cellulose Nanofibres and Nanocomposites. Journal of Materials Science. 2010;45(1):1-33.

[29] Hu G, Zhao C, Zhang S, Yang M, Wang Z. Low Percolation Thresholds of Electrical Conductivity and Rheology in Poly(ethylene terephthalate) Through the Networks of Multi-Walled Carbon Nanotubes. Polymer. 2006;47(1):480-488.

[30] Kamal MR and Khoshkava V. Effect of Cellulose Nanocrystals (CNC) on Rheological and Mechanical Properties and Crystallization Behavior of PLA/CNC Nanocomposites. Carbohydrate Polymers. 2015;123:105-14.

[31] Safdari F, Bagheriasl D, Carreau PJ, Heuzey MC, Kamal MR. High-Performance Polylactide Biocomposites Reinforced with Cellulose Nanofibers. SPE Plastics Research Online. 2016.

[32] Bagheriasl D, Carreau PJ, Riedl B, Dubois C, Hamad WY. Shear Rheology of Polylactide (PLA)–Cellulose Nanocrystal (CNC) Nanocomposites. Cellulose. 2016;23(3):1885-1897.

[33] Khoshkava V and Kamal MR. Effect of Cellulose Nanocrystals (CNC) Particle Morphology on Dispersion and Rheological and Mechanical Properties of Polypropylene/CNC Nanocomposites. ACS Applied Materials and Interfaces. 2014;6(11):8146-8157.

[34] Ghanbari A, Heuzey MC, Carreau PJ, Ton-That MT. A Novel Approach to Control Thermal Degradation of PET/Organoclay Nanocomposites and Improve Clay Exfoliation. Polymer. 2013;54(4):1361-1369.

[35] Ghanbari A, Heuzey MC, Carreau PJ, Ton-That MT. Morphological and Rheological Properties of PET/Clay Nanocomposites. Rheologica Acta. 2013;52(1):59-74.

[36] Abbasi S, Carreau PJ, Derdouri A, Moan M. Rheological Properties and Percolation in Suspensions of Multiwalled Carbon Nanotubes in Polycarbonate. Rheologica Acta. 2009;48(9):943-959.

[37] Arias A, Heuzey MC, Huneault M. Thermomechanical and Crystallization Behavior of Polylactide-Based Flax Fiber Biocomposites. Cellulose. 2013;20(1):439-452.

[38] Sanchez-Garcia M and Lagaron J. On the Use of Plant Cellulose Nanowhiskers to Enhance the Barrier Properties of Polylactic Acid. Cellulose. 2010;17(5):987-1004.

[39] Lee JY, Su KE, Chan EP, Zhang Q, Emrick T, Crosby AJ. Impact of Surface-Modified Nanoparticles on Glass Transition Temperature and Elastic Modulus of Polymer Thin Films. Macromolecules. 2007;40(22):7755-7757.

[40] Halpin JC and Kardos JL. Moduli of Crystalline Polymers Employing Composite Theory. Journal of Applied Physics. 1972;43(5):2235-2241.

[41] Wang S, Cheng Q, Rials TG, Lee SH. "Cellulose Microfibril/Nanofibril and Its Nanocompsites" in *The 8th Pacific rim bio-based composites symposium*, Kuala Lumpur, Malaysia, 2006, pp. 301-308.

[42] Bagheriasl D, Carreau PJ, Dubois C, Riedl B. Properties of Polypropylene and Polypropylene/Poly(ethylene-co-vinyl alcohol) Blend/CNC Nanocomposites. Composite Science and Technology. 2015;117:357-363.

[43] Azizi Samir MAS, Alloin F, Paillet M, Dufresne A. Tangling Effect in Fibrillated Cellulose Reinforced Nanocomposites. Macromolecules. 2004;37(11):4313-4316.

[44] Ramezani Kakroodi A, Cheng S, Sain M, Asiri A. Mechanical, Thermal, and Morphological Properties of Nanocomposites Based on Polyvinyl Alcohol and Cellulose Nanofiber from Aloe vera Rind. Journal of Nanomaterials. 2014;2014:1-7.

[45] Ambrosio-Martín J, Fabra MJ, Lopez-Rubio A, Lagaron JM. Melt Polycondensation to Improve the Dispersion of Bacterial Cellulose into Polylactide via Melt Compounding: Enhanced Barrier and Mechanical Properties. Cellulose. 2015;22(2):1201-1226.

[46] Petersson L and Oksman K. Biopolymer Based Nanocomposites: Comparing Layered Silicates and Microcrystalline Cellulose as Nanoreinforcement. Composite Science and Technology. 2006;66(13):2187-2196.

[47] Kalia S, Boufi S, Celli A, Kango S. Nanofibrillated Cellulose: Surface Modification and Potential Applications. Colloid and Polymer Science. 2014;292(1):5-31.

[48] Tercjak A, Gutierrez J, Barud HS, Domeneguetti RR, Ribeiro SJL. Nano- and Macroscale Structural and Mechanical Properties of in Situ Synthesized Bacterial Cellulose/PEO-b-PPO-b-PEO Biocomposites. ACS Applied Materials and Interfaces. 2015;7(7):4142-4150.

CHAPTER 7 ARTICLE 3 : EFFECTS OF POLY(ETHYLENE GLYCOL) ON THE MORPHOLOGY AND PROPERTIES OF BIOCOMPOSITES BASED ON POLYLACTIDE AND CELLULOSE NANOFIBERS[3]

Fatemeh Safdari[a], Pierre J. Carreau[a*], Marie C. Heuzey[a], Musa R. Kamal[b]

[a] *Research Center for High Performance Polymer and Composite Systems (CREPEC), Chemical Engineering Department, Polytechnique Montreal, Montreal, Quebec H3C 3A7, Canada*

[b] *CREPEC, Chemical Engineering Department, McGill University, Montreal, Quebec H3A 0C5, Canada*

Parts of this chapter have been presented at the:

- *CREPEC Annual Conference*, Montreal, Canada (December 2016), winner of the "*Third Prize Award*" in poster competition
- *International Conference on Bio-Based Materials and Composites (ICBMC)*, Nantes, France (March 2017)

[3] Accepted in *Cellulose*.

7.1 Abstract

Polylactide (PLA)/cellulose nanofiber (CNF) biocomposites were prepared via solution casting and direct melt mixing. To improve the compatibility, a masterbatch of CNFs and poly(ethylene glycol) (PEG) (1:2) was also prepared. The effects of PEG on the morphology and properties of the biocomposites were investigated. The dispersion/distribution of nanofibers in PLA was improved when the masterbatch was used and the composites were prepared in solution. Substantial effects on the rheological properties of solution-prepared PLA/CNF/PEG composites were observed compared to composites containing no PEG, whereas for melt-prepared composites no significant changes were detected. Increased crystalline content and crystallization temperature were observed for the composites prepared via the masterbatch and solvent casting. The storage modulus of PLA was increased by 42 and 553% at 25 and at 80 °C, respectively, for the solution-based PEG-compatibilized composite containing 2 wt% nanofibers. Also, a better light transmittance was measured for the PLA/CNF/PEG composites prepared in solution.

Keywords: *Biocomposites*, *Polylactide (PLA)*, *Cellulose nanofibers (CNFs)*, *Rheology*, *Crystallinity*, *Thermomechanical Properties*, *Transparency*

7.2 Introduction

Composites are usually designed to produce materials with new and/or enhanced properties compared to those of the matrices. Sustainability and environmental considerations have made it desirable to use polymers derived from renewable resources as alternatives to petroleum-based polymers [1]. Thus, the preparation of composites from fully bio-based components is highly desirable. In this regard, bio-derived polylactide (PLA), a semi-crystalline thermoplastic polyester [2-5], has been the frontrunner among other biopolymers, owing to its interesting mechanical properties, relatively good processability, low toxicity, moderate cost, UV stability, and gloss [1, 3-13]. PLA has found many applications in different fields such as biomedical, automotive and textile applications, in addition to electronics and packaging and many other industries [4, 5, 12, 14-22]. However, the use of PLA for many applications presents a variety of issues. Its slow crystallization [20] and low heat resistance (low stiffness at elevated temperatures) limit its applications [2, 6, 7, 9, 11, 20]. These limitations can be circumvented by different approaches including copolymerization, blending, and use of reinforcements, which has been considered as a

promising method to enhance the properties of PLA [2, 7]. It is important that the advantages of PLA such as biocompatibility, biodegradability and transparency can be maintained when choosing an appropriate reinforcement. To this end, some common nanofillers (e.g. carbon nanotubes) may not be appropriate as they are not biocompatible and biodegradable and that they may deteriorate the transparency of the matrix.

Cellulose is the most abundant biopolymer produced in nature [1, 6, 23]. It can be extracted in the form of nanofibers, that have been used in many fields including cosmetics, medical applications, food packaging, construction, electronics and automotive [12, 16, 21, 23-26]. Cellulose nanofibers (CNFs) have shown excellent properties of interest as reinforcement in composites, including high sound attenuation, high strength and modulus, large aspect ratio and surface area, biodegradability, biocompatibility, low density, low cost, low energy consumption, nontoxicity and non-abrasiveness to the processing equipment [1, 2, 6, 9-13, 15, 16, 18-22, 24-33]. Thus, the use of CNFs to develop reinforced PLA composites, considering their entirely bio-based nature, would be preferable over that of other inorganic particles [20, 24, 30].

Achieving uniformly dispersed nanofibers in PLA and assuring nanofiber–polymer interfacial compatibility are important challenges in the preparation of PLA/CNF biocomposites. This is due to the very strong hydrogen bond interactions between the long and flexible CNFs that cause their agglomeration. Furthermore, the difference in polarity between PLA and CNFs favors agglomeration [5, 10, 32, 34]. Therefore, special processing methods and compatibilization strategies are required to promote interfacial compatibility between nonpolar polymer matrices and CNFs. Good dispersion with minor agglomeration of CNFs within PLA may be obtained by compatibilization through chemical modification of either CNFs [2, 3, 5, 9, 10, 12, 15, 17, 27, 32, 35] or PLA [4, 9]. The use of a compatibilizer as a third component, which may be easier and more cost effective, can be an interesting alternative [11, 22, 27, 36]. In most cases, compatibilization is conducted in solution and a drying step is needed prior to the addition of compatibilized CNFs to the matrix. However, the tendency to agglomerate during the drying step would make re-dispersion of compatibilized CNFs in the matrix in molten state still difficult. Thus, composite preparation in solution could be a good alternative to achieve good dispersion [18, 20, 24, 30].

Several efforts have been made to produce PLA/CNF biocomposites with nanofiber contents of 1–5 wt% and using a compatibilizer to enhance the properties of PLA, but with limited success so

far. Mathew et al. [36] prepared cellulose microfiber (CMF)-reinforced PLA by adding poly(ethylene glycol) (PEG) as a processing aid. The CMF/PEG aqueous suspension was pumped into the PLA melt stream during extrusion. However, the tensile strength remained unchanged and the Young modulus increased by only 15% for the PLA/CMF/PEG composite containing 5 wt% fibers and 5 wt% PEG compared to PLA. Wang and Sain [27] modified hemp nanofibers (HPNs) using styrene maleic anhydride copolymer (SMA) in solution. The modified nanofibers were then freeze-dried and used to produce composites via an internal batch mixer. However, the dispersion of the modified nanofibers in PLA was not uniform and agglomerates were still formed. The tensile strength and Young's modulus increased by 9 and 10%, respectively, for the composite sample containing 5 wt% SMA-modified HPNs. Qu et al. [11] also prepared PLA/CNF composites using N,N-dimethylacetamide (DMAc) as the solvent and PEG as the compatibilizer in a solvent-casting method. All the components were added into DMAc with CNF/PEG at a ratio 3/2. The tensile strength was slightly increased from ca. 40 MPa for PLA to ca. 45 MPa for the PLA/CNF/PEG sample containing 2 wt% fibers. Lee et al. [22] incorporated bio-derived polylactide carbohydrate copolymer to compatibilize bacterial cellulose nanofibers (BCNFs) with PLA. They added PLA, CNFs and the copolymer into 1,4-dioxane. The suspension was then immersed in liquid nitrogen and subsequently dried using a freeze-dryer prior to the injection molding step. Both the glass transition and crystallization temperatures of the matrix were reduced for the composite containing 5 wt% BCNFs with 4.75 wt% copolymer, while the crystalline content of PLA increased. The tensile strength and Young's modulus of the composite were improved by 7 and 15%, respectively, compared to PLA.

In our previous work [34, 37], solvent casting was employed to incorporate CNFs into PLA to overcome some of its drawbacks, e.g. slow crystallization and low heat resistance, which could successfully improve the properties in different aspects without deteriorating the thermal stability and transparency of the matrix. In the current study, in order to further improve the dispersion/distribution of nanofibers within the PLA matrix, PEG is used as a compatibilizer to produce biocompatible and biodegradable PLA/CNF/PEG composites. The choice of PEG is justified by its miscibility with PLA [38-41] and its better affinity with CNFs compared to PLA. A solvent-casting technique is used to prepare PLA/CNF/PEG composites with enhanced properties at low nanofiber loadings. Effects of PEG on the morphology, rheological, thermal, mechanical, and optical properties of the CNF-reinforced PLA composites are then reported. This work shows

that the rheological properties are correlated with the quality of the dispersion/distribution of CNFs in the matrix and the thermo mechanical properties of the polymer/CNF composites. To our knowledge, such full characterization of PLA/CNF composites with the emphasis on the improved CNF dispersion/distribution that could successfully lead to major property enhancements has not been reported.

7.3 Experimental section

7.3.1 Materials

A polylactide (PLA) (Ingeo Biopolymer 3251D, NatureWorks, Minnetonka, MN, USA) with a melting point of 155–170 °C, weight-average molecular weight of 55,000 g/mol, and polydispersity index of 1.62 [42] was used. A poly(ethylene glycol) (PEG) in flake form with a number-average molecular weight of 20,000 g/mol and a melting point of 63–66 °C was purchased from Sigma-Aldrich Canada Co. (Oakville, ON, Canada). The solvent, N,N-dimethylformamide (DMF), was used as received (anhydrous 99.8% from Sigma-Aldrich Canada Co., Oakville, ON, Canada). An aqueous suspension containing 2.3 wt% cellulose nanofibers (CNFs), with a diameter less than 50 nm and length of several micrometers, was kindly provided by Prof. Mohini M. Sain following the methodology described in [43]. A copper(II)-ethylenediamine complex 1.0 M in H_2O (Sigma-Aldrich Canada Co., Oakville, ON, Canada) was used to stain the CNFs in composites prior to the transmission electron microscopy.

7.3.2 Sample preparation

The aqueous suspension of CNFs was freeze-dried for 48 h (Labconco Freezone 2.5^{Plus}). The freeze-dried CNFs were mixed with an appropriate amount of DMF in an Erlenmeyer to form CNF suspensions containing 4–10 g of CNFs per L of DMF. The suspension was sonicated for 1 h using a water-bath sonicator (FS30 100 Watts Ultrasonic Cleaner, Fisher Scientific, Pittsburgh, PA, USA) and, then, stirred for 1 more hour using a magnetic stirrer at 400 rpm. Vacuum-dried PLA, at 80 °C for 24 h, was added to the suspension and stirred at 400 rpm, 70 °C and for 2 h until the PLA pellets were completely dissolved. Finally, the mixture was vacuum dried in an oven at 80 °C for 24 h, and, the product was then ground into small granules using a laboratory grinder (Janke & Kunkel A10S1 model, IKA WERK, Germany) and kept again for 48 h in a vacuum oven at 60 °C.

A masterbatch of CNFs and PEG was prepared via an aqueous mixing method at ambient temperature. The original CNF aqueous suspension was diluted with distilled water in an Erlenmeyer using a magnetic stirrer at 400 rpm for 1 h to form a 1 wt% CNF suspension and the desired amount of PEG was added for a weight ratio of CNFs to PEG 1:2, then, stirred for 1 more hour. Finally, the mixture was vacuum dried for 48 h at 50 °C to be used as the masterbatch of compatibilized CNFs for the composite fabrication following the same solution preparation technique described above. The various samples containing CNFs or PEG or CNF/PEG masterbatch are identified based on their fiber and PEG contents, 0–5 and 0–4 wt%, respectively. For instance, PLA/2CNF/4PEG denotes composite containing 2 wt% CNFs and 4 wt% PEG of the overall composite. The samples of the neat PLA and PLA/4PEG were also produced using a similar procedure to compare the results.

To investigate the effect of different preparation techniques on the dispersion and distribution of nanofibers and final properties of the biocomposites, the neat PLA and biocomposites were also prepared in the melt using an internal mixer, DDRV501 Brabender (C. W. Brabender Instruments Inc., NJ, USA). These samples are denoted with a "(M)", referring to preparation in the molten state. For this purpose, the as-received PLA and PEG were dried at 80 and 50 °C, respectively, under vacuum for 24 h. The freeze-dried CNFs, the masterbatch or PEG were directly melt-compounded with PLA for 7 min, at 100 rpm and 180 °C under nitrogen. Thereafter, the samples were immersed in liquid nitrogen, then ground into small granules and dried.

Finally, all the samples formulated using both methods, solution and melt, were molded using a compression press (12 Ton Manual Hydraulic Press, Carver, Inc., Wabash, IN, USA) at 175 °C for 10 min in the presence of nitrogen to prepare different test specimens. The pressure was gradually increased up to 29 kPa. After compression molding, the samples were cooled in the press under 29 kPa at room temperature for 5 min and, then, were kept under vacuum before subsequent testing.

7.3.3 Characterization

7.3.3.1 Microscopy

Gold-coated microtomed sample surfaces were investigated by scanning electron microscopy (SEM) using a JSM 7600TFE microscope (JEOL USA, Inc., Peabody, MA, USA).

For transmission electron microscopy (TEM), the samples were microtomed at ca. -100 °C with a diamond knife into slices with an approximate thickness of 50–80 nm using an Ultracut FC microtome (Leica Biosystems Inc., Concord, ON, Canada). Then, the ultra-microtomed sample slices were characterized by TEM using a JEM 2100F microscope (JEOL USA, Inc., Peabody, MA, USA). For a better visualization of nanofibers, the samples were stained using a copper(II)-ethylenediamine complex 1.0 M in H_2O. The details of the staining are given elsewhere [44].

Images of ultra-microtomed surfaces of composites were obtained using a multimode scanning probe in tapping mode on Dimension FastScan atomic force microscope (AFM) with ScanAsyst^{TM} from BRUKER (Billerica, MA, USA).

7.3.3.2 Rheology

The rheological properties were measured at 175 °C in the presence of nitrogen using a stress-controlled rheometer (MCR 301, Anton Paar, Austria). A cone-and-plate geometry with 0.051 mm cone truncation, ca. 2° cone angle and 25 mm diameter, was used to perform the measurements in small-amplitude oscillatory shear (SAOS) mode in the linear viscoelastic region. The thermal stability in time sweep tests was assessed at 1 rad/s frequency for 15 min. All the samples exhibited stable rheological properties, with changes less than 4%, in time-sweep tests. A strain amplitude of 0.05 was used to perform frequency sweeps within the time limit of measurements (i.e., 15 min).

7.3.3.3 Mechanical and thermal properties

For thermogravimetric analysis (TGA), a TGA Q500 (TA Instruments, New Castle, DE, USA) was used in high-resolution mode. The samples were heated to 800 °C at a rate of 10 °C/min and a nitrogen flow rate of 60 mL/min. The tests were performed twice on typically 15 mg specimens for each sample.

Differential scanning calorimetry (DSC) was performed using a DSC Q1000 (TA Instruments, New Castle, DE, USA), under nitrogen. A rate of 2 °C/min was chosen to heat the samples, from room temperature to 200 °C, and then, the samples were held at 200 °C for 3 min, and finally cooled (2 °C/min) to 20 °C. Two replicates were tested for each sample.

Tensile tests were performed on specimens with dumb-bell shape type V (standard ASTM D638) using an Instron 3365 (Instron, Norwood, MA, USA). The tests were carried out at room

temperature with a load cell of 5 kN and a crosshead speed of 5 mm/min. At least seven specimens per sample were tested.

Dynamic mechanical thermal analysis (DMTA) was performed in flexion mode using a DMA 2980 analyzer (TA Instruments, New Castle, DE, USA). The frequency, amplitude and heating rate were 1 Hz, 30 μm and 2 °C/min (from room temperature to 120 °C), respectively. At least three replicates per sample were tested.

7.3.3.4 Optical properties

The optical transparency was investigated on films of 102 ± 6 μm thickness, using a LAMBDA 1050 UV/Vis/NIR Spectrophotometer (PerkinElmer, Waltham, MA, USA). The wavelength range was 250–800 nm with 5 nm spectral bandwidth and 141 nm/min scanning rate. The test was performed three times for each sample.

7.4 Results and discussion

7.4.1 SEM

Figure 7.1 illustrates SEM images of the freeze-dried CNFs (from an aqueous suspension containing 0.1 wt% nanofibers) and PLA containing 2 wt% CNFs with and without PEG. A web-like structure of individual nanofibers and bundles are observed in Figure 7.1a-c, even when the nanofibers are dispersed in the preferred medium, i.e., water [31]. The SEM images of PLA/2CNF, presented in Figure 7.1d-f, show a moderately fair dispersion and uniform distribution of the fibers in PLA at the micro level. However, Figure 7.1g-i show that CNFs are very well dispersed/distributed within the matrix for the PLA/2CNF/4PEG composite, which is related to the efficient compatibilization effect of PEG; also, there is no fiber pull-out for this composite, contrary to the PLA/2CNF sample, suggesting a better adhesion between CNFs and PLA in the presence of PEG. Moreover, the SEM images of PLA/2CNF/4PEG (Figure 7.1g-i) do not show a two-phase system indicating that PEG is miscible with PLA; hence, the nanofibers are distributed over the whole sample.

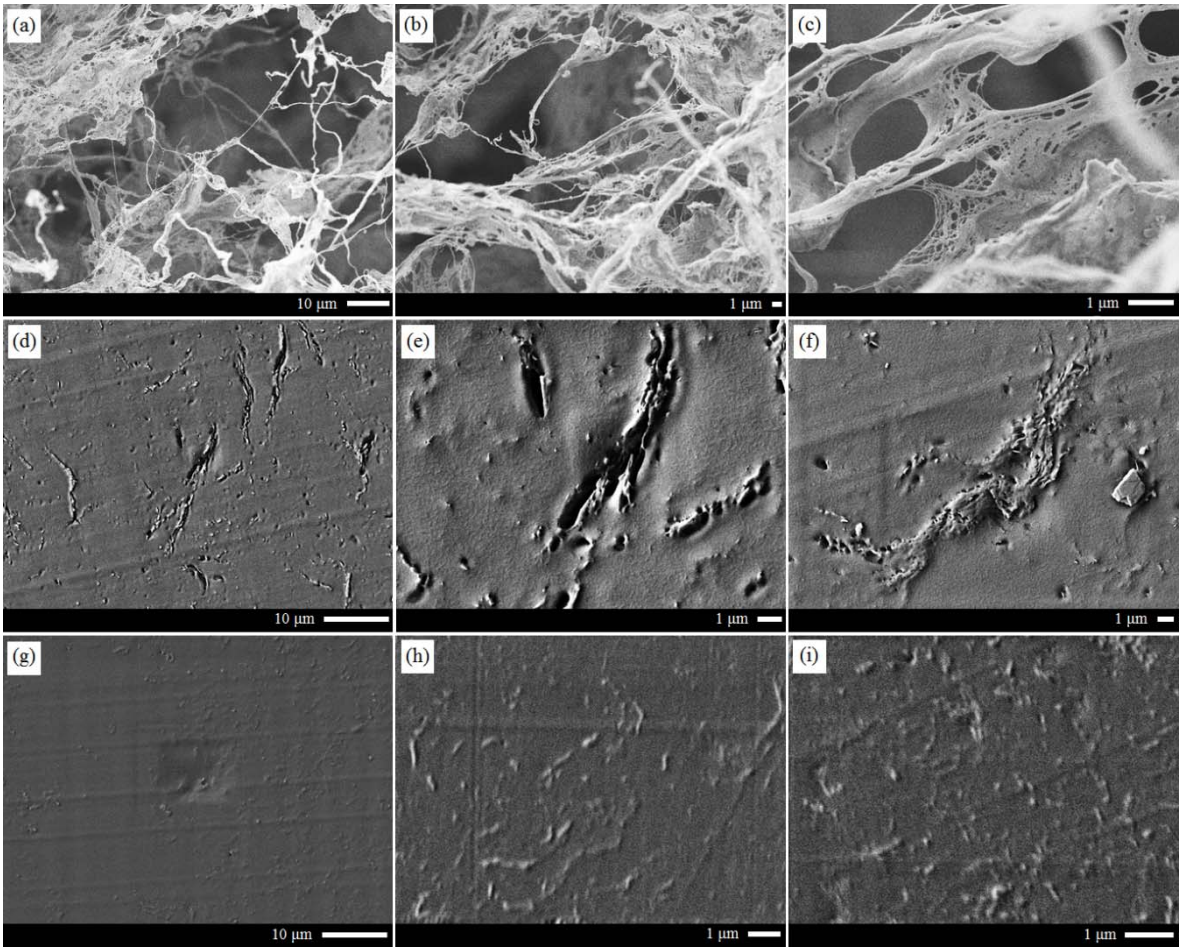

Figure 7.1: SEM images of (a-c) freeze-dried CNFs, (d-f) PLA/2CNF and (g-i) PLA/2CNF/4PEG, taken from different samples and/or at different magnifications.

7.4.2 Transmission electron microscopy (TEM)

Figure 7.2a shows the web-like structure of single CNFs and bundles of nanofibers after water evaporation (CNF concentration of 0.5 wt% in the aqueous suspension). TEM images of PLA/2CNF and PLA/2CNF/4PEG are presented in Figure 7.2b-e and Figure 7.2f-i, respectively. The quality of the nanofiber dispersion/distribution for composites prepared without PEG is clearly different from that for PEG-compatibilized composites (Figure 7.2b-e compared to Figure 7.2f-i). For PLA/2CNF in Figure 7.2b-e, no large agglomerates are seen, but there are not many single fibers; however, for PLA/2CNF/4PEG in Figure 7.2f-i, more CNFs are dispersed individually and/or in the form of bundles with few fibers. Also, the CNF distribution at the nano level is quite good for the sample containing PEG over the other composites. This is a consequence of using the CNF/PEG masterbatch to produce the PLA/2CNF/4PEG sample.

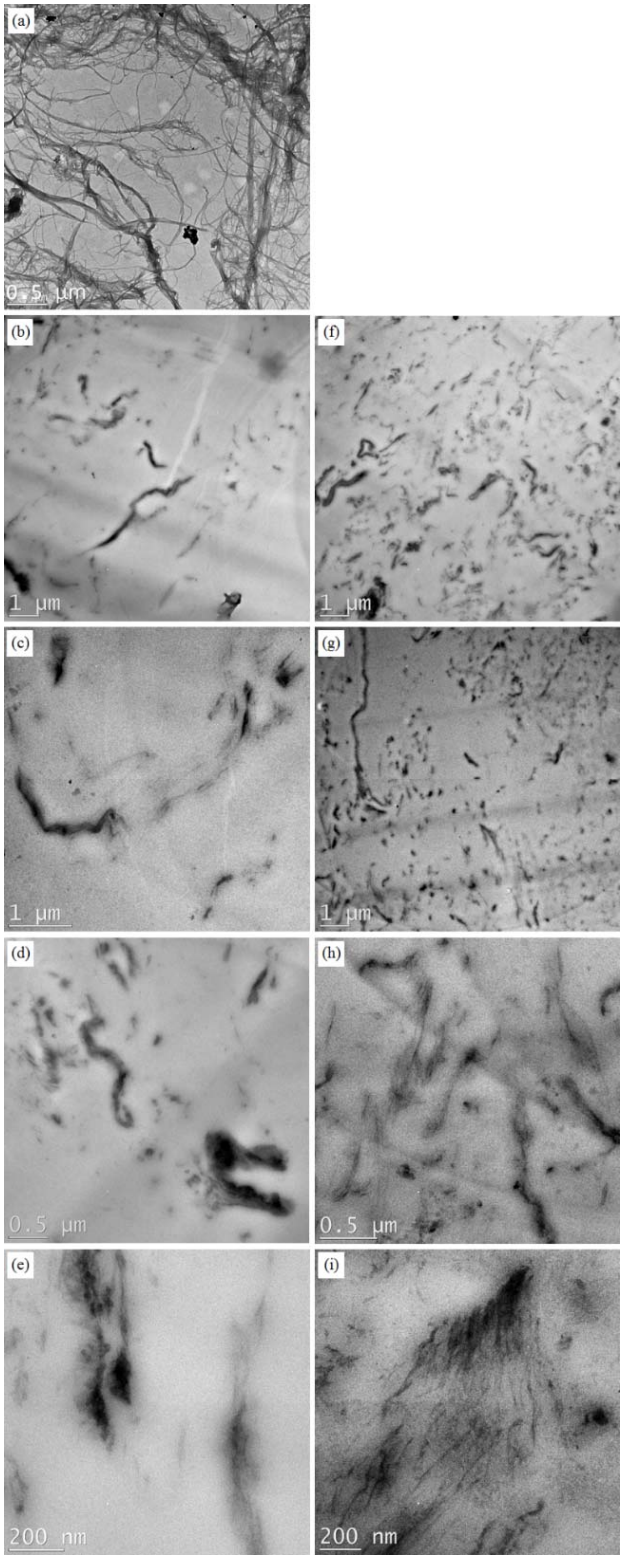

Figure 7.2: TEM images of (a) dried CNFs (from an aqueous suspension containing 0.5 wt% fibers), (b-e) PLA/2CNF and (f-i) PLA/2CNF/4PEG, taken from different samples and/or at different magnifications.

7.4.3 Atomic force microscopy (AFM)

Figure 7.3a and b presents AFM images for the 2 wt% nanofiber composite without PEG and AFM images for the PEG-compatibilized composite are presented in Figure 7.3c-h. As both height and adhesion (and modulus, if applicable) modes show clearly, the distribution for the composite without PEG (Figure 7.3a and b) is not as uniform as that for PLA/2CNF/4PEG (Figure 7.3c-e). The CNFs for the sample prepared using the masterbatch are well distributed throughout the matrix (Figure 7.3c-e); also the presence of fibers with a diameter of few nanometers is evident in Figure 7.3f-h, revealing the good dispersion of the CNFs. Hence, the AFM analysis confirms that a better dispersion and distribution of CNFs may be achieved when they are first dispersed in PEG.

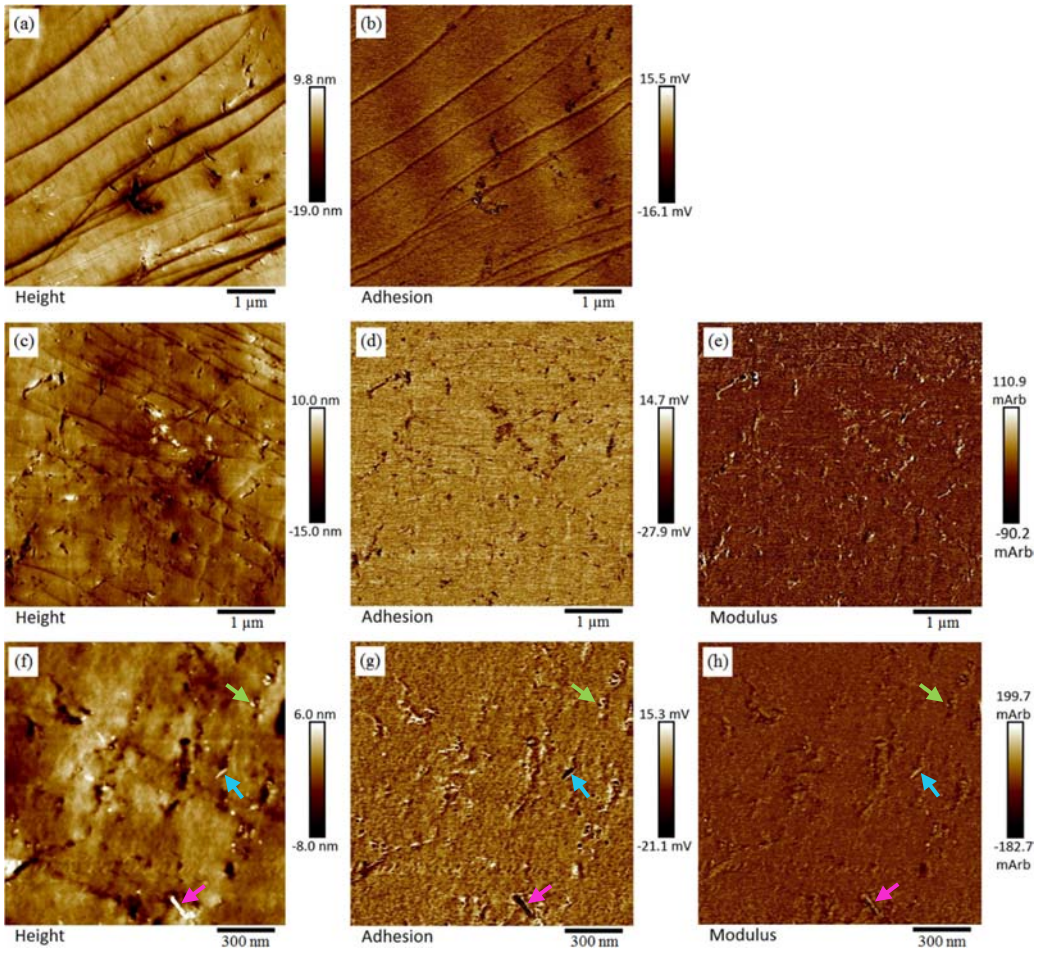

Figure 7.3: AFM images of (a and b) PLA/2CNF and (c-h) PLA/2CNF/4PEG, at different magnifications and for different modes of height, adhesion and modulus. Positive height, negative adhesion, and positive modulus represent the nanofibers, e.g. the arrows in (f-h) indicate how a nanofiber or fiber bundle appears in different modes.

7.4.4 Rheology

Figure 7.4 presents SAOS data in terms of the complex viscosity, η^*, and storage and loss moduli, G' and G'', as functions of frequency, ω, for all solution-produced samples. PLA exhibits a long plateau for η^* followed by shear thinning (Figure 7.4a). Also terminal zones with slopes of two and one are observed for G' and G'' versus ω, respectively (Figure 7.4b). All composites show a shear-thinning behavior without a plateau region for η^* (Figure 7.4a) and a less frequency-dependency behavior for G' and G'' (Figure 7.4b), especially at lower frequencies. Large increases in η^*, G' and G'' by one, four and one orders of magnitude, respectively, are observed for PLA/2CNF relative to the neat PLA (extrapolating the PLA G' data at low frequencies). The results suggest a network formation, which consequently leads to a transition from liquid- to solid-like behavior, with an upturn in viscosity and plateaus in G' and G'' at low frequencies. On the other hand, by introducing the masterbatch into PLA, i.e., PLA/2CNF/4PEG sample, the values for η^*, G' and G'' of PLA/4PEG at low frequencies increase by two, six and two orders of magnitude (extrapolating the PLA/4PEG G' data), respectively. Also, Figure 7.4b shows that G' and G'' for PLA/2CNF/4PEG cross over at a frequency higher than that for PLA/2CNF. Interestingly, PLA/2CNF/4PEG exhibits a similar low-frequency complex viscosity behavior as the composite containing more CNFs, but without PEG, i.e., PLA/5CNF (Figure 7.4a). In contrast, η^* of PLA/4PEG is lower than that of PLA due to the lower complex viscosity of PEG compared to PLA. In fact, PEG has a Newtonian behavior in the whole range of frequencies tested, with a very low value of η^*, ca. 20 Pa.s at 75 °C (already lower than that of PLA at 175 °C), so that it was not feasible to measure its rheological properties at 175 °C for the sake of comparison.

These are indications of a more solid-like behavior in the composite with PEG compared to PLA/2CNF, which suggests that the better dispersion/distribution of nanofibers in the matrix using the masterbatch method could make a stronger CNF network, as strong as the network that is made in the presence of larger content of nanofibers, i.e., 5 wt%. Therefore, the rheological results (Figure 7.4) confirm the SEM, TEM and AFM observations of Figures 7.1–7.3. Composites containing other particles such as cellulose nanocrystals [44-47], organoclays [48, 49] and carbon nanotubes [50] also showed similar rheological behavior.

If no apparent yield stress is observed as expected for PLA and PLA/4PEG in Figure 7.4a, the composites obviously show an apparent yield stress that can be quantified according using the modified Carreau-Yasuda model [34, 45]:

$$\eta^* = \sigma_y/\omega + \eta_0(1 + (\lambda\omega)^a)^{(n-1/a)} \qquad (7.1)$$

where σ_y, a, λ, n and η_0 are the apparent yield stress, Yasuda parameter, time constant, flow index and zero-shear viscosity, respectively. Figure 7.4a shows that the model fits all the composite data very well. The parameters of the model are listed in Table 7.1. Since this is a 5-parameter (empirical) model, justifying the variations of the parameters with the CNF content is not easy. As the CNF content increases and/or a better CNF dispersion/distribution is achieved σ_y increases, while n decreases. Also, η_0 and λ increase significantly by incorporating the nanofibers. The changes are more significant when the PEG-compatibilized CNFs is incorporated into the matrix. Therefore, the rheological percolation for PLA/CNF/PEG system might occur at a lower CNF content than that for the system without PEG; however, the determination of a precise percolation threshold for the PLA/CNF/PEG system requires further investigations for composites containing less CNFs. A percolation threshold of 0.5–1 and 1–2 wt% CNFs has been already reported in our previous investigations focused on PLA/CNF [34, 37] and poly(ethylene oxide)/CNF [51] systems, respectively.

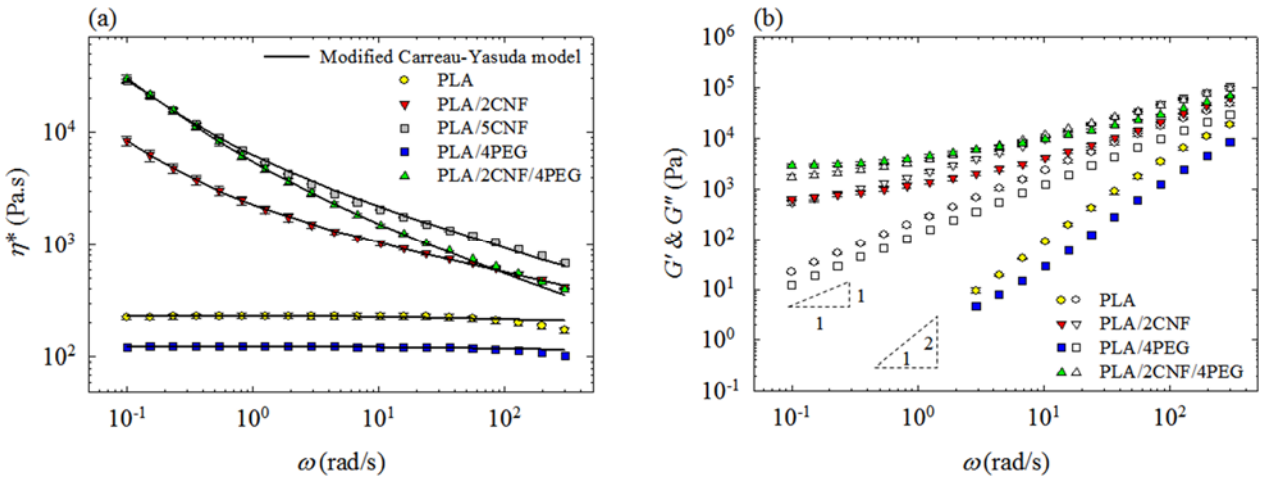

Figure 7.4: (a) Complex viscosity, and (b) storage and loss moduli (*filled* and *open symbols*, respectively) vs frequency at 175 °C and 0.05 strain amplitude for all solution-based samples. The solid lines in (a) represent the modified Carreau-Yasuda model fits, Eq. 7.1.

Table 7.1: Modified Carreau-Yasuda model parameters, Eq. 7.1.

Sample	n	σ_y (Pa)	λ (s)	η_0 (Pa.s)	a
PLA	0.97	0.00	0.100	232	0.99
PLA/2CNF	0.75	531	777	9170	0.87
PLA/5CNF	0.66	1990	963	43600	0.78
PEO/4PEG	0.98	0.00	0.100	124	0.99
PEO/2CNF/4PEG	0.61	2250	1230	53500	0.66

Figure 7.5 presents η^* as a function of ω, for the samples prepared in the melt. Contrary to the results achieved for the samples prepared in solution, the complex viscosity of PLA/2CNF (M) does not increase much relative to the PLA (M). Also, using the CNF/PEG masterbatch does not lead to better results than direct melt mixing of PLA and CNFs. This confirms that because of the long length and high flexibility of the nanofibers that make a highly entangled structure, the CNF dispersion in a matrix remains challenging when a melt mixing step is used. This suggests that the solution preparation method is an effective method to disperse/distribute the fibers within the matrix. Therefore, further measurements in this investigation are mainly reported for solution-based samples.

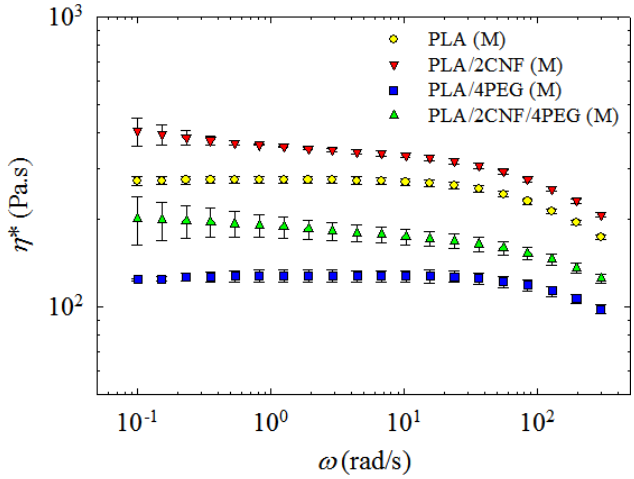

Figure 7.5: Complex viscosity vs frequency at 175 °C and 0.05 strain amplitude for the samples prepared in the melt.

7.4.5 TGA

Figure 7.6 presents the thermal degradation behavior in terms of TGA and derivative TGA (DTG) data of the samples prepared in solution. The temperature at which the sample loses 5% of its weight after evaporation of the absorbed moisture occurs at 306, 327 and 380 °C for CNFs, PLA and PEG, respectively (Figure 7.6a). All samples, i.e., PLA/2CNF, PLA/4PEG and PLA/2CNF/4PEG, exhibit almost similar values relative to the neat PLA (with differences of 1 °C). DTG data are plotted in Figure 7.6b. The onset temperature of degradation occurs at 317 °C for CNFs and at 324 and 378 °C for PLA and PEG, respectively. This occurs at ca. 329 °C for other PLA samples containing either CNFs, PEG or masterbatch. However, the DTG peak temperature for PLA/2CNF, PLA/4PEG and PLA/2CNF/4PEG increases to 334, 338 and 342 °C, respectively, compared to that of PLA (330 °C); for CNFs this temperature appears at 340 °C. The presence of PEG with a higher peak degradation temperature, i.e., 383 °C, increases the peak degradation temperature of PLA. Moreover, the dispersed/distributed nanofibers raise the peak temperature of PLA due to suppression of the polymer chain motion [34, 51-53]. Thus, when PEG-compatibilized CNFs are used to prepare the composite, this temperature shifts to a higher temperature affected by both components, i.e., PEG and CNFs.

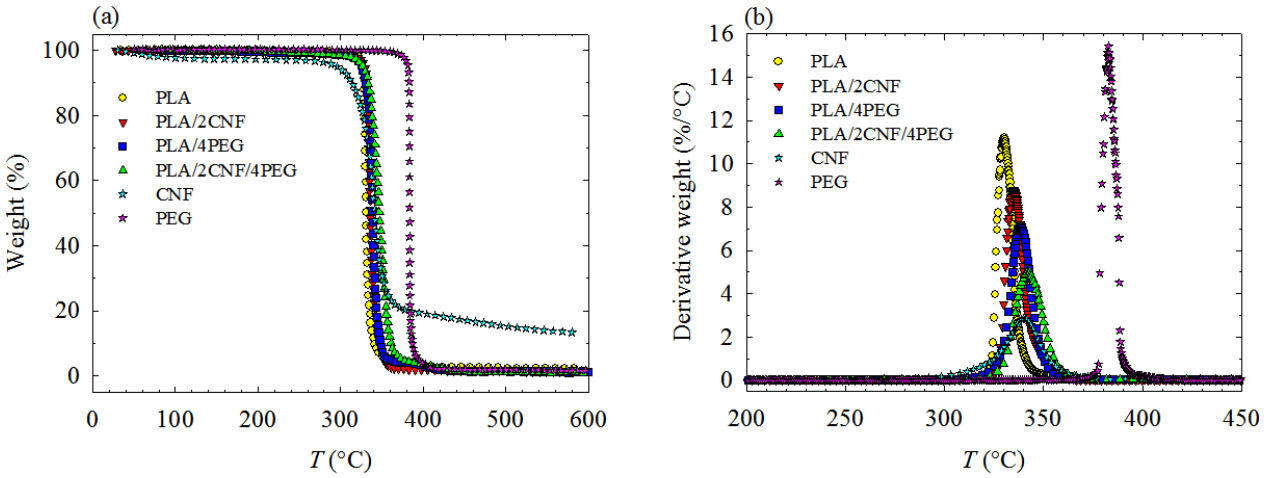

Figure 7.6: TGA (a) and DTG (b) plots of samples prepared in solution.

7.4.6 DSC

Table 7.2 reports cold crystallization (T_{cc}), crystallization (T_c), and melting (T_m) temperatures as well as crystalline contents upon the first heating and first cooling sequences ($X_c^{heating}$ and

$X_c^{cooling}$) of DSC measurements for PEG and samples prepared in solution. The $X_c^{heating}$ and $X_c^{cooling}$ values are reported based on the following equations [48]

$$X_c^{heating} = (\Delta H_m - \Delta H_{cc}) \times 100/(w_m \Delta H_m^0) \qquad (7.2)$$

$$X_c^{cooling} = \Delta H_c \times 100/(w_m \Delta H_m^0) \qquad (7.3)$$

where the enthalpies of cold crystallization, melting and crystallization are ΔH_{cc}, ΔH_m and ΔH_c, respectively; the melting enthalpy of 100% crystalline PLA (ΔH_m^0) is 93 J/g [53], and w_m is the PLA weight fraction. To calculate crystalline contents for PEG sample, ΔH_{cc} is zero and ΔH_m^0 is equal to 201.2 J/g [25]; w_m refers to the PEG weight fraction and is equal to 1.

Table 7.2 shows that $X_c^{heating}$ of PLA is not affected by the addition of 2 wt% CNFs. The crystalline content increases when PEG is added to PLA, this is mostly due to the plasticization role of PEG that increases the polymer chain mobility. However, PLA/2CNF/4PEG exhibits a lower crystallinity than PLA/4PEG due to the restriction of the polymer chain mobility caused by the nanofibers that disrupt the crystalline growth. $X_c^{cooling}$ of PLA increases up to 33% by adding 2 wt% CNFs and 4 wt% PEG for PLA/2CNF/4PEG. Moreover, T_c is shifted to higher temperatures for both PLA/2CNF and PLA/2CNF/4PEG samples relative to that of PLA, up to 19 °C for the latter case. This is due to a synergistic effect of PEG and CNFs on the crystallization of PLA. PEG could play two roles: first it acts as a plasticizer and, second, it helps the dispersion/distribution of CNFs. On the other hand, nanofibers can have a nucleating effect on the crystallization of the plasticized PLA. Similar synergistic effects of plasticization and nucleation have been reported for PLA/talc/PEG composites [54, 55]. Contrary to our results, Lee et al. [22] reported a decrease in the crystallization temperature of PLA in presence of 5 wt% BCNFs and 4.75 wt% copolymer. The values of T_{cc} and T_m for the composite sample without PEG are similar to those of PLA. However, T_{cc} of PLA decreases by 9 °C for PEG-contained samples; this fact supports the idea that PEG acts as a plasticizer.

Table 7.2: DSC results of PEG and solution-prepared samples for first heating and cooling sequences.

Sample	T_g^* (°C)	T_{cc} (°C)	T_c (°C)	T_m (°C)	$X_c^{heating}$ (%)	$X_c^{cooling}$ (%)
PEG	N/A	N/A	48.4 ± 0.1	65.3 ± 0.1	75.6 ± 0.3	75.3 ± 0.2
PLA	59.4 ± 0.4	85.2 ± 0.3	105.2 ± 0.2	170.3 ± 0.3	29.1 ± 0.2	38.4 ± 0.1
PLA/2CNF	63.2 ± 0.4	85.6 ± 0.5	114.1 ± 0.3	170.4 ± 0.4	29.4 ± 0.4	45.4 ± 0.1
PLA/4PEG	58.7 ± 0.7	75.9 ± 0.1	114.8 ± 0.2	170.1 ± 0.2	34.2 ± 0.1	49.1 ± 0.1
PLA/2CNF/4PEG	58.6 ± 0.6	76.1 ± 0.1	124.1 ± 0.2	169.9 ± 0.1	32.0 ± 0.1	51.0 ± 0.1

All temperatures indicate the values at the corresponding peak; PEG-contained samples showed single peaks for melting and crystallization.

* The T_g data have been extracted from the DMTA tests.

7.4.7 Tensile properties

Figure 7.7 presents normalized values of the Young modulus, tensile strength, and elongation at break for the solution- and melt-prepared samples. The Young modulus of PLA increases for solution-prepared samples containing either CNFs or PEG-compatibilized CNFs (Figure 7.7a). In all cases, the incorporation of nanofibers enhances the Young modulus due to their reinforcing role. Indeed, as the first heating sequence crystallinity of the samples containing 2 wt% CNFs with and without PEG is lower than that of the PLA/4PEG or the same as that of the PLA, respectively (Table 7.2), the reinforcing role of nanofibers is the dominant factor that improves the modulus rather than the nucleating/crystallization effect. In other words, when the crystalline content of PLA/4PEG decreases in presence of the nanofibers and this may lead to a lower modulus, the presence of a strong CNF network in the PLA/2CNF/4PEG compensates that effect. The tensile strength shows almost the same trend (Figure 7.7b). It is interesting to note that other investigators have reported lower enhancements for the Young modulus and tensile strength of PLA/CNF composites with a similar or larger CNF contents, although compatibilization and/or CNF modification were employed [11, 22, 27, 36]. As expected, the elongation at break decreases in the presence of nanofibers (Figure 7.7c) as is the case for many composite systems. Figure 7.7 also depicts no property enhancement for the melt-prepared composites relative to the neat PLA as the nanofibers are probably poorly dispersed/distributed in the samples.

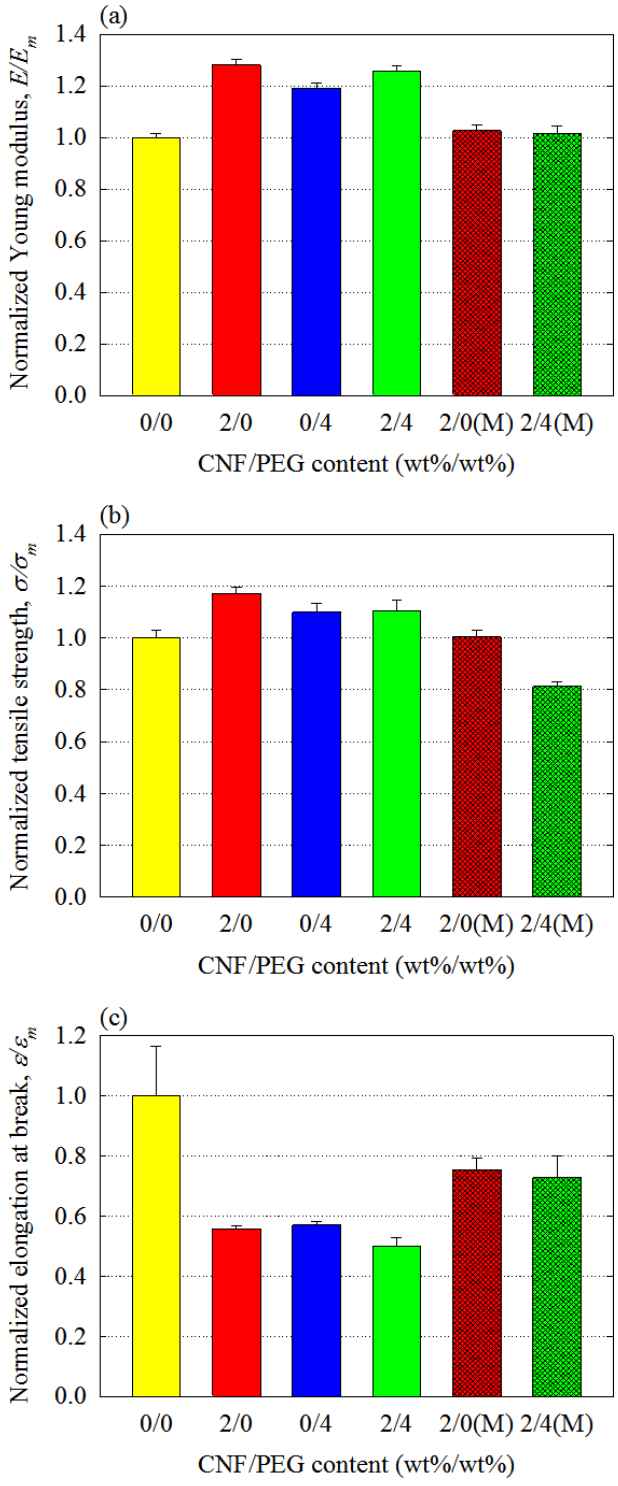

Figure 7.7: Normalized values of tensile properties: Young's modulus (a), tensile strength (b) and elongation at break (c) for the samples prepared in the solution and molten states. Subscript m refers to the PLA with Young's modulus, tensile strength and elongation at break of 2.96 GPa, 66.3 MPa and 4%, respectively.

7.4.8 DMTA

Figure 7.8 presents the flexural storage modulus, E', and $\tan\delta$ for the samples prepared in solution as functions of temperature. The storage modulus of PLA increases over a wide range of temperatures by incorporating the nanofibers; the largest increases are observed in the rubbery region when CNFs are added to the PLA via the masterbatch (Figure 7.8a). In fact, a good dispersion and strong entangled network of the nanofibers within the matrix can make the material stiffer [18, 34, 51, 56]. The $\tan\delta$ peak (Figure 7.8b), which is taken as the glass transition temperature, T_g, is reported in Table 7.2 for the different samples. T_g of PLA is not affected significantly by the addition of the CNFs, compatibilizer nor the masterbatch; it increases from ca. 59 to ca. 63 °C for PLA and PLA/2CNF, respectively. However, with the incorporation of either the CNFs or the compatibilizer within the PLA phase, the area under the $\tan\delta$ peak of PLA decreases. In the case where a masterbatch has been used to prepare the final composite, i.e., PLA/2CNF/4PEG, this reduction is more significant. The normalized area, A/A_m (where subscript m refers to the PLA), under the $\tan\delta$ peaks of PLA/2CNF and PLA/2CNF/4PEG decreases to 0.66 and 0.51, respectively. This indicates restricted PLA chain motion as a result of the good dispersion of the CNFs creating a large interfacial area [34, 51, 57] and the effect of PEG on the crystallinity of PLA (see Table 7.2).

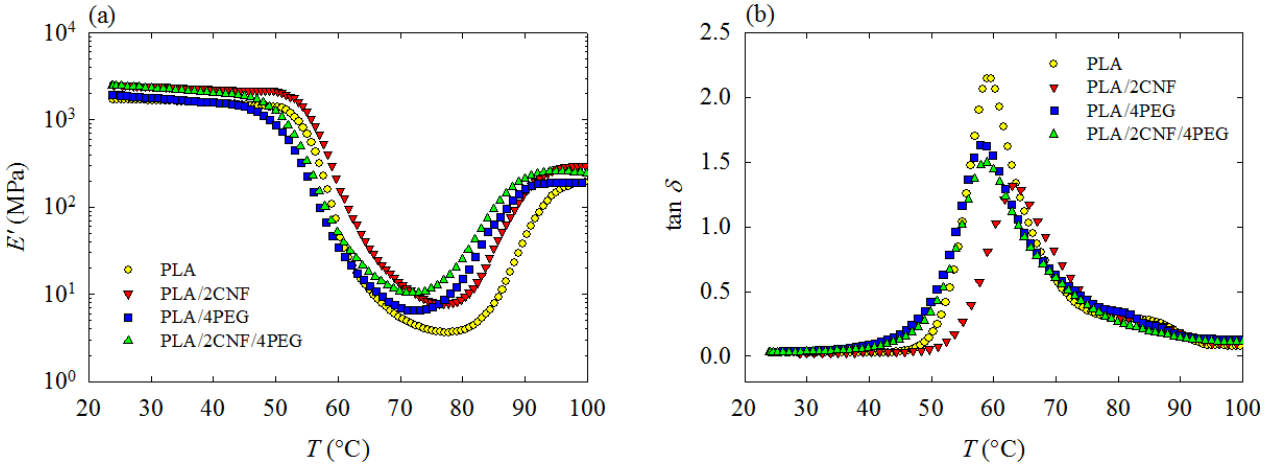

Figure 7.8: Flexural storage modulus (a) and $\tan\delta$ (b) of the solution-prepared samples.

Figure 7.9 compares the normalized flexural storage modulus, E'/E'_m, at 25 and 80 °C. The storage modulus of PLA at 25 °C (1.71 GPa) increases up to 42% for PLA/2CNF/4PEG (Figure 7.9a).

Moreover, in the rubbery region, 132 and 553% enhancement in the storage modulus of PLA (3.9 MPa at 80 °C) is achieved for the samples containing 2 wt% CNFs without and with PEG, respectively (Figure 7.9b). This shows that the reinforcement of the nanofibers is more effective when the matrix has a lower modulus in the rubbery region [20], and also confirms that a good state of dispersion is achieved using the compatibilizer; thus, PLA products can be exposed to higher temperatures.

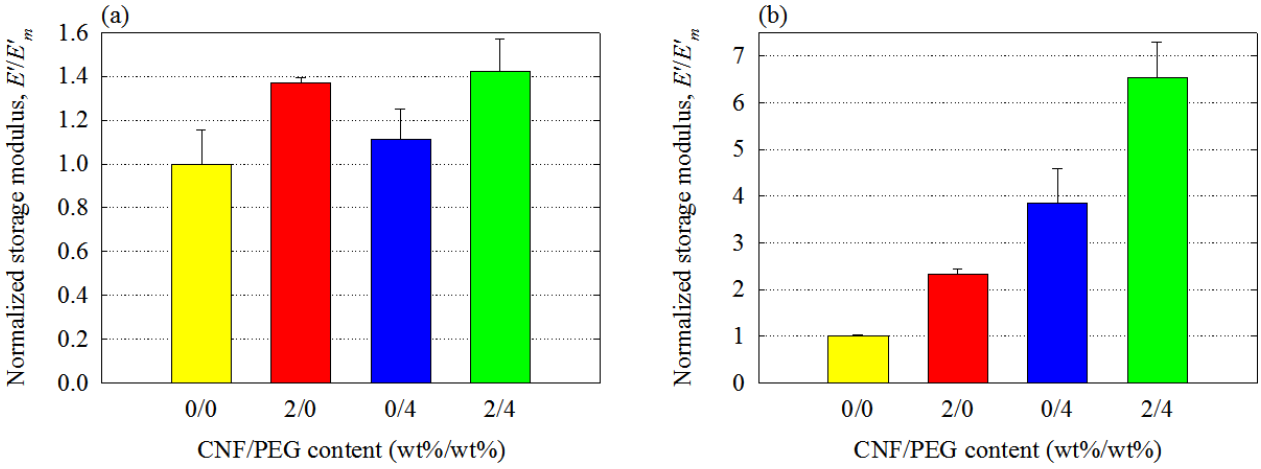

Figure 7.9: Normalized flexural storage modulus at 25 °C (a) and 80 °C (b) for samples prepared in the solution state.

7.4.9 Optical properties

Good dispersion/distribution of nanoparticles in the composite does not usually deteriorate the original transparency of the matrix [28, 31, 34, 51], which could be beneficial for many applications. Figure 7.10 shows the transmittance for PLA, PLA/2CNF and PLA/2CNF/4PEG films as a function of wavelength, λ. In the visible light range, i.e., λ = 390–700 nm, the light transparency of PLA does not change significantly due to the presence of the nanofibers. Furthermore, the PLA/2CNF/4PEG film shows even smaller deviations from the transmittance values of the neat PLA film compared to the PLA/2CNF film, even though the crystalline content and the ratio of CNFs to PLA are slightly larger in the former. This confirms that in the presence of PEG the CNFs are better dispersed/distributed in PLA [28, 34]. Nevertheless, both composites show adequate transparency characteristics, since optical transmittance greater than 75% is considered as acceptable transparency for films [34, 51, 53]. Therefore, these materials can be of interests for optical [43, 58, 59] and optoelectronic [7, 26, 59] applications, whereas it is not the

case for composites containing other nano-reinforcements such as carbon nanotubes [58]. Lower levels of transparency for CNF-filled composites have been reported where CNFs were poorly dispersed/distributed in the matrix, as translucent films and films with visible agglomerates were seen in some investigations [12, 18].

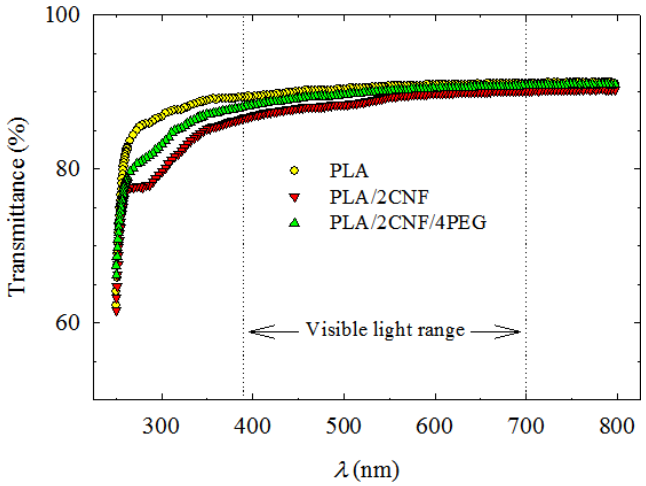

Figure 7.10: Light transmittance of PLA, PLA/2CNF and PLA/2CNF/4PEG films.

7.5 Concluding remarks

Simple methods were utilized to prepare a CNF/PEG masterbatch and nanofiber-reinforced PLA composites in order to investigate the effects of PEG on the morphology, rheological, thermal, mechanical, and optical properties of PLA/CNF composites. The results of SEM, TEM and AFM indicated a more uniform dispersion/distribution of the nanofibers in the matrix when the CNFs were initially dispersed in PEG prior to mixing with PLA via a solution method. Moreover, a two-phase system was not observed suggesting that PEG and PLA were miscible. Incorporation of CNFs caused substantial increases in the complex viscosity and the storage and loss moduli of PLA for the samples prepared in the solution state; an apparent yield stress was also observed. However, the effect of CNFs on the rheological properties of PLA was more pronounced upon employing the masterbatch method. Increases of one order of magnitude in the complex viscosity, storage and loss moduli for PLA/2CNF/4PEG were observed over the other composite (PLA/2CNF), suggesting better dispersion and distribution of CNFs in this case. The composites prepared using melt processing show much lower increases in rheological properties of the matrix. This confirms

that dispersing highly-entangled CNFs in a matrix via direct mixing in the melt is very challenging, even if a well-dispersed/distributed masterbatch has been already prepared.

The T_c of PLA shifted up to 19 °C and $X_c^{cooling}$ of PLA increased by 33% for the compatibilized composite, i.e., PLA/2CNF/4PEG. The storage modulus in DMTA was significantly enhanced for the composites in comparison with the PLA over a wide range of temperatures, especially in the rubbery zone; the storage modulus of PLA at 80 °C was improved by 132 and 553% for the samples containing 2 wt% CNFs without and with PEG, respectively. In the limit of visible light, similar transparencies were observed for both composite films compared to the neat PLA, especially for the composites prepared via the masterbatch.

The results of this study point out to the efficiency of the solution preparation method and the substantial potential of PEG to further increase the properties of PLA/CNF biocomposites. This would promote the use of PLA in applications where its low heat resistance and slow crystallization are serious drawbacks (e.g. film blowing, blow molding and pipes and products exposed to high temperatures); also good optical properties of PLA/CNF films are of interest for optical and optoelectronic applications.

7.6 Acknowledgments

This work was supported by the Natural Sciences and Engineering Research Council of Canada (NSERC) through the Network for Innovative Plastic Materials and Manufacturing Processes (NIPMMP). The authors also wish to thank Prof. Mohini M. Sain of the University of Toronto for providing the CNFs.

7.7 References

[1] Raquez JM, Habibi Y, Murariu M, Dubois P. Polylactide (PLA)-Based Nanocomposites. Progress in Polymer Science. 2013;38(10–11):1504-1542.

[2] Abdulkhani A, Hosseinzadeh J, Ashori A, Dadashi S, Takzare Z. Preparation and Characterization of Modified Cellulose Nanofibers Reinforced Polylactic Acid Nanocomposite. Polymer Testing. 2014;35:73-79.

[3] Li ZQ, Zhou XD, Pei CH. Preparation and Characterization of Bacterial Cellulose/Polylactide Nanocomposites. Polymer-Plastics Technology and Engineering. 2010;49(2):141-146.

[4] Marais A, Kochumalayil JJ, Nilsson C, Fogelström L, Gamstedt EK. Toward an Alternative Compatibilizer for PLA/Cellulose Composites: Grafting of Xyloglucan with PLA. Carbohydrate Polymers. 2012;89(4):1038-1043.

[5] Tome LC, Pinto RJB, Trovatti E, Freire CSR, Silvestre AJD, Neto CP, Gandini A. Transparent Bionanocomposites with Improved Properties Prepared from Acetylated Bacterial Cellulose and Poly(lactic acid) through a Simple Approach. Green Chemistry. 2011;13(2):419-427.

[6] Adeosun SO, Lawal GI, Balogun SA, Akpan EI. Review of Green Polymer Nanocomposites. Journal of Minerals and Materials Characterization and Engineering. 2012;11(4):385-416.

[7] Siró I and Plackett D. Microfibrillated Cellulose and New Nanocomposite Materials: a Review. Cellulose. 2010;17(3):459-494.

[8] La Mantia FP and Morreale M. Green Composites: A Brief Review. Composites Part A: Applied Science and Manufturing. 2011;42(6):579-588.

[9] Lu T, Liu S, Jiang M, Xu X, Wang Y, Wang Z, Gou J, Hui D, Zhou Z. Effects of Modifications of Bamboo Cellulose Fibers on the Improved Mechanical Properties of Cellulose Reinforced Poly(lactic acid) Composites. Composites Part B: Engineering. 2014;62:191-197.

[10] Plummer CG, Choo CC, Boissard CR, Bourban PE, Månson JA. Morphological Investigation of Polylactide/Microfibrillated Cellulose Composites. Colloid and Polymer Science. 2013;291(9):2203-2211.

[11] Qu P, Gao Y, Wu G, Zhang L. Nanocomposites of Poly(lactic acid) Reinforced with Cellulose Nanofibrils. Bioresources. 2010;5(3):1811-1823.

[12] Tingaut P, Zimmermann T, Lopez-Suevos F. Synthesis and Characterization of Bionanocomposites with Tunable Properties from Poly(lactic acid) and Acetylated Microfibrillated Cellulose. Biomacromolecules. 2010;11(2):454-464.

[13] Wu CS. Renewable Resource-Based Composites of Recycled Natural Fibers and Maleated Polylactide Bioplastic: Characterization and Biodegradability. Polymer Degradation and Stability. 2009;94(7):1076-1084.

[14] Zhou C, Shi Q, Guo W, Terrell L, Qureshi AT, Hayes DJ, Wu Q. Electrospun Bio-Nanocomposite Scaffolds for Bone Tissue Engineering by Cellulose Nanocrystals Reinforcing Maleic Anhydride Grafted PLA. ACS Applied Materials and Interfaces. 2013;5(9):3847-3854.

[15] Frone AN, Berlioz S, Chailan JF, Panaitescu DM. Morphology and Thermal Properties of PLA-Cellulose Nanofibers Composites. Carbohydrate Polymers. 2013;91(1):377-84.

[16] Nakagaito AN, Fujimura A, Sakai T, Hama Y, Yano H. Production of Microfibrillated Cellulose (MFC)-Reinforced Polylactic Acid (PLA) Nanocomposites from Sheets Obtained by a Papermaking-Like Process. Composite Science and Technology. 2009;69(7–8):1293-1297.

[17] Frone AN, Berlioz S, Chailan JF, Panaitescu DM, Donescu D. Cellulose Fiber-Reinforced Polylactic Acid. Polymer Composites. 2011;32(6):976-985.

[18] Jonoobi M, Harun J, Mathew AP, Oksman K. Mechanical Properties of Cellulose Nanofiber (CNF) Reinforced Polylactic Acid (PLA) Prepared by Twin Screw Extrusion. Composite Science and Technology. 2010;70(12):1742-1747.

[19] Sanchez-Garcia M and Lagaron J. On the Use of Plant Cellulose Nanowhiskers to Enhance the Barrier Properties of Polylactic Acid. Cellulose. 2010;17(5):987-1004.

[20] Suryanegara L, Nakagaito AN, Yano H. The Effect of Crystallization of PLA on the Thermal and Mechanical Properties of Microfibrillated Cellulose-Reinforced PLA Composites. Composite Science and Technology. 2009;69(7-8):1187-1192.

[21] Wang T and Drzal LT. Cellulose-Nanofiber-Reinforced Poly(lactic acid) Composites Prepared by a Water-Based Approach. ACS Applied Materials and Interfaces. 2012;4(10):5079-5085.

[22] Lee KY, Tang M, Williams CK, Bismarck A. Carbohydrate Derived Copoly(lactide) as the Compatibilizer for Bacterial Cellulose Reinforced Polylactide Nanocomposites. Composite Science and Technology. 2012;72(14):1646-1650.

[23] Lee KY, Quero F, Blaker JJ, Hill CAS, Eichhorn SJ, Bismarck A. Surface Only Modification of Bacterial Cellulose Nanofibres with Organic Acids. Cellulose. 2011;18(3):595-605.

[24] Iwatake A, Nogi M, Yano H. Cellulose Nanofiber-Reinforced Polylactic Acid. Composite Science and Technology. 2008;68(9):2103-2106.

[25] Brown EE and Laborie MPG. Bioengineering Bacterial Cellulose/Poly(ethylene oxide) Nanocomposites. Biomacromolecules. 2007;8(10):3074-3081.

[26] Tercjak A, Gutierrez J, Barud HS, Domeneguetti RR, Ribeiro SJL. Nano- and Macroscale Structural and Mechanical Properties of in Situ Synthesized Bacterial Cellulose/PEO-b-PPO-b-PEO Biocomposites. ACS Applied Materials and Interfaces. 2015;7(7):4142-4150.

[27] Wang B and Sain M. The Effect of Chemically Coated Nanofiber Reinforcement on Biopolymer Based Nanocomposites. Bioresources. 2007;2(3):371-388.

[28] Petersson L and Oksman K. Biopolymer Based Nanocomposites: Comparing Layered Silicates and Microcrystalline Cellulose as Nanoreinforcement. Composite Science and Technology. 2006;66(13):2187-2196.

[29] Xu X, Wang H, Jiang L, Wang X, Payne SA, Zhu JY, Li R. Comparison between Cellulose Nanocrystal and Cellulose Nanofibril Reinforced Poly(ethylene oxide) Nanofibers and Their Novel Shish-Kebab-Like Crystalline Structures. Macromolecules. 2014;47(10):3409-3416.

[30] Kowalczyk M, Piorkowska E, Kulpinski P, Pracella M. Mechanical and Thermal Properties of PLA Composites with Cellulose Nanofibers and Standard Size Fibers. Composites Part A: Applied Science and Manufturing. 2011;42(10):1509-1514.

[31] Eichhorn SJ, Dufresne A, Aranguren M, Marcovich NE, Capadona JR, Rowan SJ, Weder C, Thielemans W, Roman M, Renneckar S, Gindl W, Veigel S, Keckes J, Yano H, Abe K, Nogi M, Nakagaito AN, Mangalam A, Simonsen J, Benight AS, Bismarck A, Berglund LA, Peijs, T. Review: Current International Research into Cellulose Nanofibres and Nanocomposites. Journal of Materials Science. 2010;45(1):1-33.

[32] Jonoobi M, Mathew AP, Abdi MM, Makinejad MD, Oksman K. A Comparison of Modified and Unmodified Cellulose Nanofiber Reinforced Polylactic Acid (PLA) Prepared by Twin Screw Extrusion. Journal of Polymers and the Environment. 2012;20(4):991-997.

[33] Azizi Samir MAS, Alloin F, Dufresne A. Review of Recent Research into Cellulosic Whiskers, Their Properties and Their Application in Nanocomposite Field. Biomacromolecules. 2005;6(2):612-626.

[34] Safdari F, Bagheriasl D, Carreau PJ, Heuzey MC, Kamal MR. Rheological, Mechanical, and Thermal Properties of Polylactide/Cellulose Nanofiber Biocomposites. Polymer Composites. 2016.

[35] Lee KY, Blaker JJ, Bismarck A. Surface Functionalisation of Bacterial Cellulose as the Route to Produce Green Polylactide Nanocomposites with Improved Properties. Composite Science and Technology. 2009;69(15–16):2724-2733.

[36] Mathew AP, Chakraborty A, Oksman K, Sain M. "The Structure and Mechanical Properties of Cellulose Nanocomposites Prepared by Twin Screw Extrusion" in *Cellulose Nanocomposites: Processing, Characterization, and Properties*. vol. 938, K. Oksman and M. Sain, Eds., ed: Oxford University Press, 2006, pp. 114-131.

[37] Safdari F, Bagheriasl D, Carreau PJ, Heuzey MC, Kamal MR. High-Performance Polylactide Biocomposites Reinforced with Cellulose Nanofibers. SPE Plastics Research Online. 2016.

[38] Arias A, Heuzey MC, Huneault MA, Ausias G, Bendahou A. Enhanced Dispersion of Cellulose Nanocrystals in Melt-Processed Polylactide-Based Nanocomposites. Cellulose. 2015;22(1):483-498.

[39] Sheth M, Kumar RA, Davé V, Gross RA, McCarthy SP. Biodegradable Polymer Blends of Poly(lactic acid) and Poly(ethylene glycol). Journal of Applied Polymer Science. 1997;66(8):1495-1505.

[40] Baiardo M, Frisoni G, Scandola M, Rimelen M, Lips D, Ruffieux K, Wintermantel E. Thermal and Mechanical Properties of Plasticized Poly(L-lactic acid). Journal of Applied Polymer Science. 2003;90(7):1731-1738.

[41] Buddhiranon S, Kim N, Kyu T. Morphology Development in Relation to the Ternary Phase Diagram of Biodegradable PDLLA/PCL/PEO Blends. Macromolecular Chemistry and Physics. 2011;212(13):1379-1391.

[42] Zhang K, Nagarajan V, Misra M, Mohanty AK. Supertoughened Renewable PLA Reactive Multiphase Blends System: Phase Morphology and Performance. ACS Applied Materials and Interfaces. 2014;6(15):12436-12448.

[43] Janardhnan S and Sain M. Bio-Treatment of Natural Fibers in Isolation of Cellulose Nanofibres: Impact of Pre-Refining of Fibers on Bio-Treatment Efficiency and Nanofiber Yield. Journal of Polymers and the Environment. 2011;19(3):615-621.

[44] Bagheriasl D, Carreau PJ, Riedl B, Dubois C, Hamad WY. Shear Rheology of Polylactide (PLA)–Cellulose Nanocrystal (CNC) Nanocomposites. Cellulose. 2016;23(3):1885-1897.

[45] Kamal MR and Khoshkava V. Effect of Cellulose Nanocrystals (CNC) on Rheological and Mechanical Properties and Crystallization Behavior of PLA/CNC Nanocomposites. Carbohydrate Polymers. 2015;123:105-14.

[46] Khoshkava V and Kamal MR. Effect of Cellulose Nanocrystals (CNC) Particle Morphology on Dispersion and Rheological and Mechanical Properties of Polypropylene/CNC Nanocomposites. ACS Applied Materials and Interfaces. 2014;6(11):8146-8157.

[47] Bagheriasl D, Carreau PJ, Riedl B, Dubois C. Enhanced Properties of Polylactide by Incorporating Cellulose Nanocrystals. Polymer Composites. 2016.

[48] Ghanbari A, Heuzey MC, Carreau PJ, Ton-That MT. A Novel Approach to Control Thermal Degradation of PET/Organoclay Nanocomposites and Improve Clay Exfoliation. Polymer. 2013;54(4):1361-1369.

[49] Ghanbari A, Heuzey MC, Carreau PJ, Ton-That MT. Morphological and Rheological Properties of PET/Clay Nanocomposites. Rheologica Acta. 2013;52(1):59-74.

[50] Abbasi S, Carreau PJ, Derdouri A, Moan M. Rheological Properties and Percolation in Suspensions of Multiwalled Carbon Nanotubes in Polycarbonate. Rheologica Acta. 2009;48(9):943-959.

[51] Safdari F, Carreau PJ, Heuzey MC, Kamal MR, Sain MM. Enhanced Properties of Poly(ethylene oxide)/Cellulose Nanofiber Biocomposites. Cellulose. 2017;24(2):755-767.

[52] Ramezani Kakroodi A, Cheng S, Sain M, Asiri A. Mechanical, Thermal, and Morphological Properties of Nanocomposites Based on Polyvinyl Alcohol and Cellulose Nanofiber from Aloe vera Rind. Journal of Nanomaterials. 2014;2014:1-7.

[53] Ambrosio-Martín J, Fabra MJ, Lopez-Rubio A, Lagaron JM. Melt Polycondensation to Improve the Dispersion of Bacterial Cellulose into Polylactide via Melt Compounding: Enhanced Barrier and Mechanical Properties. Cellulose. 2015;22(2):1201-1226.

[54] Courgneau C, Ducruet V, Avérous L, Grenet J, Domenek S. Nonisothermal Crystallization Kinetics of Poly(lactide)—Effect of Plasticizers and Nucleating Agent. Polymer Engineering and Science. 2013;53(5):1085-1098.

[55] Wang Y, Li M, Hu D, Shen C. Accelerating the Crystallization of Poly(lactic acid). SPE Plastics Research Online. 2010.

[56] Azizi Samir MAS, Alloin F, Paillet M, Dufresne A. Tangling Effect in Fibrillated Cellulose Reinforced Nanocomposites. Macromolecules. 2004;37(11):4313-4316.

[57] Bagheriasl D, Carreau PJ, Dubois C, Riedl B. Properties of Polypropylene and Polypropylene/Poly(ethylene-co-vinyl alcohol) Blend/CNC Nanocomposites. Composite Science and Technology. 2015;117:357-363.

[58] Xu X, Liu F, Jiang L, Zhu JY, Haagenson D, Wiesenborn DP. Cellulose Nanocrystals vs. Cellulose Nanofibrils: A Comparative Study on Their Microstructures and Effects as Polymer Reinforcing Agents. ACS Applied Materials and Interfaces. 2013;5(8):2999-3009.

[59] Kalia S, Boufi S, Celli A, Kango S. Nanofibrillated Cellulose: Surface Modification and Potential Applications. Colloid and Polymer Science. 2014;292(1):5-31.

CHAPTER 8 GENERAL DISCUSSION

One of the problems encountered during the planning and execution of this project was related to literature review and comparison with published results. In few investigations, the word “cellulose nanofibers (CNFs)” is used in the title and in the text, while the material is not CNFs as referred to in this dissertation (network- or web-like structure of nanofibers that comprises both crystalline and amorphous parts of cellulose). For instance, authors have used CNFs to refer to particles that consist mainly of crystalline parts of cellulose fibers, i.e., where the word “cellulose nanocrystals (CNCs)” is intended. Moreover, in some investigations CNFs can be found under other nomenclatures, e.g. cellulose microfibers/microfibrils (CMFs) and micro-fibrillated cellulose (MFC). Besides, CNFs used in different investigations were obtained from various sources and had different aspect ratios and level of entanglements; hence, it is difficult to compare results of the different investigations. It is worth mentioning that determining the nanofiber length is difficult if not impossible as the CNFs are long, flexible and highly entangled.

A major challenge in using hydrophilic CNFs to prepare enhanced polymer composites is that most of the polymers of industrial interest are hydrophobic, such as polylactide (PLA), polypropylene, polyethylene, polystyrene, and so on. Poor compatibility between nanofibers and polymers causes limited or no enhancement in properties as a result of poor CNF dispersion and distribution. Hence, normally a compatibilization or modification step is needed to overcome strong inter-molecular hydrogen bonds of nanofibers and reduce entanglements. Besides, the addition of a third component such as a compatibilizer, can alter the initial properties of the matrix. Therefore, it is important to choose a compatibilizer that is miscible with the polymer matrix, and yet compatible with the CNFs. Also, having good mechanical properties for the compatibilizer, comparable to those of the neat polymer is desirable. In case of surface modification, it is important to keep the degradation temperature of the modified CNFs well above the processing temperature of the polymer matrices. The degree of substitution is also a key issue. Moreover, the length of the chains to be grafted on the CNF surface has a significant influence on different properties. Each of these techniques, if conducted in solution, usually requires a drying step prior to the addition of the compatibilized or modified CNFs to the matrix. However, upon drying, the nanofibers might stick together and re-agglomerate. Therefore, the final composites may still contain many agglomerates and, consequently, exhibit poor mechanical properties.

In the case of hydrophilic polymers, such as poly(ethylene oxide), the dispersion and distribution of nanofibers in the molten state is also quite challenging, as these long and flexible nanofibers can form many entanglements and, therefore, agglomerates remain in the polymer. In fact, the hydrogen bonds between CNFs and hydrophilic matrices may not be effective at the high temperatures required for melt mixing and that may affect the state of CNF dispersion and distribution within the matrices.

Hence, one of the challenges of using CNFs as potential reinforcement in industry is that conventional direct melt mixing techniques, which are simple and desirable from an industrial point of view, are not commonly effective in producing CNF-reinforced composites due to the long length, flexibility, and level of entanglements. Therefore, the use of solution preparation techniques is inevitable.

Attempts were made to finely disperse/distribute CNFs in polymer matrices and, consequently, to enhance the properties, however, with limited success at low contents of nanofibers, as reported in the literature, even after modification or compatibilization in the case of hydrophobic matrices such as PLA. In this research project, simple preparation methods are proposed to well disperse and distribute CNFs into hydrophobic and hydrophilic matrices and, consequently, to enhance the properties in different aspects, i.e., thermal, mechanical, and optical. Moreover, the methods used here can be applied to other polymer matrices, where CNFs can be dispersed in appropriate solvents. Thus, without any modification or compatibilization step, composites with a dispersed/distributed structure can be achieved. Moreover, the masterbatch method with the aim of compatibilization that has been used in this research project can further improve the quality of dispersion/distribution and different properties, as well. Organic solvents, such as N,N-dimethylformamide (DMF) used in this thesis for the fabrication of PLA-based biocomposites, however, are not desirable on an industrial scale and the interest to employ melt-mixing still remains. Nevertheless, there are some industrial-scale solution-based techniques such as polymerization and *in-situ* polymerization that require the use of organic solvents.

CHAPTER 9 CONCLUSIONS AND RECOMMENDATIONS

9.1 Conclusions

This research studied the use of a bio-based reinforcing agent, i.e., cellulose nanofibers (CNFs), to enhance the properties of polymer matrices. In this regard, a commercialized bio-derived polymer, i.e., polylactide (PLA), which has found many applications, and a biocompatible and biodegradable polymer, i.e., poly(ethylene oxide) (PEO), were chosen as matrices.

In the first step of this project the CNFs were incorporated in PLA using a simple solution technique and without any compatibilization. The following concluding remarks highlight the results of the first paper:

1. Dispersed CNFs could form an interconnected network within PLA and the network became stronger with the CNF content.
2. The rheological percolation threshold was estimated to occur at a CNF content of 0.5–1 wt% for the PLA/CNF systems studied at 175 °C.
3. The Young modulus and tensile strength of PLA increased by 50 and 31%, respectively, upon the use of 5 wt% CNFs due to their reinforcing potential.
4. The storage modulus of PLA measured in DMTA increased over a wide range of temperatures in the presence of CNFs, especially in the rubbery region; 51 and 264% increases were observed at room temperature and 70 °C, respectively, for PLA/5CNF. That showed the potential of CNFs to improve the heat resistance of PLA, which is one of its major drawbacks.
5. CNFs could play a nucleating role and this could increase the crystalline content of PLA (by up to 18%) and shift the crystallization temperature towards higher temperatures (from 105 °C for PLA to 116 °C for PLA/5CNF). Hence, the crystallization of PLA was more rapid in the presence of CNFs.
6. The thermal stability of PLA did not decrease in the presence of CNFs.
7. The transparency of the composite films in the visible light range remained comparable to that of neat PLA.

The second step of this project focused on the incorporation of the CNFs in PEO via a simple aqueous solution method. The effect of preparation techniques, melt and solution, on

dispersion/distribution of the CNFs was studied. The main conclusions based on the second article are:

1. Melt-based preparation could not disperse/distribute CNFs properly within the PEO as large agglomerates were observed and no increases in properties, rheological and tensile, were achieved.
2. Following solution-based preparation, a good dispersion/distribution of CNFs was obtained within PEO. Well-dispersed nanofibers could form a strong interconnected network within the matrix and the network became stronger as the nanofiber content increased.
3. The rheological percolation threshold was estimated to occur at the CNF content of 1–2 wt% for the PEO/CNF systems studied at 85 °C.
4. CNFs restricted PEO chains mobility and did not act as nucleating agents. This would decrease the crystalline content of PEO (from ca. 65% for PEO to ca. 55% for PEO/3CNF). However, this decrease would be of interest in some applications, e.g. when PEO is used in the electrochemical field as electrolyte.
5. The Young modulus and tensile strength of PEO increased upon the use of CNFs (by 49 and 35%, respectively, in the presence of only 3 wt% nanofibers) due to their reinforcing effect; PEO and CNFs are both hydrophilic and can have possible interactions.
6. The DMTA storage modulus of PEO increased over a wide range of temperatures for the PEO/CNF composites, e.g. at room temperature, a 47% enhancement was achieved for PEO/3CNF.
7. The thermal stability of the PEO increased in the presence of CNFs due to the possible interactions between the two components.
8. Final composites could maintain optical transmittance of the PEO film within the visible light range.

The last step of this research was conducted to compatibilize PLA and CNFs in order to achieve better dispersed/distributed nanofibers within the matrix. To do so, poly(ethylene glycol) (PEG) was used to prepare compatibilized CNFs via a simple aqueous solution method. Moreover, the efficiency of different preparation techniques, i.e., melt and solution, on dispersing/distributing the nanofibers was investigated. The main findings of the third paper are listed below.

1. Melt-based preparation was not successful to properly disperse/distribute either CNFs or PEG-compatibilized CNFs within the PLA and as a result, no increase in rheological and tensile properties was observed.
2. PEG was miscible with PLA and could result in a better dispersion/distribution of nanofibers within the matrix when the composites were prepared via the solution-based method.
3. Dispersed CNFs could form an interconnected network within the PLA and that network was stronger when PEG was used as the compatibilizer. The increases of the complex viscosity and storage modulus of PLA/2CNF/4PEG were one order of magnitude larger than those of PLA/2CNF, compared to PLA. Also, the network of nanofibers in PLA/2CNF/4PEG was stronger relative to the PLA/5CNF composite.
4. The percolation for PLA/CNF system occurred at a CNF content in the range of 0.5–1 wt%; for PLA/CNF/PEG systems it would occur at a lower nanofiber loading, i.e., lower than 0.5 wt% CNFs or in the range of 0.5–1 wt%.
5. The nucleating effect of CNFs was more evident when PEG-compatibilized nanofibers were used to prepare the composites. The crystallization temperature increased from 105 °C for PLA to 124 °C for PLA/2CNF/4PEG; similarly, the crystalline content increased from ca. 38 to 51%.
6. Up to ca. 30 and ca. 20% enhancements in the Young modulus and tensile strength of PLA were achieved, respectively, in the presence of 2 wt% CNFs.
7. The DMTA storage modulus of PLA increased over a wide range of temperatures, especially in the rubbery region and when the masterbatch was used to prepare the final composites. 42 and 553% improvements were achieved for the storage modulus at room temperature and 80 °C, respectively, for PLA/2CNF/4PEG compared to PLA. That showed the potential of nanofibers to act as reinforcing agents and to improve the heat resistance of PLA.
8. The thermal stability of the PLA did not decrease in the presence of PEG-compatibilized CNFs.
9. A better light transmittance was measured for the PLA/CNF/PEG composite films relative to the PLA/CNF films.

9.2 Original contributions

In the first and second parts of this research, simple solution methods were designed through which the CNFs were well dispersed/distributed into PLA, without any compatibilization/modification, and PEO. This resulted in the development of high-performance fully bio-based PLA/CNF and biocompatible/biodegradable PEO/CNF composites, at low nanofiber contents, with superior property enhancement in different aspects relative to the other investigations on similar systems. Furthermore, quantifying the optical properties was reported for both systems and the effect of CNFs on the molten-state rheological properties of PEO was investigated for the first time that related to the dispersion/distribution of the nanofibers in the matrix. In addition, there is no report in the literature on using empirical models to fit the rheological data to determine the apparent yield stress and subsequently the rheological percolation threshold for CNF-filled PLA and PEO. Therefore, rheology was used as a powerful tool to understand the efficiency of the preparation methods in dispersing/distributing the nanofibers in polymer matrices. To our knowledge, such a full characterization of PLA/CNF and PEO/CNF biocomposites, i.e., morphological, rheological, thermal, mechanical and optical, with consistent property enhancements, has not been reported in the literature.

In the last part of this research, PEG, that is a biocompatible and biodegradable polymer, was used as a miscible compatibilizer for the PLA/CNF system via an effective masterbatch preparation. As a consequence, improved PLA/CNF/PEG biocomposites were obtained compared with PLA/CNF biocomposites (prepared in the first part). In addition, to our knowledge, this is the most efficient compatibilization method for the PLA/CNF system in terms of dispersion/distribution, rheological and thermomechanical properties. Also, there is no report in the literature on the optical transmittance and rheological characterization for PEG-compatibilized PLA/CNF system.

The findings of this research light up more clearly the substantial potential of CNFs to be used as a new bio-based reinforcement of polymers.

9.3 Recommendations

The following aspects are recommended for future studies:

1. To prepare a solution-based masterbatch made of well-dispersed CNFs and the polymer matrix (and a compatibilizer, if necessary) prior to the dilution with the same polymer

matrix via melt-mixing, e.g. a PEO/CNF masterbatch to be diluted with the PEO matrix or PLA/CNF and PLA/CNF/PEG masterbatches for the PLA matrix. As demonstrated in the second and third papers, melt mixing of either CNFs or CNF/PEG masterbatch without the presence of the main polymer, PEO or PLA, could not lead to any increase in properties. This will minimize the use of solvents in the composite fabrication step and help to develop enhanced polymer/CNF composites by melt mixing that is desirable from an industrial point of view.

2. To use a non-toxic solvent in composite fabrication. In this regard, dihydrolevoglucosenone (Cyrene^{TM}), a dipolar bio-derived solvent from waste cellulose, may be considered as a green alternative to N,N-dimethylformamide (DMF). However, the high boiling point of Cyrene, ca. 203 °C, will make the drying step longer and may cause some thermal degradation of polymers sensitive to high temperature. Dimethyl sulfoxide (DMSO) would be considered as another choice, although it has a high boiling point of 189 °C.
3. To optimize the ratio of compatibilizer, PEG, to CNFs (only the ratio of 2 was studied in the third paper) as a function of final properties of the products. Also, the effect of PEG molecular weight can be investigated. Moreover, composites with larger CNF contents could be employed.
4. To incorporate other miscible compatibilizers, preferably bio-based ones, with superior mechanical properties relative to PEG for PLA/CNF systems in order to achieve further-enhanced composites. Polyvinyl acetate, polyvinyl acetate-co-vinyl alcohol, polyacetals, poly(meth)acrylates and copolymers of (meth)acrylates are examples that are reported to be miscible with PLA, at least partly.
5. To investigate the effects of CNFs on the crystallization of PLA and PEO polymers through rheometry and microscopy techniques.
6. To anneal the PLA/CNF samples to obtain high crystalline contents and synergistic effects on the mechanical properties of PLA.
7. To perform other rheological and mechanical tests such as elongational flows and impact tests. This will help acquire more information about the melt strength and solid-state properties and, consequently, expand PLA applications. As the neat PLA exhibits low melt strength, which affects its use in film blowing, and poor impact strength.

8. To produce films and injection-molded parts via film blowing and injection molding, respectively, and characterize them. Polymer/CNF composites show many potential applications especially for the automotive and packaging industry.

9. To develop other CNF-reinforced bio-based and commodity polymer composites. In this regard, one can mention bio-derived polyethylene, polyhydroxyalkanoates, polybutyrate, polybutylene succinate, polycaprolactone, polyamide, polyethylene terephthalate, polyvinyl chloride, and polypropylene.

REFERENCES

[1] Abdul Khalil HPS, Bhat AH, Ireana Yusra AF. Green Composites from Sustainable Cellulose Nanofibrils: A Review. Carbohydrate Polymers. 2012;87(2):963-979.

[2] Siró I and Plackett D. Microfibrillated Cellulose and New Nanocomposite Materials: a Review. Cellulose. 2010;17(3):459-494.

[3] Lee SH, Wang S, Pharr GM, Xu H. Evaluation of Interphase Properties in a Cellulose Fiber-Reinforced Polypropylene Composite by Nanoindentation and Finite Element Analysis. Composites Part A: Applied Science and Manufacturing. 2007;38(6):1517-1524.

[4] Spoljaric S, Genovese A, Shanks RA. Polypropylene–Microcrystalline Cellulose Composites with Enhanced Compatibility and Properties. Composites Part A: Applied Science and Manufacturing. 2009;40(6-7):791-799.

[5] Raquez JM, Habibi Y, Murariu M, Dubois P. Polylactide (PLA)-Based Nanocomposites. Progress in Polymer Science. 2013;38(10-11):1504-1542.

[6] Eichhorn SJ, Dufresne A, Aranguren M, Marcovich NE, Capadona JR, Rowan SJ, Weder C, Thielemans W, Roman M, Renneckar S, Gindl W, Veigel S, Keckes J, Yano H, Abe K, Nogi M, Nakagaito AN, Mangalam A, Simonsen J, Benight AS, Bismarck A, Berglund LA, Peijs, T. Review: Current International Research into Cellulose Nanofibres and Nanocomposites. Journal of Materials Science. 2010;45(1):1-33.

[7] Adeosun SO, Lawal GI, Balogun SA, Akpan EI. Review of Green Polymer Nanocomposites. Journal of Minerals and Materials Characterization and Engineering. 2012;11(4):385-416.

[8] Frone AN, Berlioz S, Chailan JF, Panaitescu DM. Morphology and Thermal Properties of PLA-Cellulose Nanofibers Composites. Carbohydrate Polymers. 2013;91(1):377-84.

[9] Nakagaito AN, Fujimura A, Sakai T, Hama Y, Yano H. Production of Microfibrillated Cellulose (MFC)-Reinforced Polylactic Acid (PLA) Nanocomposites from Sheets Obtained by a Papermaking-Like Process. Composite Science and Technology. 2009;69(7–8):1293-1297.

[10] Jonoobi M, Harun J, Mathew AP, Oksman K. Mechanical Properties of Cellulose Nanofiber (CNF) Reinforced Polylactic Acid (PLA) Prepared by Twin Screw Extrusion. Composite Science and Technology. 2010;70(12):1742-1747.

[11] Iwatake A, Nogi M, Yano H. Cellulose Nanofiber-Reinforced Polylactic Acid. Composite Science and Technology. 2008;68(9):2103-2106.

[12] Tercjak A, Gutierrez J, Barud HS, Domeneguetti RR, Ribeiro SJL. Nano- and Macroscale Structural and Mechanical Properties of in Situ Synthesized Bacterial Cellulose/PEO-b-PPO-b-PEO Biocomposites. ACS Applied Materials and Interfaces. 2015;7(7):4142-4150.

[13] Tingaut P, Zimmermann T, Lopez-Suevos F. Synthesis and Characterization of Bionanocomposites with Tunable Properties from Poly(lactic acid) and Acetylated Microfibrillated Cellulose. Biomacromolecules. 2010;11(2):454-464.

[14] Wang B and Sain M. The Effect of Chemically Coated Nanofiber Reinforcement on Biopolymer Based Nanocomposites. Bioresources. 2007;2(3):371-388.

[15] Petersson L and Oksman K. Biopolymer Based Nanocomposites: Comparing Layered Silicates and Microcrystalline Cellulose as Nanoreinforcement. Composite Science and Technology. 2006;66(13):2187-2196.

[16] Xu X, Wang H, Jiang L, Wang X, Payne SA, Zhu JY, Li R. Comparison between Cellulose Nanocrystal and Cellulose Nanofibril Reinforced Poly(ethylene oxide) Nanofibers and Their Novel Shish-Kebab-Like Crystalline Structures. Macromolecules. 2014;47(10):3409-3416.

[17] Xie Y, Hill CAS, Xiao Z, Militz H, Mai C. Silane Coupling Agents Used for Natural Fiber/Polymer Composites: A Review. Composites Part A: Applied Science and Manufacturing. 2010;41(7):806-819.

[18] Sanchez-Garcia M and Lagaron J. On the Use of Plant Cellulose Nanowhiskers to Enhance the Barrier Properties of Polylactic Acid. Cellulose. 2010;17(5):987-1004.

[19] Frone AN, Berlioz S, Chailan JF, Panaitescu DM, Donescu D. Cellulose Fiber-Reinforced Polylactic Acid. Polymer Composites. 2011;32(6):976-985.

[20] Zhou C, Chu R, Wu R, Wu Q. Electrospun Polyethylene Oxide/Cellulose Nanocrystal Composite Nanofibrous Mats with Homogeneous and Heterogeneous Microstructures. Biomacromolecules. 2011;12(7):2617-2625.

[21] Kaczmarek H, Bajer K, Gałka P, Kotnowska B. Photodegradation Studies of Novel Biodegradable Blends Based on Poly(ethylene oxide) and Pectin. Polymer Degradation and Stability. 2007;92(11):2058-2069.

[22] Park OH, Eo YJ, Choi YK, Bae BS. Preparation and Optical Properties of Silica-Poly(ethylene oxide) Hybrid Materials. Journal of Sol-Gel Science and Technology. 1999;16(3):235-241.

[23] Elimat ZM. Optical Characterization of Poly (ethylene oxide)/Zinc Oxide Thin Films. Radiation Effects and Defects in Solids. 2014;169(8):686-695.

[24] Hendrick E and Frey M. Increasing Surface Hydrophilicity in Poly(Lactic Acid) Electrospun Fibers by Addition of Pla-b-Peg Co-Polymers. Journal of Engineered Fibers and Fabrics. 2014;9(9):153-164.

[25] Sheth M, Kumar RA, Davé V, Gross RA, McCarthy SP. Biodegradable Polymer Blends of Poly(lactic acid) and Poly(ethylene glycol). Journal of Applied Polymer Science. 1997;66(8):1495-1505.

[26] Baiardo M, Frisoni G, Scandola M, Rimelen M, Lips D, Ruffieux K, Wintermantel E. Thermal and Mechanical Properties of Plasticized Poly(L-lactic acid). Journal of Applied Polymer Science. 2003;90(7):1731-1738.

[27] Buddhiranon S, Kim N, Kyu T. Morphology Development in Relation to the Ternary Phase Diagram of Biodegradable PDLLA/PCL/PEO Blends. Macromolecular Chemistry and Physics. 2011;212(13):1379-1391.

[28] Arias A, Heuzey MC, Huneault MA, Ausias G, Bendahou A. Enhanced Dispersion of Cellulose Nanocrystals in Melt-Processed Polylactide-Based Nanocomposites. Cellulose. 2015;22(1):483-498.

[29] Siqueira G, Bras J, Dufresne A. Cellulosic Bionanocomposites: A Review of Preparation, Properties and Applications. Polymers. 2010;2(4):728-765.

[30] Moon RJ, Martini A, Nairn J, Simonsen J, Youngblood J. Cellulose Nanomaterials Review: Structure, Properties and Nanocomposites. Chemical Society Reviews. 2011;40(7):3941-94.

[31] Klemm D, Heublein B, Fink HP, Bohn A. Cellulose: Fascinating Biopolymer and Sustainable Raw Material. Angewandte Chemie International Edition. 2005;44(22):3358-93.

[32] Klemm D, Kramer F, Moritz S, Lindstrom T, Ankerfors M, Gray D, Dorris A. Nanocelluloses: A New Family of Nature-Based Materials. Angewandte Chemie International Edition. 2011;50(24):5438-66.

[33] Dahlke B, Larbig H, Scherzer HD, Poltrock R. Natural Fiber Reinforced Foams Based on Renewable Resources for Automotive Interior Applications. Journal of Cellular Plastics. 1998;34(4):361-379.

[34] Azizi Samir MAS, Alloin F, Dufresne A. Review of Recent Research into Cellulosic Whiskers, Their Properties and Their Application in Nanocomposite Field. Biomacromolecules. 2005;6(2):612-626.

[35] Herrmann AS, Nickel J, Riedel U. Construction Materials Based Upon Biologically Renewable Resources—from Components to Finished Parts. Polymer Degradation and Stability. 1998;59(1–3):251-261.

[36] Abdulkhani A, Hosseinzadeh J, Ashori A, Dadashi S, Takzare Z. Preparation and Characterization of Modified Cellulose Nanofibers Reinforced Polylactic Acid Nanocomposite. Polymer Testing. 2014;35:73-79.

[37] Li ZQ, Zhou XD, Pei CH. Preparation and Characterization of Bacterial Cellulose/Polylactide Nanocomposites. Polymer-Plastics Technology and Engineering. 2010;49(2):141-146.

[38] Marais A, Kochumalayil JJ, Nilsson C, Fogelström L, Gamstedt EK. Toward an Alternative Compatibilizer for PLA/Cellulose Composites: Grafting of Xyloglucan with PLA. Carbohydrate Polymers. 2012;89(4):1038-1043.

[39] Tome LC, Pinto RJB, Trovatti E, Freire CSR, Silvestre AJD, Neto CP, Gandini A. Transparent Bionanocomposites with Improved Properties Prepared from Acetylated Bacterial Cellulose and Poly(lactic acid) through a Simple Approach. Green Chemistry. 2011;13(2):419-427.

[40] Kaihara S, Matsumura S, Mikos AG, Fisher JP. Synthesis of Poly(L-lactide) and Polyglycolide by Ring-Opening Polymerization. Nature Protocols. 2007;2(11):2767-2771.

[41] La Mantia FP and Morreale M. Green Composites: A Brief Review. Composites Part A: Applied Science and Manufturing. 2011;42(6):579-588.

[42] Lu T, Liu S, Jiang M, Xu X, Wang Y, Wang Z, Gou J, Hui D, Zhou Z. Effects of Modifications of Bamboo Cellulose Fibers on the Improved Mechanical Properties of Cellulose Reinforced Poly(lactic acid) Composites. Composites Part B: Engineering. 2014;62:191-197.

[43] Plummer CG, Choo CC, Boissard CR, Bourban PE, Månson JA. Morphological Investigation of Polylactide/Microfibrillated Cellulose Composites. Colloid and Polymer Science. 2013;291(9):2203-2211.

[44] Qu P, Gao Y, Wu G, Zhang L. Nanocomposites of Poly(lactic acid) Reinforced with Cellulose Nanofibrils. Bioresources. 2010;5(3):1811-1823.

[45] Wu CS. Renewable Resource-Based Composites of Recycled Natural Fibers and Maleated Polylactide Bioplastic: Characterization and Biodegradability. Polymer Degradation and Stability. 2009;94(7):1076-1084.

[46] Zhou C, Shi Q, Guo W, Terrell L, Qureshi AT, Hayes DJ, Wu Q. Electrospun Bio-Nanocomposite Scaffolds for Bone Tissue Engineering by Cellulose Nanocrystals Reinforcing Maleic Anhydride Grafted PLA. ACS Applied Materials and Interfaces. 2013;5(9):3847-3854.

[47] Suryanegara L, Nakagaito AN, Yano H. The Effect of Crystallization of PLA on the Thermal and Mechanical Properties of Microfibrillated Cellulose-Reinforced PLA Composites. Composite Science and Technology. 2009;69(7-8):1187-1192.

[48] Wang T and Drzal LT. Cellulose-Nanofiber-Reinforced Poly(lactic acid) Composites Prepared by a Water-Based Approach. ACS Applied Materials and Interfaces. 2012;4(10):5079-5085.

[49] Lee KY, Tang M, Williams CK, Bismarck A. Carbohydrate Derived Copoly(lactide) as the Compatibilizer for Bacterial Cellulose Reinforced Polylactide Nanocomposites. Composite Science and Technology. 2012;72(14):1646-1650.

[50] Miao C and Hamad WY. Cellulose Reinforced Polymer Composites and Nanocomposites: A Critical Review. Cellulose. 2013;20(5):2221-2262.

[51] Herzberger J, Niederer K, Pohlit H, Seiwert J, Worm M, Wurm FR, Frey H. Polymerization of Ethylene Oxide, Propylene Oxide, and Other Alkylene Oxides: Synthesis, Novel Polymer Architectures, and Bioconjugation. Chemical Reviews. 2016;116(4):2170-2243.

[52] Yamaguchi Y, Li Z, Zhu X, Liu C, Zhang D, Dou X. Polyethylene Oxide (PEO) and Polyethylene Glycol (PEG) Polymer Sieving Matrix for RNA Capillary Electrophoresis. PLOS One. 2015;10(5):e0123406.

[53] Cai Z and Kim J. Bacterial Cellulose/Poly (ethylene glycol) Composite: Characterization and First Evaluation of Biocompatibility. Cellulose. 2010;17(1):83-91.

[54] Brown EE and Laborie MPG. Bioengineering Bacterial Cellulose/Poly(ethylene oxide) Nanocomposites. Biomacromolecules. 2007;8(10):3074-3081.

[55] Xu X, Liu F, Jiang L, Zhu JY, Haagenson D, Wiesenborn DP. Cellulose Nanocrystals vs. Cellulose Nanofibrils: A Comparative Study on Their Microstructures and Effects as Polymer Reinforcing Agents. ACS Applied Materials and Interfaces. 2013;5(8):2999-3009.

[56] Azizi Samir MAS, Alloin F, Sanchez JY, Dufresne A. Cellulose Nanocrystals Reinforced Poly(oxyethylene). Polymer. 2004;45(12):4149-4157.

[57] Azizi Samir MAS, Mateos AM, Alloin F, Sanchez JY, Dufresne A. Plasticized Nanocomposite Polymer Electrolytes Based on Poly(oxyethylene) and Cellulose Whiskers. Electrochimica Acta. 2004;49(26):4667-4677.

[58] Azizi Samir MAS, Chazeau L, Alloin F, Cavaillé JY, Dufresne A, Sanchez JY. POE-Based Nanocomposite Polymer Electrolytes Reinforced with Cellulose Whiskers. Electrochimica Acta. 2005;50(19):3897-3903.

[59] Mathew AP, Chakraborty A, Oksman K, Sain M. "The Structure and Mechanical Properties of Cellulose Nanocomposites Prepared by Twin Screw Extrusion" in *Cellulose Nanocomposites: Processing, Characterization, and Properties*. vol. 938, K. Oksman and M. Sain, Eds., ed: Oxford University Press, 2006, pp. 114-131.

[60] Kowalczyk M, Piorkowska E, Kulpinski P, Pracella M. Mechanical and Thermal Properties of PLA Composites with Cellulose Nanofibers and Standard Size Fibers. Composites Part A: Applied Science and Manufturing. 2011;42(10):1509-1514.

[61] Kiziltas A, Nazari B, Erbas Kiziltas E, Gardner DJ, Han Y, Rushing TS. Method to Reinforce Polylactic Acid with Cellulose Nanofibers via a Polyhydroxybutyrate Carrier System. Carbohydrate Polymers. 2016;140:393-399.

[62] Jonoobi M, Mathew AP, Abdi MM, Makinejad MD, Oksman K. A Comparison of Modified and Unmodified Cellulose Nanofiber Reinforced Polylactic Acid (PLA) Prepared by Twin Screw Extrusion. Journal of Polymers and the Environment. 2012;20(4):991-997.